



Republic of Iraq

Ministry of Higher Education & Scientific Research

University of Kerbala

College of Engineering

Department of Civil Engineering

**Flexural Behavior of Reinforced Concrete Beams  
Containing SIFCON and Strengthened by CFRP  
Sheets.**

**A Thesis Submitted to the Council of the College of Engineering  
/University of Kerbala in Partial Fulfillment of the Requirements for  
Master's Degree in Civil Engineering**

**By:**

**Isam Yousif Jabbar**

**Supervised by:**

**Prof. Dr. Laith Shakir Rasheed**

**Asst. Prof. Dr. Wajde Shober Sahib Alyhya**

**May. 2023 A.D**

**Shawwal-1444 AH**

بِسْمِ اللَّهِ الرَّحْمَنِ الرَّحِيمِ

يَرْفَعِ اللَّهُ الَّذِينَ آمَنُوا مِنْكُمْ وَالَّذِينَ أُوتُوا الْعِلْمَ  
دَرَجَاتٍ

صدق الله العلي العظيم

(المجادلة: من الآية 11)

## Examination Committee Certification

We certify that we have read the thesis entitled "Flexural Behavior of Reinforced Concrete Beams Containing SIFCON and Strengthened CFRP Sheets", and as an examining committee, we examined the student "Isam Yousif Jabbar" in its content and what is connected with it and that in our opinion it is adequate as a thesis for the degree of Master of Science in Civil Engineering.

**Supervisor**

Signature: 

Name: Prof. Dr. Laith Shakir Rasheed

Date: / / 2023

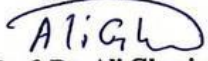
**Supervisor**

Signature: 

Name: Asst. Prof. Dr. Wajde Shoher Saheb


Date: / / 2023

**Member**

Signature:   
Name: Asst. Prof. Dr. Ali Ghanim Abbas


Date: / / 2023

**Member**

Signature:   
Name: Asst. Prof. Dr. Mushtaq Sadiq Radhi

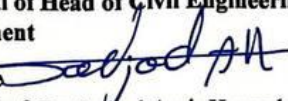
Date: / / 2023

**Chairman**

Signature:   
Name: Prof. Dr. Ali Homeed Aziz

Date: / / 2023

**Approval of Head of Civil Engineering Department**

Signature:   
Name: Prof. Dr. Sajjad Amir Hemzah

Date: / / 2023

**Approval of Deanery of the College of Engineering**

Signature:   
Name: Prof. Dr. Laith Shakir Rasheed

Date: / / 2023

## Supervisors' Certificate

We certify that the thesis entitled "**Flexural Behavior of Reinforced Concrete Beams Containning SIFCON and Strengthened by CFRP Sheets**" was prepared by **Isam Yousif Jabbar** under our supervision at the Department of Civil Engineering, Faculty of Engineering, University of Kerbala as a partial fulfilment of the requirements for the Master's Degree in Civil Engineering Science.

Signature: 

**Prof. Dr. Laith Shakir Rasheed**

Date: / / 2023

Signature: 

**Asst. Prof. Dr. Wajde Shobar Saheb Alyhya**

Date: / / 2023

## **Linguistic Certificate**

I certify that the thesis entitled "**Flexural Behavior of Reinforced Concrete Beams Containning SIFCON and Strengthened by CFRP Sheets**", submitted by **Isam Yousif Jabbar**, has been proofread, and its language has been amended to meet the English style.

Signature:



Name: Asst. Dr. Zena Dhiah Mohamed Husan

Date: / / 2023

## **Undertaking**

I certify that the research work titled “**Flexural Behavior of Reinforced Concrete Beams SIFCON and Strengthened CFRP Sheets**” is my work, and it has not been presented elsewhere for assessment. All material used from other sources has been properly acknowledged/referred to.

Signature:

**Isam Yousif Jabbar**

Date: / / 2023

## **Abstract**

Mortar infiltrated within the fibers (SIFCON) is one of the new usages of concrete, which has become more important for the success of its use as a way to reinforce and repair old structures and modernize them, or as a result of increased loads resulting from design errors.

Hybrid concrete (Sifcon) is distinguished by its very ductile substance and excellent energy absorption capacity. Additionally, it has great impact resistance and explosive loading. The resulting hybrid concrete matrix functions as a composite member to distribute loads and absorb shocks on the structural member due to the high values of elasticity and potential energy of the steel fibers.

The present study aims to investigate experimentally the behaviors of reinforced concrete beams containing SIFCON and strengthened by Carbon Fiber Reinforced Polymer sheet (CFRP) at their bottom flexural faces. Fourteen specimens of reinforced concrete beams, divided into five groups were made and tested according to the percentage of steel fiber, thickness of SIFCON layer and CFRP sheets presence.

The results of the experimental program showed that the percentage of steel fiber has an impact on the compressive strength of SIFCON, as increasing the percentage of steel fiber from 0 % to 6% has increased the compressive strengths from (30 to 77%) in comparison with the control specimen at the age 28 days, respectively.

Moreover, it was proved that the percentage of steel fiber has a significant effect on the splitting tensile strength (fct). The splitting tensile strengths increased by approximately (160% to 417%) for the added steel fiber percentages from 0% to 6% relative to the reference specimen for age 28 days, respectively.

The experimental results also revealed that the percentage of steel fiber has an impact on the ultimate flexural force of SIFCON, for the increase of the percentage of steel fiber increased the ultimate flexural force by about (16 and 30%) for the added steel fiber percentage of 4 and 6% concerning the reference specimen of 2% for SIFCON specimens with a thickness of 30mm respectively. At the same time, the increase of the percentage of steel fiber increased the ultimate flexural force concerning the reference specimen of 2% for SIFCON specimens with a thickness of 20mm respectively.

It is worth mentioning that the ductility index is greatly affected by the percentage of added steel fibers and the thickness of the SIFCON layer in the presence of CFRP. And, in this regard, failure is controlled by debonding of the SIFCON layer, which makes it close to failure in the absence of CFRP. This indicates that the CFRP fixation length is insufficient to raise the ductility index. It has been demonstrated that adding more CFRP sheets increases stiffness. Similarly increasing the percentage of steel fibers increases the stiffness, and likewise, increasing the SIFCON layer thickness from 20 to 30 mm increases the stiffness by a small amount.



## **Dedication**

I dedicate my thesis to God Almighty, my dear father, the martyr, Dr. Yousif Jabbar, my kind mother, my beloved wife and family and friends.

## **Acknowledgements**

First and foremost, many praises and thanks to ALLAH for enabling me to finish this work.

I would like to thank my supervisors, Dr. Laith Shakir Rasheed and Dr. Wajde Shobar Saheb, for their excellent assistance, guidance, and valuable suggestions throughout the research period.

Thanks, are also due to the Head and staff of the Civil Engineering Department, the construction materials laboratory, and all those who stood with me to finish this work.

I would like to extend my special thanks and gratitude to my family, especially my father, my mother, and all my family members, for their care, patience, and encouragement throughout the research period.

Finally, I would like to express my extreme love and appreciation to everyone who has supported this work.

## Table of Contents

Subject	Page
Dedication	I
Acknowledgments	II
Table of Contents	III
List of Tables	VI
List of Figures	VIII
List of Abbreviation	XII
List of Symbols	XIII
Chapter One (Introduction)	
1.1 General	1
1.2 Slurry Infiltrated Fiber Concrete (SIFCON) technique	2
1.3 Strengthening Technique for Beams	3
1.4 Fiber-Reinforced Polymer (FRP)	5
1.5 Aim and Objective of the Study	6
1.6 Layout of Thesis	7
Chapter Two (Literature review)	
2.1 Introduction	8
2.2 Slurry Infiltrated Fiber Concrete SIFCON)	9
2.3 Advantages of Slurry Infiltrated Fibers Concrete	11
2.4 Disadvantages of Slurry Infiltrated Fibers Concrete	12
2.5 Experimental studies of SIFCON	12
2.6 SIFCON in Reinforced Beams	15
2.7 Reinforced Concrete Beams with FRP	20
2.7.1 Experimental Studies on Reinforced Concrete Beams with CFRP	22
2.8 Concluding Remarks	28
Chapter Three (The experimental work)	

<b>Subject</b>	<b>Page</b>
3.1 Introduction	29
3.2 Materials	29
3.2.1 Fine aggregate	30
3.2.2 Coarse aggregate	31
3.2.3 Silica fume	32
3.2.4 High-range water-reducing Admixture (HRWR)	33
3.2.5 Water	34
3.2.6 Steel fibers	34
3.2.7 Steel- Reinforcing Bars	35
3.2.8 CFRP Sheets	36
3.2.9 Epoxy	37
3.3 Concrete Mixes	38
3.4 Preparation and Casting of SIFCON Specimens	38
3.5 Mixing of Concrete	39
3.6 Casting and Curing of Sifcon Specimens	39
3.7 Slump Test:	42
3.8.1 Compressive Strength	42
3.8.2 Splitting Tensile Strength	43
3.8.3 Flexural Strength of SIFCON	44
3.9 Molds and Reinforcement	44
3.10 The Experimental Program	46
3.10.1 The mechanism used to prepare the Sifcon mixture	48
3.10.2 External Strengthening with CFRP Sheets	50
3.11 Beam Test	51
3.11.1 Deflection Measurements	51
3.11.2 Strain Indicator	51
3.11.3 Microscopic Observation	52

<b>Subject</b>	<b>Page</b>
3.12 Loading Test Setup	53
<b>Chapter Four (Experimental Results and Discussion)</b>	
4.1 Introduction	55
4.2 Test Results of Control Specimens	55
4.2.1 Compressive Strength	55
4.2.2 Splitting Tensile Strength	57
4.2.3 Flexural ultimate force	58
4.3 Crack Behavior and Failure Modes of RcBeams	60
4.3.1 First Crack Loads and Crack Patterns	60
4.3.2 Failure Modes	66
4.3.3 Width of Crack	66
4.4 Load-Deflection curves of RC Beams	67
4.5 Parameters Study	75
4.5.1 Effect of Steel fiber	75
4.5.2 Effect of CFRP Sheets	78
4.5.3 Effect of SIFCON Layer Thickness	80
4.5.4 Deflections at Mid-span of Beams at Service and Ultimate Loads	81
4.6 Ductility Index	82
4.7 Ultimate Load	84
4.8 Flexural Toughness	86
4.9 Flexural Stiffness	88
<b>Chapter Five (Conclusions and recommendation)</b>	
5.1 General	90
5.2 Conclusions	90
5.3 Recommendations for future research work	93
References	94
Appendix	99

## List of Tables

No.	Title of Tables	Page
Chapter Two (Literature review)		
2.1	Beams distribution.	19
2.2	Loads results.	19
Chapter Three (The experimental work)		
3.1	Sulfate-resistant Portland cement's chemical make-up and key ingredients	29
3.2	Physical characteristics of cement	30
3.3	Fine aggregate grading	31
3.4	Some properties of fine aggregate	31
3.5	Coarse aggregate grading	32
3.6	Some properties of coarse aggregate	32
3.7	Chemical analysis of Silica fume	33
3.8	Technical description of Glenium 51	34
3.9	Tensile properties of the used steel reinforcing bars	35
3.10	Mechanical properties of CFRP	36
3.11	Mechanical properties of epoxy resin	37
3.12	SIFCON slurry and normal concrete mix proportions and properties.	38
3.13	Number and classification of Control specimens.	40
Chapter Four (Experimental Results and Discussion)		
4.1	Test results of compressive strength ( $f_{cu}$ ) of SIFCON	56
4.2	Test results of splitting tensile strength ( $f_{ct}$ ) of SIFCON	58
4.3	Test results of flexural strength of SIFCON plates	59
4.4	Crack and Ultimate Loads of all beams	61
4.5	Crack width at ultimate loads of beams with CFRP	67

<b>No.</b>	<b>Title of Tables</b>	<b>Page</b>
4.6	Deflections at mid-span of specimens at service and ultimate loads	82
4.7	Ductility Index of all beams	83
4.8	Ultimate Loads of all tested beams	85
4.9	The toughness of tested beams	87
4.10	Stiffness of tested beams	88

## List of Figures

No.	Title of Figures	Page
Chapter one (Introduction)		
1.1	The application of CFRP in strengthening beams	5
Chapter Two (Literature review)		
2.1	Fiber direction and edge effect in a cylinder-shaped SIFCON specimen	10
2.2	Direction of fiber in cored SIFCON as influenced by the coring orientation concerning fiber placement directions	11
2.3	Beam details	18
2.4	Stress-strain relationship of fibers and steel	21
2.5	Profile section of the test beams (units: mm)	25
2.6	Cross-section of beams (dimensions are in mm)	25
2.7	Reinforcement arrangement and test setup	27
Chapter Three (The experimental work)		
3.1	Steel Fibers.	34
3.2	Steel Bar Testing Machine	35
3.3	CFRP Sheets.	36
3.4	Epoxy Material.	37
3.5	Wooden prismatic specimens' moulds	41
3.6	steel cubes and cylindrical moulds	41
3.7	Figure 3.7 slump test	42
3.8	Compressive Test Machine.	43
3.9	Splitting Tensile Strength Test.	43
3.10	SIFCON Flexural Strength Test	44
3.11	Wooden moulds and Steel Reinforcement Details.	45
3.12	Beam Specimens Cast process	45



<b>No.</b>	<b>Title of Figures</b>	<b>Page</b>
3.13	Schematic Layout of Beams and Details of Steel Reinforcement	47
3.14	Preparation and Casting of SIFCON Layers	49
3.15	15 External Strengthening with CFRP sheets of Tested Beams	50
3.16	Strain Indicator Device and Software Interface Window.	51
3.17	Crack Meter Microscopic Device.	52
3.18	Test Setup.	53
<b>Chapter Four (Experimental Results and Discussion)</b>		
4.1	Effect of steel fiber percent on compressive strength at various ages.	57
4.2	Effect of steel fiber percent on splitting tensile strength at various ages.	58
4.3	Effect of steel fiber percent on the ultimate flexural force at various thicknesses of SIFCON plates.	60
4.4	Cracking Pattern of Specimen A-N	62
4.5	Cracking Pattern of Specimen A-NF	62
4.6	Cracking Pattern of Specimen B20-2	63
4.7	Cracking Pattern of Specimen B20-4	63
4.8	Cracking Pattern of Specimen B20-6	63
4.9	Cracking Pattern of Specimen C30-2	64
4.10	Cracking Pattern of Specimen C30-4	64
4.11	Cracking Pattern of Specimen C30-6	64
4.12	Cracking Pattern of Specimen D20-2F	64
4.13	Cracking Pattern of Specimen D20-4F	65
4.14	Cracking Pattern of Specimen D20-6F	65
4.15	Cracking Pattern of Specimen E30-2F	65
4.16	Cracking Pattern of Specimen E30-4F	65
4.17	Cracking Pattern of Specimen E30-6F	66

<b>No.</b>	<b>Title of Figures</b>	<b>Page</b>
4.18	Load deflection Curve for Beam A-N	68
4.19	Load deflection Curve for Beam A-NF.	69
4.20	Load deflection Curve for Beam B20-2.	69
4.21	Load deflection Curve for Beam B20-4.	70
4.22	Load deflection Curve for Beam B20-6.	70
4.23	Load deflection Curve for Beam C30-2.	71
4.24	Load deflection Curve for Beam C30-4.	71
4.25	Load deflection Curve for Beam C30-6.	72
4.26	Load deflection Curve for Beam D20-2F.	72
4.27	Load deflection Curve for Beam D20-4F.	73
4.28	Load deflection Curve for Beam D20-6F.	73
4.29	Load deflection Curve for Beam E30-2F.	74
4.30	Load deflection Curve for Beam E30-4F.	74
4.31	Load deflection Curve for Beam E30-6F.	75
4.32	Effect of steel fiber percent on load-deflection Behavior.	77
4.33	Effect of CFRP sheets on load-deflection behavior. (F=CFRP).	79
4.34	Effect of SIFCON layer on load-deflection behavior.	81
4.35	A comparison in ductility factor for tested beams.	84
4.36	Ultimate load comparisons of specimen beams.	86
4.37	A comparison in the toughness of tested beams.	87
4.38	A comparison in stiffness values of tested beams.	89

## List of Abbreviations

Symbol	Description
ABAQUS	Finite Element Package
ACI	American Concrete Institute
AFRP	Aramid Fiber Reinforced Polymer
ASTM	American Society for Testing and Materials
BS	British Standard
CFRP	Carbon fiber reinforcement polymer
DoF	Degrees of freedom
EFNARC	European guidelines for Self-Compacting Concrete
et al.	Others
FEA	Finite Element Analysis
FRC	Fiber Reinforced Concrete
FRP	Fiber Reinforcement Polymer
GFRP	Glass fiber reinforcement polymer
HVFA	high-volume fly ashes
IQs.	Iraqi specification
mm	Millimeter
MPa	Mega Pascal (N/mm <sup>2</sup> )
No.	Number
NSM	Near-Surface Mounted technique
NVC	Normal Vibrated Concrete
RC	Reinforced Concrete
SIFCON	Slurry-infiltrated fiber concrete

## List of Symbols

Symbol	Description
a	The total length of the column (mm)
$A_c$	The cross-sectional area of concrete (mm <sup>2</sup> )
$A_g$	The cross-sectional area of section (mm <sup>2</sup> )
$A_s$	The cross-sectional area of steel reinforcement (mm <sup>2</sup> )
b	Total width of column (mm)
$d_b$	Diameter of steel reinforcement (mm)
$E_c$	Concrete modulus of elasticity (GPa)
$E_s$	Steel modulus of elasticity (GPa)
$f_{cu}$	Concrete compressive strength (MPa)
$f_{fe}$	The effective FRP strengthening stress (MPa)
$f_{sp}$	Splitting tensile strength of concrete (MPa)
$f_{su}$	The ultimate strength of steel reinforcement (MPa)
$f_{sy}$	Strength of steel reinforcement (MPa)
$f_y$	Yield strength of steel reinforcement (MPa)
$P_{cr}$	Cracked load (kN)
t	CFRP sheets thickness (mm)
V	Volume of specimen (m <sup>3</sup> )
w	CFRP sheets width (mm)
$W_{dry}$	Oven-dry mass (kg)

# Chapter One

## Introduction

### 1.1 General Overview:

It is well known that plain concrete requires additional reinforcement since it is vulnerable to cracking and collapse under tensile pressure. Various reinforcing materials, such as steel fibers and fiber reinforced polymer (FRP), have been used to tackle the inherent low tensile strength issue. In this regard, slurry-infiltrated fiber concrete (SIFCON), a relatively new type of hybrid concrete with exemplary behavior, has been invented. SIFCON is manufactured using short discrete fibers in the molds to their full capacity or the desired volume percentage. The fibers are subsequently penetrated with a fine liquid slurry or cement mortar, which can be scattered in big portions by hand or by fiber-dispensing equipment. The vibration could be applied when placing the fibers and pouring the slurry if necessary. The steel fiber content might reach up to 30 percent by the mould volume. (Jerry and Fawzi, 2022)

In traditional fiber-reinforced concrete (FRC), the proportion of fibers combined with other concrete ingredients is restricted to nearly 2% for practical workability considerations. Due to its high fiber content, SIFCON possesses unique and exceptional mechanical qualities in strength and ductility domains. In addition to the obvious difference in fiber volume percentage, the primary distinction between FRC and SIFCON is the absence of coarse aggregate in SIFCON, which, if present, would impede the infiltration of the slurry via the dense fiber network. In addition, SIFCON includes comparatively higher cement content than normal vibrated concrete (NVC). (Balaji and Thirugnanam, 2018)

Hybrid concrete (Sifcon) is distinguished by its very ductile substance and excellent energy absorption capacity. Additionally, it has great impact resistance and explosive loading. The resulting hybrid concrete matrix functions as a composite member to distribute loads and absorb shocks on the structural member

due to the high values of elasticity and potential energy of the steel fibers. (Lankard, 1985)

Although SIFCON is still a relatively new building product, it has been effectively applied since the early 1980s in a variety of applications. Such examples include storage containers designed to withstand the effects of an explosion, security vaults that can withstand the force of a bomb, and the maintenance and restoration of bridge decks, airport pavements, and abrasion-resistant surfaces. (Balaguri and Shah, 1992).

## **1.2 Slurry Infiltrated Fiber Concrete (SIFCON)**

Slurry infiltrated fiber concrete (Sifcon) is a new type of fiber-reinforced concrete characterized as an extremely ductile material with high absorb energy. It additionally possesses high resistance to impact and explosive loading.

In 1979, Lankard Materials Laboratory in Columbus, Ohio, United States, invented SIFCON by integrating significant quantities of steel fibers into steel fiber reinforced cement-based components. Related to fiber-reinforced concrete (FRC), SIFCON features a discrete fiber matrix that imparts considerable tensile capabilities to the composite matrix. The percentage of fiber by volume of conventional fiber-reinforced concrete ( $V_f$ : fibers percentage by volume) is restricted by the capacity to mix the fibers inside the fresh concrete properly. This restricts the percentage of fiber by volume  $V_f$  to between 1 % and 2 %, depending on the type of fiber employed and the mix's desired workability. On the other hand, SIFCON specimens are created with  $V_f$  between 5 % and 20 % in which the percentage of fiber by volume is determined by the fiber kind, lengths, diameters, and the vibration force used to fill the mold (Lankard, 1984).

SIFCON's matrix lacks coarse particles and has a high cementitious concentration. It may also contain micro silica, fly ash, and latex emulsion additives. The matrix must be developed to appropriately infiltrate the fiber network installed in the molds; otherwise, huge pores may form, resulting in a

significant drop in characteristics. A limited amount of high-range water-reducing admixture (superplasticizer) should be added to SIFCON to improve its flowability properties. Useful steel fibers include straight, hooked, and crimped varieties in a typical mix of cement and sand with 1:1, 1:1.5, or 1:2. Cement slurry can also be used alone for certain applications. 10% to 15% of the cement weight is replaced by fly ash or silica fume. The water-cement ratio fluctuates between 0.3 and 0.4, while the superplasticizer percentage varies between 2% and 5% by weight of cement. The percentages of fiber by volume can range from 4% to 20%; however, the practical used range was only 4 to 12% (Dagar, 2012).

### **1.3 Strengthening Technique for Beams**

The goal of the strengthening procedures is to enhance the behavior of the concrete elements, re-establish and strengthen the stiffness of the concrete. Besides, it enhances the look of the concrete surface and makes it more watertight, it also stops corrosive materials from getting to the reinforcing, and rise the concrete members' total durability. The proper strengthening of decaying concrete structures is predicated on a thorough study of the causes and effects of the degradation, as well as the techniques, processes, and materials employed for repair or strengthening. The costs and simplicity of application, in addition to the effectiveness of the strengthening process, play a significant role in the selection of materials and processes. Multiple methods can be utilized to strengthen a reinforced or broken structure to an acceptable level of function at an affordable cost. Strengthening or reinforcing concrete beams by trying to apply repairing methods to the tension side of the beam (like using reinforcement concrete layers, plates of steel, and FRP (Fiber-reinforced polymer) wrapping laminates), are among the most commonly used repairing or reinforcing methods for beams. The primary purpose of the underneath layer is to boost the concrete beam's load capacity. Depending on the wrapping layer employed, stiffness and strength are enhanced. As with any other strengthening or mending procedure, the design of the underlying layer must account for the additional stresses that may impact the beam and the

connection between the repairing material and the concrete face. The new concrete should have the same compressive strength as the previous structure (Bashandy, 2013)

Such a strategy is applicable in several ways. Typically, the lower face of the concrete beam is covered with a mending layer that is adhered to the beam's tension face. Ferrocement is a good material for structural rehabilitation and reinforcement. **It enhances fracture resistance in conjunction with high toughness, the capacity to be cast into any form, quick production without heavy gear, a minimal increase in weight, and inexpensive construction costs** (Bashandy, 2013).

Steel plate repair and reinforcement are among the most effective rehabilitation techniques. Plate end anchorages exert a stronger influence on shorter beams having a high-shear force-to-bending moments ratio than on longer beams. Typically, anchors consist of anchor bolts or bonded cover plates. The method of reinforcing reinforced concrete members by continuously connecting an FRP strip has the benefit of being quick and incorporating the essential anchoring mechanism. Using several little fasteners instead of a single large fastening bolt with a larger diameter distributes the load more equally over the strip (Bashandy, 2013)

Four different repair operations were investigated: epoxy injections, ferrocement, steel plate bonding, and a mixture of epoxy system installed and ferrocement. The results revealed that beams rebuilt by ferrocement layer, steel plate bonding, and a mixture of epoxy system installed and ferrocement had greater flexural strength than their original counterparts. The flexural strength and cracking behavior of the epoxy injection-repaired beams were identical to those of the original beams. A larger number of fractures and finer cracks were seen in rehabilitated beams compared to the unrehabilitated beams, indicating that the ferrocement layer or epoxy injection in conjunction with the provided ferrocement layer enhanced cracking behavior. The lower ductility of beams enhanced with



plate bonding can result in rapid failure, which can be mitigated partly by modifying the steel plate's design to provide a more ductile failure (Bashandy, 2013).

### 1.4 Fiber-Reinforced Polymer (FRP)

Fiber-reinforced polymer (FRP) is becoming an unbeaten material in strengthening and retrofitting existing structures. Due to its simplicity and application, FRP has a superior mix of attributes in weight, strength, stiffness, impact, durability, and corrosion resistance compared to traditional construction materials. Because of its low weight, it does not require mechanical lifting or anchoring equipment, resulting in little service disruption during the strengthening and maintenance procedure. It is with high advantages, especially in tight spaces. The application is simple, cost-effective, and short in duration, and thus substantial savings can be realized when all of the project costs are considered. **Figure 1.1** shows the application of one type of fiber reinforced polymer known as Carbon Fiber Reinforced Polymer (CFRP) in strengthening beams (Khan et al., 2004)



**Figure 1.1:** The application of CFRP in strengthening beams (Khan et al., 2004)

FRP materials have much lower densities than steel. This can result in decreased transportation costs, a marginal increase in the structure's dead load, and easier material handling and application on-site. Depending on the type of fiber, resin, and fiber's volume fraction, the coefficient of thermal expansion varies from one FRP system to another. When placed in direct tension, FRP materials show linear elastic stress-strain behavior till rupture. Consequently, failure is abrupt and possibly catastrophic. The net-fiber area or the gross-laminate area may determine the attributes of an FRP system (Sundar et al., 2016). The load-carrying strength remains constant regardless of the reported properties. Due to a lack of testing in this specific application, ACI Committee 440 [2016] recommends that FRP systems cannot be employed as compression reinforcement. When Glass Fiber Reinforced Polymers (FRP) laminates are compressed in one direction, they may fail in several ways (Sundar et al., 2016).

## 1.5 Aim and Objective of the Study

The objective of the present study is to investigate experimentally the behaviors of reinforced concrete beams strengthened with Slurry infiltrated fiber concrete (SIFCON) and Carbon Fiber Reinforced Polymer (CFRP). They were externally strengthened with SIFCON layer and CFRP attached to their tension sides. The experimental program entails testing fourteen reinforced concrete beams, most of which were strengthened with SIFCON layer and CFRP. In comparison, all beams were with identical dimensions and reinforcement details.

The research presented in this thesis covers the following areas of study:

- 1- Laboratory tests of fresh and hardened SIFCON and normal concrete.
- 2- Experimental study and a comparison of the performance of reinforced beams strengthened with SIFCON layer and CFRP sheets attached to flexural sides. The main variables of the experimental work were the thickness of the

SIFCON layer, the volume ratio of steel fiber for the SIFCON layer, and the length of CFRP strips.

- 3- In the present study, the SIFCON layer thickness and the amount of existing CFRP have been used to categorize the tested beams into five categories. Each group has contained three beams with different percentage of steel fiber (2, 4, or 6) %, except for the first group which contains two beams un strengthened with SIFCON, while another one is strengthened with CFRP. The last two groups have improved their resistance with the addition of exterior CFRP sheets.

## **1.6 Layout of Thesis**

The thesis is divided into five chapters:

**Chapter one:** It Introduces the fundamental ideas behind SIFCON and the properties of fiber-reinforced polymers (FRP). It also outlines the objective and parameters of the work.

**Chapter two:** Chapter two provides a review of prior studies related to the properties and uses of SIFCON and Fiber reinforced polymer (FRP). Experimental studies on reinforced concrete beams with FRP were also discussed.

**Chapter three:** This chapter explains the experimental work and the specimens' details, as well as the materials and the preparation of SIFCON in addition to the proposed strengthening techniques.

**Chapter four:** It presents and discusses the experimental findings, and provides an assessment of all findings.

**Chapter five:** It presents the inferences that may be derived from this study, along with a recommendation and a proposal for more investigation.

## **Chapter two**

### **Literature review**

#### **2.1 Introduction**

SIFCON is a unique form of fiber-reinforced concrete (FRC) with a fiber-rich concentration, in which the fibers are shaped and penetrated with a cement-based slurry or pouring mortar. Despite its high cost, SIFCON is increasingly utilized worldwide, particularly in explosive and impact buildings. This is because most of these materials' ultimate capabilities and durability are superior when compared with traditional FRC (Manolia et al., 2018). Moreover, SIFCON offers excellent application potential, especially in areas that require high impact resistance and high ductility, including the design of seismic retrofits, impact and explosive constructions, and the restoration of reinforced concrete structural elements. Generally, fibers reinforced with concrete (FRC) comprises a fiber percentage of 1 % to 2 % by volume, whereas SIFCON has 4 % to 20% (Rao et al., 2010). Unlike FRC, which is an aggregate concrete matrix, SIFCON is a cement slurry or fluid mortar matrix. SIFCON is formed by penetrating a bed of pre-placed fibers with cement slurry and securely packing in the moulds. In contrast, FRC is formed by inserting fibers into new concrete (Shanthini and Mohanraj, 2015).

Several studies have shown that adding fibers, particularly steel fibers, to reinforced concrete can reduce or eliminate the need for conventional primary reinforcement under some conditions. According to McMahon and Anna (2018) steel fibers boost reinforced concrete's post-cracking tensile response and fracture control capabilities. Deformed fibers, such as hook, corrugated, and twisted fibers, may enhance the mechanical strength of composite materials (Mohammed et al., 2020) reported that the fiber-matrix binding strength of twisted steel fibers is three to seven times that of straight fibers. Several variables, including fiber form, length,

and curing conditions, affect the degree to which mechanical qualities are improved.

## 2.2 Slurry Infiltrated Fiber Concrete (SIFCON)

Compared to FRC, SIFCON is a high-behavior, high-strength material with a comparatively high-volume proportion of steel fibers. High-volume fibrous concrete is another name for this material. A cement matrix with a much higher proportion of steel fibers would provide a material with exceptional strength. Steel fiber percentage in traditional FRC ranges typically from 1% to 2% by volume. In contrast, it may be anywhere from 4% to 20% in SIFCON, depending on the geometry of the fibers and the intended use. To produce SIFCON, a low-viscosity cement slurry is infused into a bed of steel fibers that have been "pre-packed" in molds (Dagar, 2012).

The fiber orientation phenomena must be considered when planning SIFCON deployments in the field or producing specimens for testing. When preparing SIFCON test specimens, care must be taken to prevent biases in fiber distribution and orientation. A lower fiber density near the mold's periphery is quite acceptable. In addition, certain fibers may run in a vertical orientation (parallel to the long axis of the mold) along the outer surface. Edge effects in shaped SIFCON are shown in **Figure 2.1**.

The issues of fiber orientation and edge impact may be mitigated by casting a slab and then coring it to generate the test specimens. The orientation of fibers is of utmost importance once again. As opposed to a cylinder in which the fibers are oriented along its axis, substantially greater compressive strength may be predicted if the fibers are aligned along the diameter of the cylinder. According to **Figure 2.3**, specimens with fibers arranged perpendicular to the loading axis may have double the strength of specimens with fibers placed parallel to the load direction. (Lankard, 1984). **Figure 2.2** depicts the vertical and horizontal coring of a slab with horizontally arranged steel fibers to produce the cylinders seen in the figure.

Once the steel fibers are placed on a substrate or in a mold, they are infiltrated with a fine-grained cement-based slurry. The slurry must be flowable, liquid enough, and have sufficient fineness to infiltrate the dense matrix thoroughly in fiber-filled forms. The infiltration step is accomplished by simple gravity-induced flow or gravity flow aided by external vibration or pressure grouting from the bottom of the bed(Lankard, 1985). Slurry infiltration by gravity flow aided by a vibrating table.

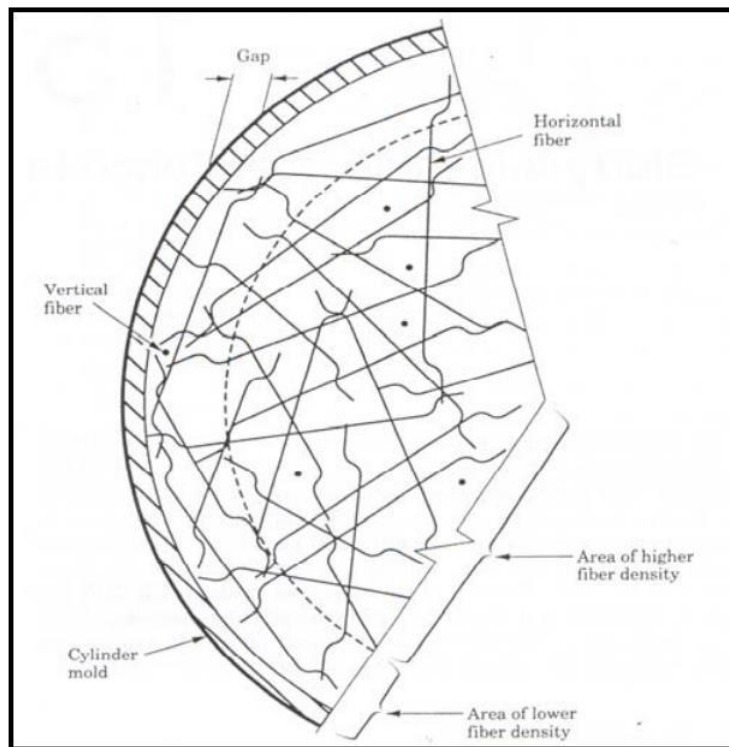


**Figure 2.1:** Fiber direction and edge effect in a cylinder-shaped SIFCON specimen(Lankard, 1985).

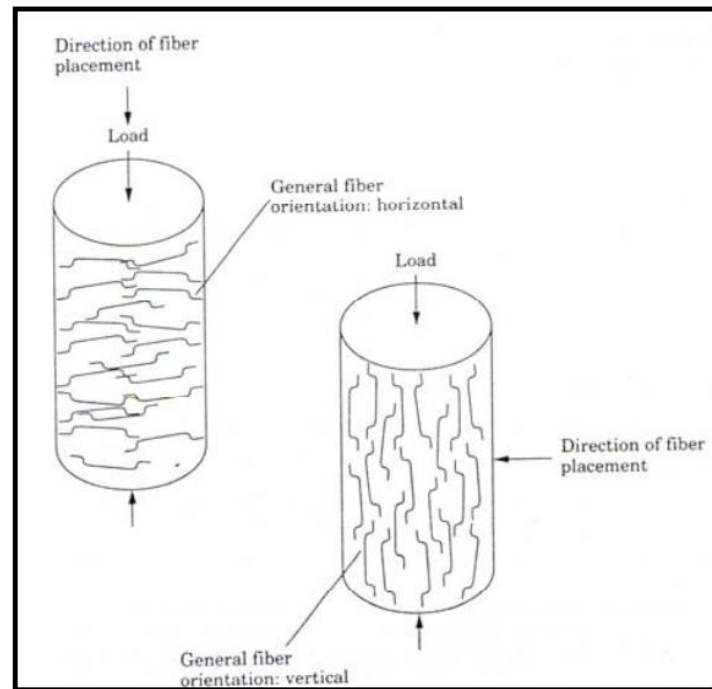


**Figure 2.2:** Direction of fiber in cored SIFCON as influenced by the coring orientation concerning fiber placement directions(Lankard, 1985).

The fluidity of the slurry determines mostly the selected infiltration method through the packed fiber bed. depicts what occurs when the slurry is not fluid enough or when the vibration is not severe enough. The degree of voids or honeycombing relies on the flowability and vibrational intensity of the slurry(Lankard, 1985).

### 2.3 Advantages of Slurry Infiltrated Fibers Concrete

In general, slurry infiltrated fibers concrete with strong ductility makes it ideal for usage in constructions with similar requirements. Utilizing Sifcon has numerous advantages, which are listed below:

- 1- Durability, energy absorption capacity, impact, and abrasion resistance, and toughness are all enhanced in slurry-infiltrated fiber concrete.
- 2- Modulus of elasticity ( $E_c$ ) values for slurry infiltrated fibers concrete samples are higher in contrast to FRC.
- 3- The balling problem of fibers caused by the increase in fiber volume in (FRC) can be resolved by mortar infiltrated fibers concrete.

- 4- Deflection for mortar-infiltrated fibers concrete will be significantly less than normal concrete structural components (Rajasekhar, 2013).

## **2.4 Disadvantages of Slurry Infiltrated Fibers Concrete**

Mortar-infiltrated fiber concrete has some unusual features, although it's not very restricted. Widespread use of these composites was hampered by issues with fiber distribution uniformity and quality control, as well as the high placement cost involved with the hand adding of fibers (Newman and Choo, 2003).

## **2.5 Experimental studies of SIFCON**

The influence of steel fiber content and silica fume-cement substitution on the mechanical characteristics of SIFCON was investigated by (Salih et al., 2018). The replacement ratio of silica fume in the SIFCON slurry was 10 % by weight of cement, and four different volume fractions of steel fiber with hooked ends were utilized (6, 8, 5, and 11) %. Compressive strength and splitting tensile strength were measured on standard-sized cubes and cylinders at ages 7 and 28 days, respectively. Using silica fume as a partial substitution for cement and adding steel fiber reinforcement in varying percentages was discovered to have a favorable effect on the mechanical qualities of SIFCON. At 28 days, the compressive and splitting tensile strengths reached 83.7 MPa and 17.3 MPa, respectively. (Salih et al., 2018) (Abd-Ali and Essa, 2019) found non-fibrous concrete is a brittle material that fails suddenly. However, when steel fibers are added to the concrete (SIFCON), it changes the failure mode from brittle to ductile, resulting in improved ductility, load-bearing capacity, and toughness. The addition of steel fibers reduces crack width, enhances resistance to deformations, and increases the compressive and splitting tensile strength of the concrete. Compared to conventional concrete and steel fiber-reinforced concrete, SIFCON shows significant improvements in compressive and splitting tensile strengths at various fiber volume fractions.



(Jerry and Fawzi, 2022) found that the SIFCON is a fiber reinforced concrete known for its superior properties. It excels in compressive strength, flexural strength, tensile strength, impact resistance, energy absorption, and ductility. This investigation focuses on fiber type's impact on SIFCON's density and impact resistance. Steel and polyolefin fibers, used alone and in hybrid combinations, are tested. Results show SIFCON with 2/3 polyolefin and 1/3 steel fibers achieves reduced density, lowering self-weight and costs while maintaining high impact resistance. Silica fume improves workability and strength in SIFCON by enhancing mortar strength through pozzolanic reaction. SIFCON mix SFS shows maximum impact resistance, 53 times greater than the reference mix after 60 days of curing. Polyolefin fibers reduce SIFON's apparent density by 17.7% compared to steel fibers (SFS) due to their lower density. Mix SFS1P2 achieves a significant density decrease (17.7%) and excellent impact resistance comparable to the maximum achieved in mix SFS. It also shows improved impact resistance.

**(Shelorkar and Jadhao, 2018) found that slurry infiltrated fiber concrete with fly ash, Metakaolin, and hook-ended steel fibers.** Steel fiber addition enhances strength, impact resistance, and elasticity. The optimal fiber content is 4% volume, while Metakaolin and fly ash should be at 10% by weight. Steel fibers with Metakaolin increase compressive strength by 71.64%, flexural strength by 87.5%, and splitting tensile strength by 67.45%. With fly ash, strength increases by 60.98%, 73.11%, and 51.04% respectively. Impact resistance is significantly improved by 158.80% (Metakaolin) and 182.40% (fly ash) compared to the control mix.

(Elavarasi, 2016) showed that Silica fume is commonly used to replace cement in SIFCON production due to its ability to enhance mechanical properties. The inclusion of silica fume improves the consistency and workability of fresh slurry by adding fines to the mixture and reducing voids in the concrete microstructure. Replacing cement with silica fume in SIFCON leads to increased compressive and split tensile strength, with the maximum strength achieved at a 15% replacement

level. SIFCON beams containing 10% fiber content exhibit higher energy absorption and ductility compared to other SIFCON and FRC specimens. The energy absorption capacity of SIFCON specimens increases by 7.45% to 116.83%, and the ductility factor ranges from 22.74% to 96.03% compared to FRC specimens. Increasing the volume of fiber content in SIFCON enhances toughness and ductility while decreasing flexural strength when comparing different SIFCON specimens.

(Salih et al., 2018) found that when silica fume replaced cement, the viscosity of the SIFCON slurry rose, resulting in a decreased spread diameter of mini slump and increased V-funnel time. This can be managed by using an appropriate dosage of superplasticizer (SP) to achieve proper filling ability and flowability of the slurry. The addition of steel fibers in increasing volume fractions enhanced the mechanical properties of SIFCON, including compressive strength and splitting tensile strength. Increasing the volume fraction of steel fibers from 6% to 11% resulted in a 12% increase in compressive strength and a 44.3% increase in splitting tensile strength for M1F-11 mix at a 7-day age. Incorporating silica fume as a partial replacement for cement in the SIFCON matrix improved its mechanical properties. The use of silica fume in the M2F-11 mix resulted in approximately 9.4% increase in compressive strength and 18.5% increase in splitting tensile strength at a 28-day age.

(Al-Abdalay et al., 2020) investigated the use of silica fume and fly ash as supplementary cementing materials in cement mortars to evaluate the mechanical properties of Slurry Infiltrated Fibrous concrete (SIFCON). The mechanical properties studied included flexural, compressive, and splitting strength, as well as impact load resistance. Plate specimens with micro steel fibers were cast and tested under impact load at 90 days of age. The results showed that SIFCON outperforms conventional mortar in terms of compressive, splitting, flexural strength, and impact resistance. SIFCON exhibits significant improvements in impact resistance at first crack and failure, with the energy demand for failure increasing by 9.97

times compared to conventional mortar. This demonstrates that SIFCON can be a viable alternative in construction applications where conventional mortar or steel fiber-reinforced concrete may not meet the required strength criteria. Also, the strength (compressive, splitting, flexural) of both conventional mortar and SIFCON increases with age. SIFCON exhibits enhanced strength (compressive, splitting, flexural) compared to conventional mortar at all ages tested. SIFCON demonstrates significant improvements in impact resistance compared to the reference mix. SIFCON shows the highest impact resistance among the tested mixes. It was found that the energy demand for failure in SIFCON is 9.97 times higher than that of the reference mix.

## **2.6 SIFCON in Reinforced Beams**

Reinforced concrete beams repaired using SIFCON were investigated by (Shannag et al., 2001), who presented a straightforward mathematical method for estimating the restored beams' shear strength. To create SIFCON, short, discontinuous steel fibers were first placed into the mould before infiltrating with a cement slurry. For this work, 14 shear-deficient reinforced concrete rectangular beams were subjected to third-point loading to determine the efficacy of externally applied SIFCON jackets in enhancing the beams' shear capacity. The ratio of the shear span to the effective depth ( $a/d$ ), the quantity of longitudinal reinforcement ( $A_s$ ), and the jacket thickness ( $t$ ) were the studied factors. All beams failed under the shear tests, while the ones fixed with SIFCON showed a far higher shear capacity than the originals. Beams that had previously experienced brittle shear failure were able to have their ultimate shear strength enhanced by 25-55% after being strengthened using SIFCON jackets as external shear reinforcement. As a result, SIFCON is considered a promising material for the maintenance and rehabilitation of concrete structures.

(Ali and Riyadh, 2018) investigated slurry-infiltrated fiber reinforcement testing specimens through experimental and numerical studies. The laboratory work

consisted of twelve specimens with a dimension of 1250 mm in length and 150 mm in height, and 100 mm in depth. All specimens had the same geometry, longitudinal, and stirrups reinforcements designed to fail in flexural mode. Eight specimens with varied steel fiber percentages such as (6%) and (8%) were divided up from the total of four specimens used as a reference. The load was applied for all specimens up to failure with mid-deflections for each test. The numerical method was the finite element approach by ANSYS (16.2) that was adopted to simulate all models, compare the analysis results with experimental tests, and examine specimens with  $V_f$  of 12% numerically. The test results were close to that of the numerical analysis. They indicated that the increase in steel fiber percentages leads to increased concrete mechanical properties, enhancing the specimens' capacity and reducing deflection.

According to the values list in Table 2, the (8%) of SF provides higher compressive strength than other mixes, and the result of mix 1:1 is better than of mix 1:1.5 because of the amount of sand is increase in this mix that lead to weak the strength of the cubes.

The increase in SFs to tested specimens with different volume fraction (6% or 8%) by volume of mold used it was observed increasing in cracking load for the specimens and ultimate load and the failure changed from brittle material to ductile material that was clear in specimens (A1, A2, A3, A4, B1, B2, B3, and B4).

In comparison with 2% steel fibers concrete, increasing the  $V_f$  steel fibers to 6% and 8% volume fraction actually increases the modulus of elasticity ( $E_c$ ) by (19.9 and 28%), respectively in mix 1:1.5. Inserting steel fiber into the concrete mix leads afterwards to elevating in the elastic modulus value. The presence of steel fibers and different sand-to-mix ratios affect the workability of the concrete mixes. The mix with 8% silica fume (SF) shows higher compressive strength, and the mix with a ratio of 1:1 performs better than the 1:1.5 ratio mix. SF improves the tensile strength and prevents micro cracks. Increasing the volume fraction of steel fibers enhances the modulus of elasticity. Steel fibers reduce crack width and increase

ductility. Specimens with SF exhibit improved performance and failure behavior. Numerical analysis aligns with experimental results.

The flexural behavior of ordinary reinforced concrete beams with SIFCON at different places along the beam was studied by (Balaji and Thirugnanam, 2018). A layer of SIFCON was cast into the composite beam at different spots along the typical RC beams. Moreover, beams constructed solely from RC, Fiber Reinforced Concrete (FRC), and SIFCON were studied and compared. Twenty-seven specimens from seven test series were cast and evaluated using a two-point flexural forward cyclic loading technique. The characteristics such as load-bearing capability, stiffness degradation, ductility, and energy absorption capacity were evaluated. The concrete used in constructing RC beams was specifically formulated to provide a grade of M30. The volume fraction of fiber used in producing the SIFCON was 9%. Indeed, the steel fibers utilized in the research were crimped with a spherical diameter of 0.5 mm, and an aspect ratio of 60. The application of SIFCON in traditional RC beams improved the cracking behavior, as the initial crack load and the emergence of a greater number of finer fractures increased substantially. Compared to traditional RC beams, composite beams had an improved ultimate load-bearing capability, stiffness, ductility, and energy absorption capacity. The ductility factor of RC beams with SIFCON in the tension zone surpasses that of conventional RC beams and FRC beams by a significant margin. SIFCON beams have the highest ductility among all types, exceeding conventional RC beams by 270% and FRC beams by 200%. RC beams with SIFCON demonstrate enhanced energy absorption capacity compared to conventional RC beams and FRC beams. When SIFCON is utilized, the energy absorption capacity is significantly higher, surpassing conventional RC beams by 140% and FRC beams by 95%. **Fibrous** concrete beam specimens, including SIFCON, experience less degradation in stiffness compared to conventional RC beam specimens. This behavior is particularly beneficial in seismic loading conditions.

SIFCON was used in conjunction with reinforced concrete beams in a study carried out by (Mohammed et al., 2020) to investigate the possibility of increasing flexural capacity. Two beams were completely cast using normal vibrated concrete (NVC) and SIFCON as control for the experimental work. While the rest of the built-up beam's depths were accomplished using normal vibrated concrete (NVC), it was bolstered by a layer of SIFCON that varied in thickness and placement. Further research on SIFCON's mechanical qualities was conducted using test specimen controls. When SIFCON was applied in stress zones, the findings demonstrated stiffer behavior and a significant improvement in the load-carrying ability. When SIFCON was placed in the compression zones, a little increase in the ultimate stress was observed; however, it showed good ductility and energy dissipation when it was placed in the tension zone. SIFCON's remarkable tensile qualities may be attributed to its construction's high volumetric ratio of steel fibers. Six reinforced concrete beams, each having a total length of 1600 mm and a cross-section of 125×200 mm, were constructed and tested under static flexure stress per ACI 318M-14. As can be seen in **Figure 2.7**, 2Ø16 mm bars were employed as the primary longitudinal reinforcement, while 8mm bars were used for shear resistance and 2Ø4mm bars were only used on the top side to support stirrups.

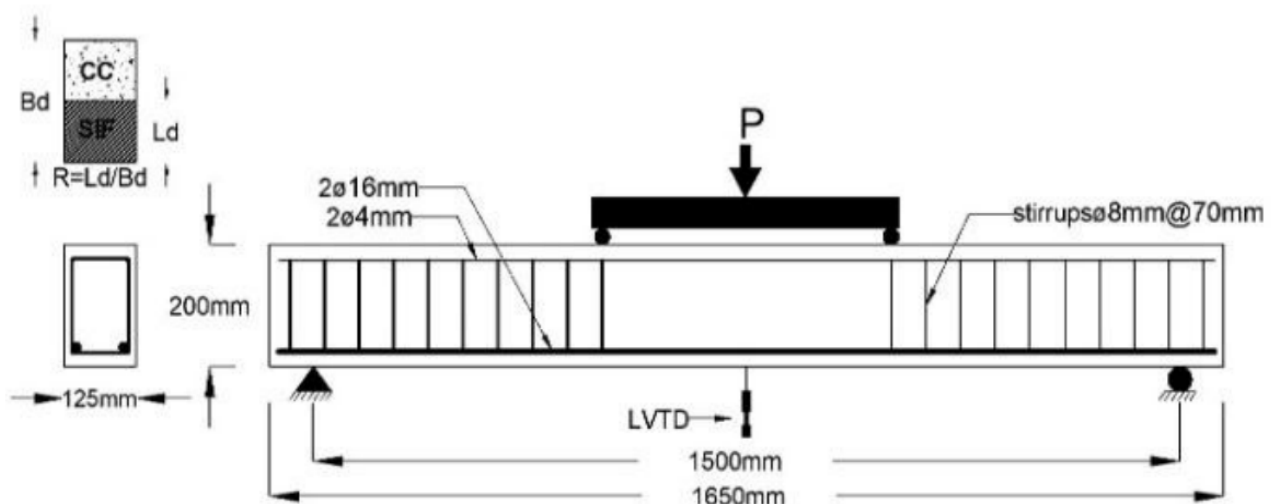


**Figure 2.3:** Beam details (Mohammed et al., 2020)

**Table 2.1** depicts the details of the RC beams [Reference beams (No. 1 and No. 2) were made to be compared with other beams. Indeed, **Table 2.2** shows the results of cracking and ultimate loads for all beams. Where  $R=Ld / Bd$ .

**Table 2.1:** Beams details (Mohammed et al., 2020)

Beams	R	Description
Ref No:1	-	CC beam
Ref No:2	1	SIFCON beam
S-B-25%T	1/4	Built-up beam with 5 cm of SIFCON in tension zone
S-B-50%T	1/2	Built-up beam with 10 cm of SIFCON in tension zone
S-B-25%C	1/4	Built-up beam with 5 cm of SIFCON in compression zone
S-B-50%C	1/2	Built-up beam with 10 cm of SIFCON in compression zone

**Table 2.2:** Test results. (Mohammed et al., 2020)

Beams	Pu (kN)	Pcr (kN)	%*	%**
Ref No:1	118	25	-	-
Ref No:2	191.22	75	62.205	200
S-B-25%T	169.65	65	43.771	160
S-B-50%T	186.323	N/A	57.9	-
S-B-25%C	142.19	25	20.5	-
S-B-50%C	156.9	25	32.966	-

% \* \*\* refers to the percentage of increase in (Pu) and (Pcr) concerning Ref No:1 beam respectively. N/A not available.

## 2.7 Reinforced Concrete Beams with FRP

Steel plate bonding technology inspired the concept of bonding fiber-reinforced polymer (FRP) or composite plates to strengthen concrete constructions. This material is an excellent counterpoint to steel since it prevents plate corrosion at the interface. Small fibers with a resin matrix make up the constituent ingredients in commercially available (FRP) systems (Valerio, 2009).

The resins are utilized to saturate the reinforcing fibers, fix them in place, and provide a path for effective load transfer between them. Polyesters, vinyl esters, and epoxies are the most frequent resins utilized. The physical characteristics of the fiber composite are determined not only by the characteristics of the components but also by their relative proportions and fiber orientation. There are three types of Fiber Reinforced Polymer: Glass Fiber Reinforced Polymer (GFRP), Carbon Fiber Reinforced Polymer (CFRP), and Aramid Fiber Reinforced Polymer (AFRP). In terms of the stress-strain relationship, the basic comparison among some types of FRP composites, based on fiber area only, and reinforcing steel, is shown in **Figure 2.8**. This figure presents the linear elastic behavior of FRP, which has a higher tensile strength in the limit of (2400 - 3400) MPa. The shear forces formed among the fibers are restricted to the properties of the matrix. In addition, the matrix limits the vertical applying forces to the fibers (Valerio, 2009).



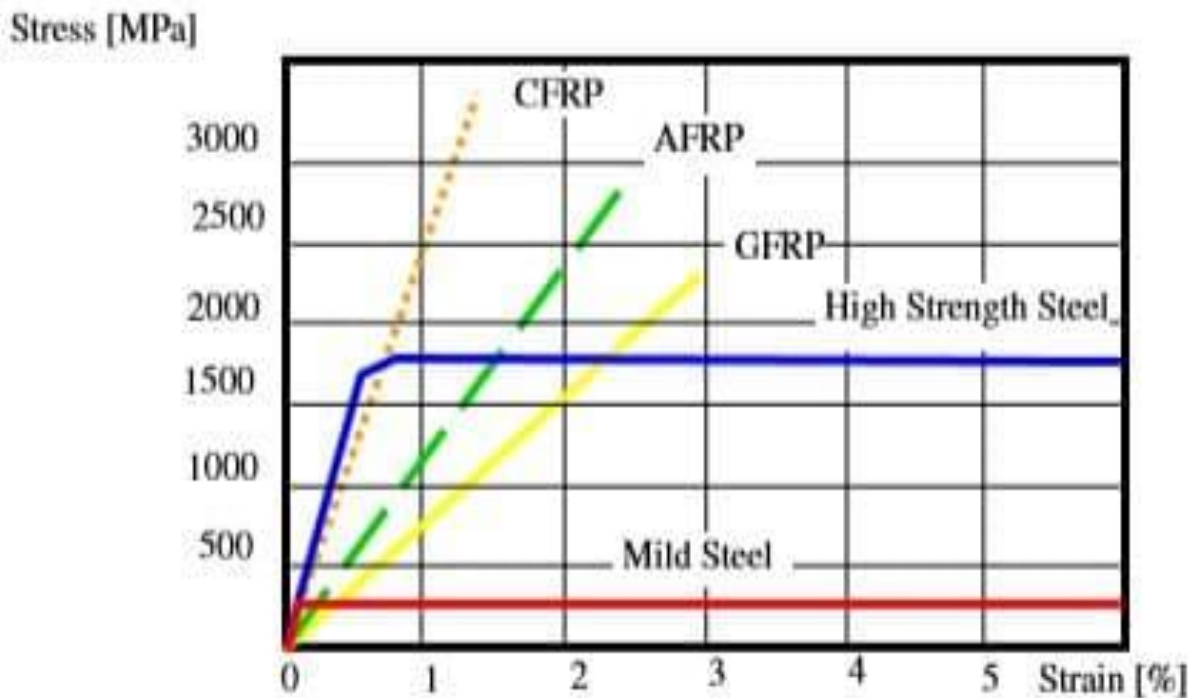


**Figure 2.4:** Stress-strain relationship of fibers and steel (Valerio, 2009).

Carbon fiber reinforced polymer (CFRP) has grown in favor of a practical choice for retrofitting and strengthening concrete structures due to its many benefits over more traditional building materials like steel and concrete. To raise the axial sectional, flexural, torsion, and shear capabilities of the reinforced concrete's structural components, the structural members' stability and serviceability are enhanced. These composites are often used as "externally bonded" arrangements. CFRP materials are then applied as a coating to the concrete surface. This method of external reinforcement is straightforward to put into action. The three CFRP reinforcements used in newly constructed buildings are internal reinforcement using CFRP bars, permanent CFRP molds for RC members, and CFRP tendons for prestressed concrete components. More details may be found in the reference (Sharifianjazi et al., 2022) .

### 2.7.1 Experimental Studies on Reinforced Concrete Beams with CFRP

Since 1987, the Swiss Laboratories for Materials Testing and Research have been performing studies incorporating bonded FRP to reinforced concrete beams (Meier, 1987). It consisted of substituting steel plates with FRP laminates to repair and strengthen reinforced concrete beams. Prior research focused on the strength and rigidity of beams constructed with unidirectional carbon fiber composite plates. (Duthinh and Starnes, 2001) examined the tensile strengths and ductility of prismatic concrete beams enhanced with carbon-fiber-reinforced polymers and reinforced with steel. Under four-point bending, seven concrete beams were strengthened inside with varying quantities of steel. External carbon fiber reinforced polymer (FRP) laminates were added just after the concrete had cracked due to service loads. Strains observed along the beam depth made it possible to calculate the beam's curvature in the zone of the constant moment. According to the findings, FRP was highly efficient for flexural strengthening. As the steel reinforcement increases, the CFRP laminates provide less additional strength. Despite their brittle failure mechanism, beams reinforced with steel and CFRP have a considerable deformation capacity compared to those reinforced with steel alone. Clamping or wrapping the laminate's edges increases the strength of adhesively bonded CFRP anchoring. Anchorage, allowable stress, ductility, and reinforcement quantity design formulae were addressed.

(Lamanna et al., 2004) examined the flexural strengthening of reinforced concrete beams by mechanically attaching fiber-reinforced polymer strips. The existing process for gluing CFRP strengthening strips to concrete buildings needs substantial time and semi-skilled labor. Attaching CFRP strips to concrete using a commercially available powder-actuated fastening system is an alternate option. Fifteen (31×31×372) cm reinforced concrete beams were subjected to flexural tests. Two unreinforced beams, twelve beams reinforced with mechanically affixed CFRP strips, and one beam reinforced with a bonded FRP strip were evaluated, as

well as the impacts of three different strip moduli, different fastener lengths and designs, and pre-drilling were all investigated. Three of the beams reinforced with mechanically attached fiber reinforced plastic strips demonstrated equivalent strength to the beam reinforced with bonded fiber reinforced plastic strips. The three identical beams reinforced with mechanically attached FRP strips were more ductile than those reinforced with bonded CFRP strips, indicating that mechanically linked CFRP strips were superior.

(Berg et al., 2006) discussed using FRP reinforcing materials and formwork for a reinforced concrete bridge deck. They described the building process and cost analysis of the projects. Elements for bridge decking reinforced with fiber-reinforced polymers were developed as a part of an ongoing research effort at the University of Wisconsin/USA. The project entailed implementing one of these ideas on a large highway bridge. The concrete deck was reinforced with FRP reinforcement: FRP stay-in-place forms, FRP reinforcing bars, and a one-of-a-kind protruded FRP reinforcing grid. With the help of the Creative Bridge Research and Building Program (IBRC) in the USA, the research effort led to the construction of a two-span bridge on Wisconsin's US Highway 151. Based on examining the short-term material and labor costs, FRP reinforcements for bridge decks may be cost-effective. Despite their currently high starting prices, they have reduced construction time savings and potential long-term durability and maintenance benefits. It is advised to optimize FRP stay-in-place formwork to reduce the cost of the FRP strengthening method in the future.

Whereas early laboratory and field research on using NSM-FRP to reinforce concrete buildings was undertaken with circular FRP bars, more current research has utilized rectangular or square NSM-FRP strips or bars. This novel strategy was developed to obtain higher FRP stresses before debonding failure. Due to the three-dimensional distribution of bond stresses created in the concrete surrounding the NSM strips as contrasted to the NSM bars (Al-Mahmoud et al., 2009), NSM-FRP

strips often have a greater average bond strength than round bars, assuming all other conditions are equivalent.

To increase its flexural ductility while retaining the high strength of the FRP bars, (Lau and Pam, 2010) advocated using steel longitudinal reinforcement to construct a Fiber reinforced polymer reinforced concrete FRPRC beam. Simple concrete beams, steel-reinforced concrete (SRC) beams, pure FRPRC beams, and hybrid FRPRC beams were all used in the construction and testing of twelve specimens. The test findings demonstrated that the hybrid FRPRC beams were more ductile than the pure FRPRC beams. A larger degree of over-reinforcement in the beam specimen resulted in a more ductile FRPRC beam. Consequently, the inclusion of steel reinforcement can enhance the flexural ductility of FRPRC members, and over-reinforcement was the ideal design technique for FRPRC members. In general, the surface features of NSM reinforcement induced frictional forces and mechanical interlocking that influenced the bonding behavior.

(Lee et al., 2013) conducted a bond test based on the strain resulting from sand-coated, ribbed, roughened, spirally coated sand, and smooth surface treatments. For each type of surface treatment, there were at least nine unique failure modes, including a mix of cracking, splitting, and FRP fracture. (Lin and Zhang, 2013) examined experimentally and analytically the flexural and bond-slip properties of FRP-reinforced concrete beams. Reinforced concrete beams enhanced with carbon, glass, and basalt fiber bars were tested to examine their flexural and bond-slip characteristics. Researchers have recently constructed finite-element models with and without the bond-slip phenomenon, and the test beams' flexural and bond-slip behaviors were computationally examined. The results of numerical modelling and experimental study were very consistent. A parametric study examined the effect of various rebar surfaces and kinds on the structural behavior of FRP-reinforced concrete beams. **Figures 2.9** and **2.10** exhibit the longitudinal and cross-section of the test beams', respectively. The results suggested that the wrapped rebar surfaces of the BFRP-reinforced concrete beams had high adhesion to the concrete. They

have significantly better load-bearing capacities before load–slip curve decay than CFRP- and GFRP-reinforced concrete beams, whose load–slip curves decay abruptly at considerably lower load values.

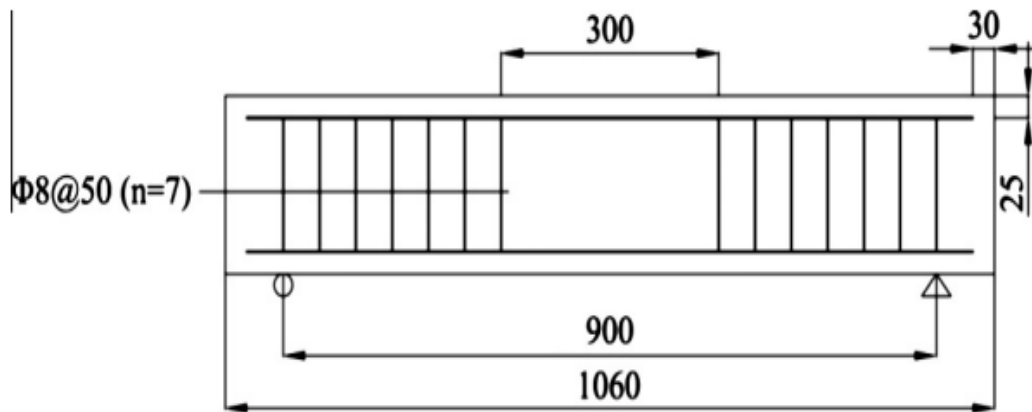


**Figure 2.5:** Profile section of the test beams (units: mm) (Lee et al., 2013)

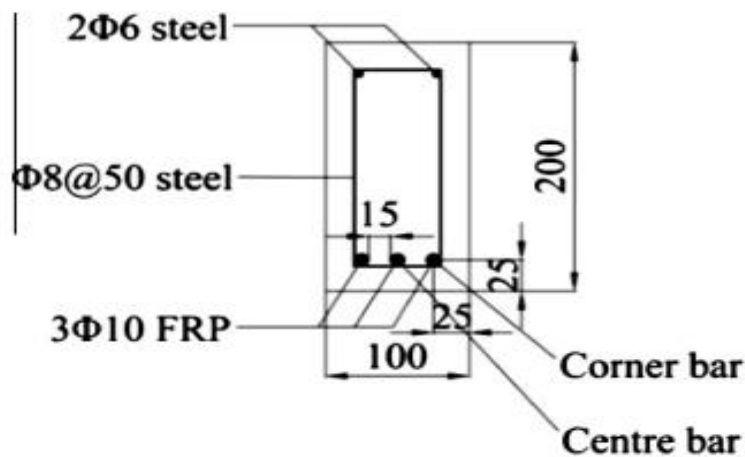


**Figure 2.6:** Cross-section of beams (dimensions are in mm) (Lin and Zhang, 2013)

(G. Karayannis et al., 2018) investigated the experimental performance of seven thin reinforced concrete beams containing CFRP bars under static loads. They presented and discussed load carrying capacities, deflections, post-cracking stiffness, fast local losses in strength, failure mechanisms, and crack propagation. Special attention has been devoted to the bond conditions of the CFRP tensile bar anchoring lengths. The application of confinement conditions throughout the

anchoring lengths of CFRP bars appeared to influence their cracking behavior in particular specimens. Nonetheless, further research is required in this field. In addition, experimental data for CFRP beams and beams reinforced with GFRP bars from the current literature were compared and analyzed. There were also comparisons between the experimental results and the predictions according to (Sundar et al., 2016).

An investigation into the flexural behavior of internally reinforced GFRP-RC beams supplemented with CFRP strips utilizing the Near-Surface Mounted (NSM) technique was made, which is available as part of a research plan (Barris et al., 2020). Cracked section analysis was used to determine their theoretical load-carrying capability. In addition, an analytical study was undertaken to reveal the effect of various factors on the flexural capacity of NSM CFRP-reinforced concrete beams with either steel or GFRP bars installed inside as reinforcement. In most cases, a greater flexural capacity may be achieved by increasing the reinforcement ratio and the internal or NSM mechanical qualities. Nevertheless, a parameter modification might affect the rise ratios differently and lead to distinct failure scenarios. **Figure 2.13** depicts the configuration and test equipment for reinforcements. The results indicated that analytical assumptions predict the experimental failure load, with a mean ratio of 0.95 between the experimental and theoretical loads. The variation of this ratio might be attributable to the smaller-than-0.003 ultimate concrete strain observed in some beams (considered in the theoretical calculations).

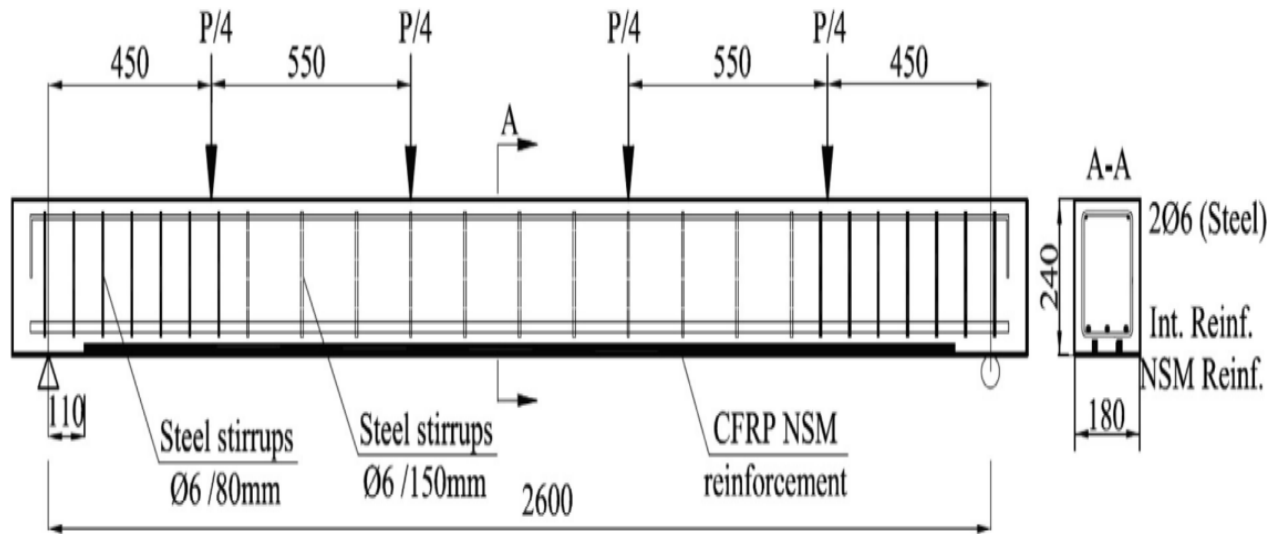


**Figure 2.7:** Reinforcement arrangement and test setup (Barris et al., 2020).

(Yang et al., 2021) experimented with the viability of strengthening beams with corroded reinforcement by directly applying FRP laminates that were externally linked to each other and coupled with U-jackets. This was performed without first repairing the damaged concrete cover. The four-point bending tests were performed on ten different beams. As standards, two beams were not utilized that were both undamaged and unreinforced. The remaining eight were subjected to preloading to bring about flexural fractures, followed by fast corrosion. Of the six damaged beam soffits, two had no reinforcement, three had laminates made of glass-fiber-reinforced plastic (GFRP), and the remaining three had plates made of carbon-fiber-reinforced plastic (CFRP). CFRP U-jackets were installed on each of the six reinforced beams that ran the bridge length. A 3D-scanning technique was used to analyze the local corrosion levels. As a result of pitting corrosion, the load-bearing and deformation capabilities of the beams were significantly reduced. Even though the mean corrosion levels were 20 percent, local corrosion levels were as high as 57 percent. Corrosion-induced cracks were as wide as 1.9 mm; the FRP strengthening technique successfully increased the load-carrying capacity and stiffness of the specimens (it was applied directly to the beams without repairing

the deteriorated concrete cover). Due to the effectiveness of the U-jackets in preventing the delamination of the concrete cover, the GFRP laminates were broken, and the usage rate for the CFRP plates was increased to as high as 64 percent. Despite this, there was no visual enhancement in the material's power to resist deformation; this calls for more research.

## **2.8 Concluding Remarks**

Based on the existing research, it is possible to infer that all studies examine the influence of individual or multiple blends of SIFCON materials with lime on the behavior (physical, dynamic, volume change duration, absorption, and durability) of the SIFCON combination. The experiments in SIFCON studies showed SIFCON as a novel construction material with enhanced energy absorption capacity, impact resistance, large ductility, and high strength. All these characteristics enable SIFCON to rehabilitate and strengthen the structures of unreinforced and reinforced concrete. The literature reviews demonstrated that the FRPs could be used to restore and strengthen reinforced concrete beams failing in shear and flexure. The degree of percentage increase in flexural capacity of strengthened beams with CFRP composite materials depends on the concrete compressive strength, steel reinforcement tensile strength, and tensile strength of the CFRP. Using CFRP decreases the propagation crack width and prevents it from expanding. It can be asserted that very limited literature is currently available on SIFCON concrete beams. Also, a few research is available to study the effect of external strengthening by CFRP in SIFCON concrete.



## Chapter three

### The Experimental Work

#### 3.1 Introduction

This part of the thesis describes and shows the detailed work performed in the laboratory. Details about material properties, mix proportions, mixing procedure, pouring and curing beam specimens' details, CFRP strengthening, and testing methods are mentioned. As part of the experimental investigation, tests were conducted on the properties of both SIFCON slurry and normal concrete mixes.

#### 3.2 Materials

This research utilized Al-Jisir, a brand of Iraqi cement, which conforms to the IQ standard [No. 5/2019]. The specific type of cement used was sulfate-resistant Portland cement, known as Type V. The physical and chemical characteristics of the cement, as outlined in Tables 3.2 and 3.3, fall within the specifications defined in the Iraqi Standard [No. 5/2019 Type V].

**Table 3.1:** Sulfate-resistant Portland cement's chemical and key ingredients\*

Oxides composition	Content %	Limits of Iraqi standard No.5/2019
CaO	62.15	---
SiO <sub>2</sub>	19.88	---
Al <sub>2</sub> O <sub>3</sub>	3.5	---
Fe <sub>2</sub> O <sub>3</sub>	4.7	---
MgO	3.23	<5.00
SO <sub>3</sub>	1.84	<2.50
Na <sub>2</sub> O	0.26	
K <sub>2</sub> O	0.51	
L.O.I.	1.25	<4.00
Insoluble residue	0.80	<1.5
Lime Saturation Factor	0.928	0.66-1.02

Main compounds (Bogue's equations)		
C <sub>3</sub> S	54.51	---
C <sub>2</sub> S	18.77	---
C <sub>3</sub> A	1.51	<3.50
C <sub>4</sub> AF	14.14	---
* Chemical analyses were carried out in the Karbala Construction Laboratory.		

**Table 3.2:** Physical characteristics of cement \*

Physical Properties		Test results	Limits of Iraqi standard No.5/2019
surface area (Blaine) m <sup>2</sup> /kg		282	≥250
Setting time (min.)	Initial setting	231	≥ 45
	Final setting	380	≤ 600
Compressive strength, MPa	2-days	23.7	≥10
	28-days	39.68	≥32.5 R
Soundness (Autoclave) %		0.13	≤0.8
* Physical analyses were carried out in the Karbala Construction Laboratory			

### 3.2.1 Fine aggregate

Natural fine aggregate/zone 2 was used according to [IQs No. 45/1984], which is found in Al-Ukhaider region. The fine aggregate grades are shown in Table 3.4. The results demonstrate that the fine aggregate complies with the grading specifications of the Iraqi standard [IQs No. 45/1984]. Table 3.5 also shows other properties of the fine aggregate.

**Table 3.3:** Fine aggregate grading. \*

Sieve size (mm)	Cumulative passing %	Iraqi standard No.45/1984 /zone (2)
10	100	100
4.75	96	90 -100
2.36	83	75 -100
1.18	67	55 – 90
0.6	54	35 -59
0.3	30	8 -30
0.15	3.3	0 -10
<b>Fineness modulus</b>		

**Table 3.4:** Some properties of fine aggregate \*

Physical properties	Test results	Iraqi specification No. 45/1984
Specific gravity (SSD)	2.66	-
Bulk Density (kg/m <sup>3</sup> )	1750	
Sulfate content (%)	0.48	≤ 0.5 %
Absorption (%)	0.63	-
* Properties of fine aggregate were performed by Karbala Construction Laboratory		

### 3.2.2 Coarse aggregate

All normal concrete mixes were made with shattered river gravel from the Al-Nebai area, with a maximum size of 14 mm. **Table 3.6** shows the coarse aggregate grading, which matches the Iraqi standard [IQs No.45/ 1984]. **Table 3.7** shows some other characteristics of the coarse aggregate.

**Table 3.5:** Coarse aggregate grading. \*

Sieve size (mm)	Cumulative passing %	IQS.No.45/1984 grade 5-14 mm
37.5	100	----
25	100	----
20	100	100
14	100	90 - 100
10	77	50 - 85
5	8.6	0 - 10
2.36	2.1	---
* Grading of coarse aggregate was performed by Karbala construction laboratory.		

**Table 3.6:** Some properties of coarse aggregate \*

Physical properties	Test results	Iraqi specification No. 45/1984
Specific gravity	2.73	-
Bulk Density (kg/m <sup>3</sup> )	1625	-
Sulfate content (%)	0.072	≤ 0.1 %
Passing from sieve 75 μm %	0.53	≤ 3 %
Absorption %	0.65	-

\* Properties of coarse aggregate were performed by Karbala construction laboratory.

### 3.2.3 Silica fume

Silica fume is a product of making silicon composite materials in electrical arch kilns. It can be utilized as a complement to cement to make concrete that works well. COMIX's construction company used Mega-Add MS (D) type Densified Micro-silica fume. **Table 3.8** shows the chemical and surface properties of the used silica fume, which are in line with [ASTM C1240/2020].

**Table 3.7:** Chemical characteristics of Silica fume\*

<b>Components</b>	<b>Silica fume %</b>	<b>ASTM C1240/2020</b>
<b>CaO</b>	1.22	
<b>SiO<sub>2</sub></b>	91.05	≥ 85
<b>Al<sub>2</sub>O<sub>3</sub></b>	0.018	
<b>Fe<sub>2</sub>O<sub>3</sub></b>	0.012	
<b>MgO</b>	0.01	
<b>SO<sub>3</sub></b>	0.225	
<b>Na<sub>2</sub>O</b>	0.205	
<b>K<sub>2</sub>O</b>	0.155	
<b>Loss on ignition</b>	2.975	≤ 6
<b>Moisture content</b>	0.68	≤ 3
<b>Activity Index with Portland cement at 7 days</b>	132.4	≥ 105
<b>Percent retained on 45µm (No. 325) sieve, max, %</b>	7	≤ 10
<b>Surface area (Blaine) m<sup>2</sup>/kg</b>	20000	≥ 15000

\*The tests were carried out by Karbala construction laboratory.

### 3.2.4 High-range water-reducing Admixture (HRWR)

**Table 3.9** shows that this additive was made by BASF Company and sold under Glenium 51. It was the third generation of superplasticizers and it meets the requirements of [ASTM C494/2017] type A and F.

**Table 3.8:** Technical description of Glenium 51 \*

Chemical Base	Polycarboxylic ether based
Appearance/colors	Amber homogenous liquid
Density	1.082 - 1.142 kg/liter at 20°C
Chlorine Content%	< 0.1
Alkaline Content%	< 3
Recommended dosage	(0.5 - 1.5) of Binder weight %

\*Giving by data sheet of the manufacturer.

### 3.2.5 Water

Concrete was mixed and cured using Tab water from Kerbala.

### 3.2.6 Steel fibers

The steel fibres were with straight ends and had a micro low-carbon RC 59/13 BN aspect ratio, measuring 13 mm in length, 0.22 mm in diameter, 2,850 MPa in tensile strength, 7.850 g/cm<sup>3</sup> in density and 210 GPa Modulus of elasticity, as shown in **Figure 3.4**.



**Figure 3.1:** Steel Fibers.

### 3.2.7 Steel- Reinforcing Bars

As reinforcing bars, two sizes of deformed bars with nominal diameters of 10 and 6 mm were employed. All of these bars' tensile tests produced the characteristics shown in **Table 3.10**. All values presented are the average of three specimens for each bar diameter. A photograph of the testing machine is shown in **Figure 3.5** The test was performed following the American Standard Specification for Deformed Steel Bars (Abdulkareem and Izzet, 2021). All tests were done at the University of Karbala /civil engineering laboratories.

**Table 3.9:** properties of the used steel reinforcing bars.

Nominal Diameter (mm)	Measured Diameter (mm)	Surface Texture	Cross sectional Area (mm <sup>2</sup> )	Yield Tensile Stress, <i>f<sub>y</sub></i> (MPa)	Ultimate Tensile Strength, <i>f<sub>u</sub></i> (MPa)	Elongation at Ultimate Stress (%)
6	6	deformed	28.3	527.5	583.5	13.2
10	10	deformed	78.5	568.1	706.5	19.6



Figure 3.2: Steel Bar Tensile Machine

### 3.2.8 CFRP Sheets

Carbon fiber sheets were used in the present study for strengthening. **Table 3.11** presents the mechanical properties of CFRP as given by the manufacturer [see **Figure 3.6**].

**Table 3.10:** Mechanical properties of CFRP\*

Product name	SikaWrap®-300 C
Tensile strength (MPa)	4,000
E- modulus (GPa)	230,000
Strain at break (min.) %	1.7
Width (mm)	600
Thickness (mm)	0.167

\* The properties were provided by the manufacturer

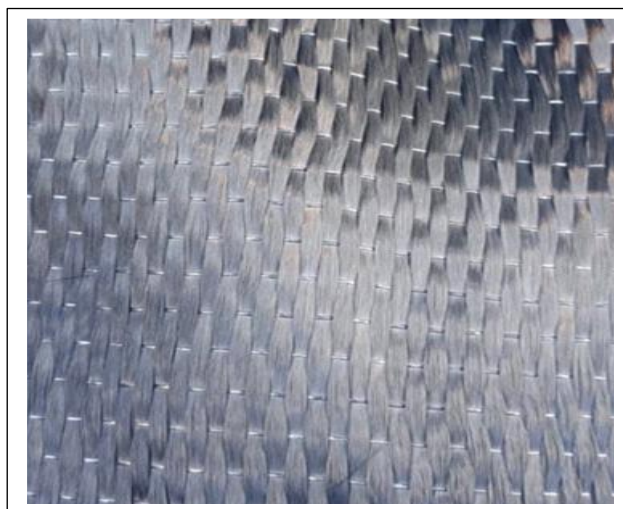


**Figure 3.3:** CFRP Sheets.



### 3.2.9 Epoxy

Epoxy (Sikadur®-330) was used in this study as a bonding material between concrete and CFRP sheet. This adhesive material consists of part A (white) and part B (black), as shown in **Figure 3.7**. These two parts were mixed with a 1B:4A ratio. The mechanical and physical properties of bonding resin are presented in **Table 3.12**.



**Figure 3.4:** Epoxy Material.

**Table 3.11:** Mechanical properties of epoxy resin\*

Product name	Sikadur®-330
Tensile strength (MPa) (7 days)	33.8
E-Modulus (MPa), (7 days)	3,489
Flexural strength (MPa) (7 days)	60.6
Compressive Strength (MPa), (7 days)	77.2
Mixing ratio	1B:4A
Elongation at Break (%), (7 days)	1.2

\* The properties were provided by the manufacturer

### 3.3 Concrete Mixes

Two mixes were used in this study, the first was for the SIFCON while the second was for normal concrete (Liu et al., 2020). **Table 3.13** illustrates the notes of the two mixes.

**Table 3.12:** SIFCON and normal concrete mix proportions.

<i>Mix</i>	<i>Materials, kg/m<sup>3</sup></i>					
	Cement	Silica fume	Fine Agg.	Coarse Agg.	W/B	Superplasticizer % by wt. of binder
<i>SIFCON</i>	872.1	96.9	969	-	0.32	2.4
<i>NORMAL CONCRETE</i>	400	-	720	1072	0.46	-

For every test assigned in the experimental program, several specimens were prepared for each batch to perform the required tests according to the necessary number of specimens required for each test as specified in the related standard test methods.

### 3.4 Preparation and Casting of SIFCON Specimens

As mentioned in Chapter 2, the first step in preparing SIFCON is placing the steel fibers into the molds up to the required volume fraction. The weight of steel fiber to be put in the mold depends on the required volume fraction, the dimensions

of the mold, and, of course, the specific gravity of the steel itself. After filling with steel fibers up to the required volume fraction, the molds were filled with the slurry or mortar matrix, which has to be flowable enough to ensure complete infiltration through the dense beds of fibers in the mold. Usually, vibration during matrix placing was necessary to avoid honeycombing or voids.

The mixing procedures for slurries, followed the requirements of (Standard, 2006). For mortars, the superplasticizer was added separately and gradually during the mixing period.

### **3.5 Mixing of Concrete**

The mixing method is essential to achieve the desired workability and uniformity of normal concrete mix. The mixing procedure was achieved according to [ASTM C192/2006] in a slanting mixer of approximately 0.03 m<sup>3</sup> capacity. Before using the mixer, it must be clean, free from water and moist. Normal concrete was put into a mixer containing coarse aggregate and a small amount of mixing water (a mixture sufficiently pressed with water). At that time, all constituents were mixed until the whole mixture was thoroughly homogenous.

### **3.6 Casting and Curing of Sifcon Specimens**

The types and dimensions of used molds for the present work were as follows:

- Cylindrical steel molds, with a diameter of 100 mm and a height of 200 mm, for splitting tensile strength of SIFCON and normal concrete.
- Steel cubes molds with dimensions of 70 mm for compressive strength of SIFCON slurry and 100 mm for normal concrete.
- Prismatic specimens' molds with dimensions of (30 or 20) × 150 × 1000 mm for the flexural strength of SIFCON.

All molds were kept clean, and the interior faces were wholly oiled to avoid the concrete sticking with molds after hardening. The concrete was poured in two layers and then comped by a tamping rod or vibration machine to remove as much

entrapped air as possible. At that moment, the top surfaces of the specimens were troweled. The specimens were covered with polyethylene sheets for 24 hours to avoid the loss of mixing water and moisture from the top surface and to prevent plastic shrinkage cracking. Finally, the specimens were de-molded and immersed in tap water until the test. The curing program for previous concrete was 7 and 28 days of water curing.

Control specimens (cubes, prisms and cylinders) were divided into four groups according to the percent of added steel fibers, as shown in Table 3.14.

**Table 3.13:** Control specimens tests details.

Specimens	Mould' Dimensions (mm)	Percent of steel fibers (%)	No. of specimens	Test type
Cube for concrete	100	0	3 3	Compressive strength 7 and 28 days
Cube for SIFCON	70	0	3 3	
		2	3 3	
		4	3 3	
		6	3 3	
Cylinder for concrete	100×200	0	3 3	splitting tensile strength 7 and 28 days
Cylinder for SIFCON		0	3 3	
		2	3 3	
		4	3 3	
		6	3 3	
Prism for SIFCON	20×150×1000	2	3	Flexural strength 7 days
		4	3	
		6	3	
	30×150×1000	2	3	
		4	3	
		6	3	

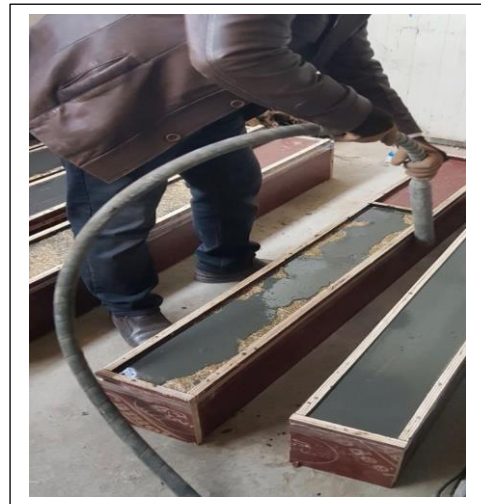


Figure 3.5 Wooden prismatic specimens' moulds

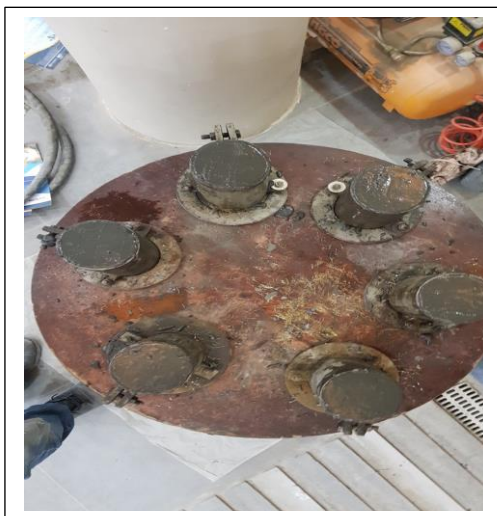


Figure 3.6 Control Specimens Proportion

### 3.7 Slump Test

A slump test was carried out according to [ASTM C143/2008 ]. It is mostly used to determine the workability of a specific batch of concrete. In practically uniform concrete, the value of slump measurement should not vary by more than about 25 mm within a batch.



Figure 3.7 slump test

## 3.8 Testing Hardened Concrete

### 3.8.1 Compressive Strength

Compressive strength was obtained according to [BS EN 12390/2019] by using a usual hydraulic digital "ELE machine of 2000 kN capacity" at a rate of loading about 0.3 MPa each second. The cubes have the dimensions of 70mm for the compressive strength of SIFCON slurry and 100mm for normal concrete. The mean compressive strength was calculated using the average compressive strength of three cubes **Figure (3.11)** shows the compressive strength test.



Figure 3.8: Concrete compressive Test Machine.

### 3.8.2 Splitting Tensile Strength

The splitting tensile strength was measured according to (Standard, 2006) [ASTM C496/2017]. A testing machine hydraulic digital "ELE machine of 2000 kN capacity" was used to load 100×200mm cylinders constantly up to failure. The mean tensile strength was calculated using three cylinders for the average splitting tensile strength **Figure (3.12)** shows the splitting tensile strength test

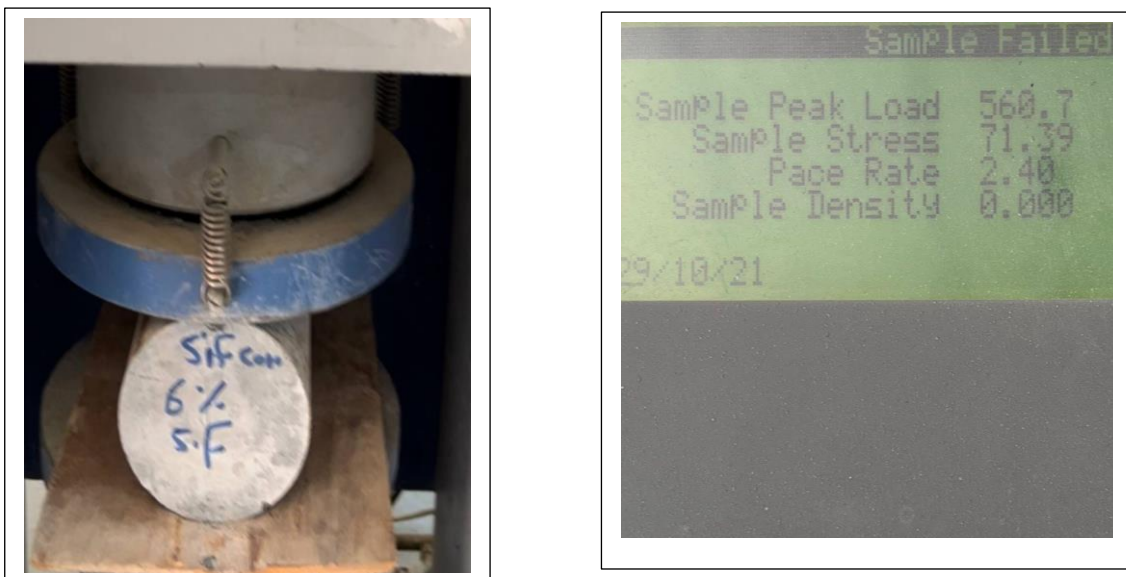
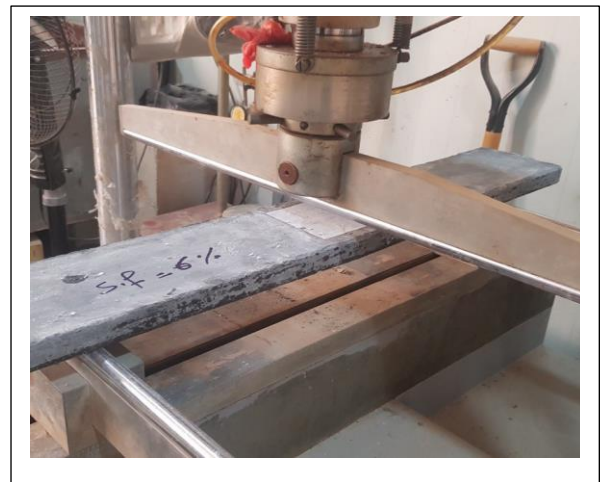
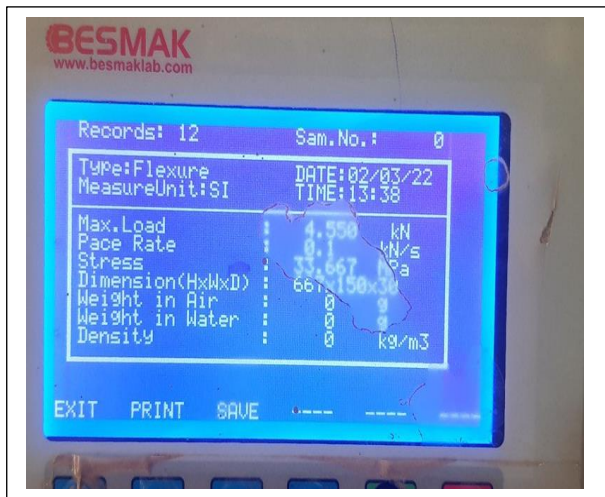


Figure 3.9: Splitting Tensile Strength Test.

### 3.8.3 Flexural Strength of SIFCON

As showed the flexural strength was measured using a digital hydraulic testing machine "ELE machine of 2000 kN capacity", to load prismatic specimens of  $(30 \text{ or } 20) \times 150 \times 1000 \text{ mm}$  (for the flexural strength of SIFCON slurry) constantly up to failure. The mean flexural strength was calculated using the average flexural strength of three specimens **Figure (3.13)** shows SIFCON flexural strength test.



**Figure 3.10:** SIFCON Flexural Strength Test

### 3.9 Molds and Reinforcement

To cast the tested beams specimens, wooden molds were fabricated and built. The molds were made of 22 mm thick plywood, and their side pieces are connected by using steel bolts that can be readily removed after casting to take off the hardened beams. Before the reinforcement cages were installed, the molds were cleaned and oiled. **Figure 3.14** illustrates how longitudinal and transverse steel bars have been placed and connected using steel wire of 2mm diameter. The reinforcing bars were previously prepared, and the reinforcing cage was then put in the wooden mold directly with bottom concrete cover of (20mm) and side concrete cover of (20mm).



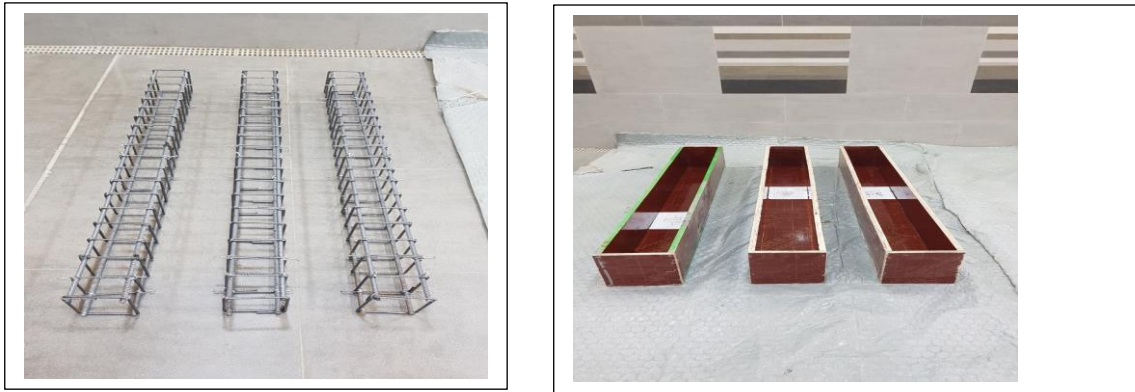


**Figure 3.11** Wooden molds and Steel Reinforcement Details.

After completing the mixing process, each beam was cast in two layers. The fresh concrete was placed in the mold, and the layer was compacted for a sufficient time using a laboratory rod vibrator after the lower layer of SIFCON. The vibration continued for the second layer. A steel trowel was used for levelling and finishing the concrete surface. Polyethylene (Nylon sheet) was used to cover the molds to avoid cracks associated with water-loss shrinkage. All concrete beam specimens' and the control specimens were removed after (1-2) days of casting date. The curing process was done using a damp canvas and continuous water soaking to ensure a good curing treatment for 28 days. **Figure 3.15** shows the cast of the concrete for each specimen.

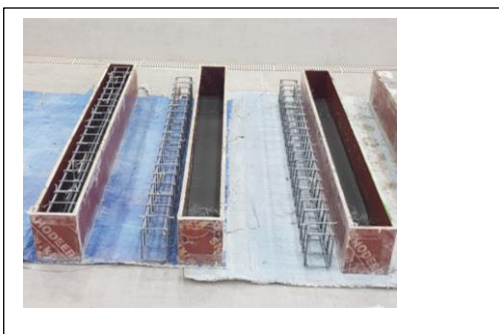
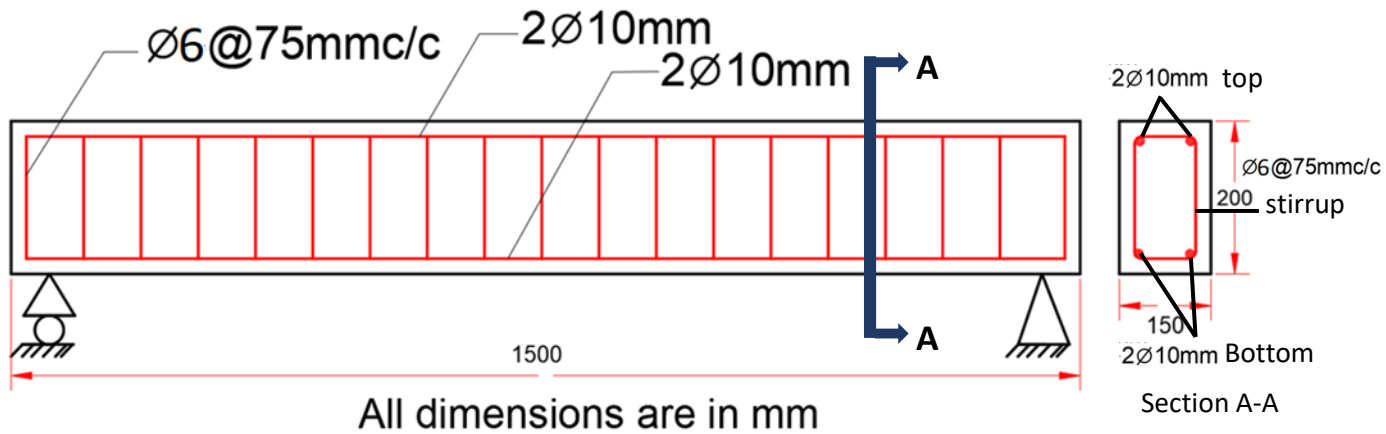


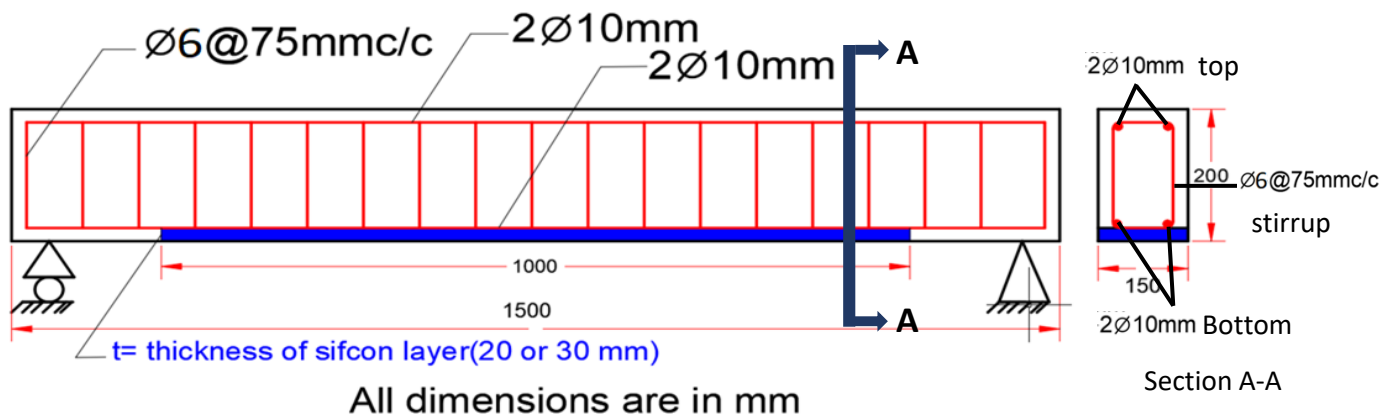
**Figure 3.12:** Beam Specimens Cast process

### 3.10 The Experimental Program

Two mixtures were utilized in this research in which the first was the SIFCON, while the second was for normal vibrated concrete (NVC). The experimental program entailed testing fourteen reinforced concrete beams constructed as beams tested until they fail for the comparison of the results. All beams were of identical size and reinforcement. They were 1500 mm in length, 1400 mm as an effective span, 150 mm in width, and 200 mm in height. All specimens were tested under two-point loads. The beams were designed using the minimum requirements of steel reinforcement according to ACI (318-19) [ACI 318, 2019] (For more details, see Appendix A). The primary reinforcement consisted of 2Ø10 mm as top reinforcement and 2Ø10 mm as bottom reinforcement, one at each corner. At the same time, the stirrups started at a distance of 20 mm from both ends and they were spaced at 75 mm, as shown in **Figure 3.1**. Specimens are divided into five groups; the first group (A), which is the reference group consists of two beams without SIFCON, one of which is strengthened with CFRP sheets and the other of which is not. The second group (B) is made up of three beams, each of which has a 20 mm-thick SIFCON layer but is not reinforced with CFRC sheets. On the other hand, the third group (C) consists of three beams, containing SIFCON layer that is 30mm thick but are not strengthened with CFRP sheets. The fourth group (D), which consists of three beams, are strengthened with sheets of CFRP and contain SIFCON with a 20mm thickness. Finally, the fifth group (E), which consists of three beams, are strengthened with CFRP sheets and contain SIFCON of 30mm thickness. As shown in **Table 3.1**. **Figure 3.2** shows the preparation and casting of the SIFCON layer, while **Figure 3.3** shows the CFRP external strengthening of the tested beams.



**A-without SIFCON**



**b-with SIFCON**

**Figure 3.13** Schematic Layout of Beams and Details of Steel Reinforcement

**Table 3.1** shows the details of the tested beams, where the letters A, B, C, D and E represents the beams, and the number 20 or 30, implies the thickness of the SIFCON layer. Indeed, the subsequent symbols, 2, 4, and 6, refer to the percentage of steel fibers. The subsequent symbol N represent normal concrete and the last subsequent symbol F, shows whether using CFRP or not.

**Table 3.14:** Details of Tested Beam Specimeance

<b>Group</b>	<b>Beam Designation</b>	<b>SIFCON thickness (mm)</b>	<b>Steel fibers (%)</b>	<b>Existing of CFRP</b>	<b>Length of CFRP (cm)</b>
1 (Ref.)	A-N	-	-	None	-
	A-NF	-	-	with	70
2	B20-2	20	2	None	-
	B20-4	20	4	None	-
	B20-6	20	6	None	-
3	C30-2	30	2	None	-
	C30-4	30	4	None	-
	C30-6	30	6	None	-
4	D20-2F	20	2	with	70
	D20-4F	20	4	with	70
	D20-6F	20	6	with	70
5	E30-2F	30	2	with	100
	E30-4F	30	4	with	100
	E30-6F	30	6	with	100

### 3.10.1 The mechanism used to prepare the Sifcon mixture

In the beginning, we start by preparing the amount of carbon fiber (steel fiber) as a volumetric ratio of 2%, 4%, and 6% of the sifcon layer in the lower part of the concrete beams. Then we prepare (slurry) which consists of cement and silicafume, mixed well at first, then we prepare the water that is mixed with 2% of the superplasticizer, and we gradually add the water and the superplasticizer together to the mixture of cement and silicafume, to reach a completely homogeneous mixture without any lumps or voids.

After that, we define a length of 100 cm with wooden barriers that prevent the infiltration of the swordcon from the outside and symmetrically in the middle at the bottom of the wooden template. So that we pour the first layer of (slurry) at the bottom of the mold so that it covers all the space and with a thickness of between 2-3 mm, then we cover this layer with a homogeneous and similar layer of carbon fiber (steel fiber) so that we ensure its spread and penetration well and homogeneously in the mortar through the use of Manual brush or table vibrator to ensure full penetration of the carbon fibers, by repeating this process 5-6 times to reach the required thickness of the sifcon layer 20-30 mm.



**Figure 3.14: Preparation and Casting of SIFCON Layers**

### 3.10.2 External Strengthening with CFRP Sheets

A mechanism for strengthening concrete beams using CFRP after applying under monotonic two point loads on the reinforced concrete beams in the structural concrete laboratory at the University of Karbala for both groups D and E, and loading them up to the service load, which was calculated from dividing the failure load by 1.7, and after cleaning the concrete beams from dust well, the epoxy material (sikadure-330) was prepared with a percentage Mix 4 A to 1 B according to the specifications shown in the details of this product. Then the lower outer surface of group D was coated with a length of 70 cm of carbon fiber (CFRP). Then the same steps were repeated with group E, but with a length of 100 cm of carbon fiber (CFRP). After that, the carbon fiber reinforced concrete beams were left for 7 days to harden according to the standard specifications shown in the data sheet.



Figure 3.15 External Strengthening with CFRP sheets of Tested Beams

### 3.11 Beam Test

Deflection and crack width at each load step were measured in this study to predict the behavior of reinforced concrete beams under 2 points of monotonic loading.

#### 3.11.1 Deflection Measurements

One type of deflection measurement was used: linear displacement sensor (LVDT-KTR-50mm) used to find the deflections at mid span and under the point load.

#### 3.11.2 Strain Indicator

A multi-channel data logger is used to measure strain, as shown in **Figure 3.15**. This device consists of 11 channels for strain gauges and four channels for LVDT-KTR-50 mm, which means 15 channels were provided. The operating software of the strain indicator permits recording the channel's reading every five seconds; this facility assists in obtaining a proper estimation of the behavior of the concrete surface under consideration.

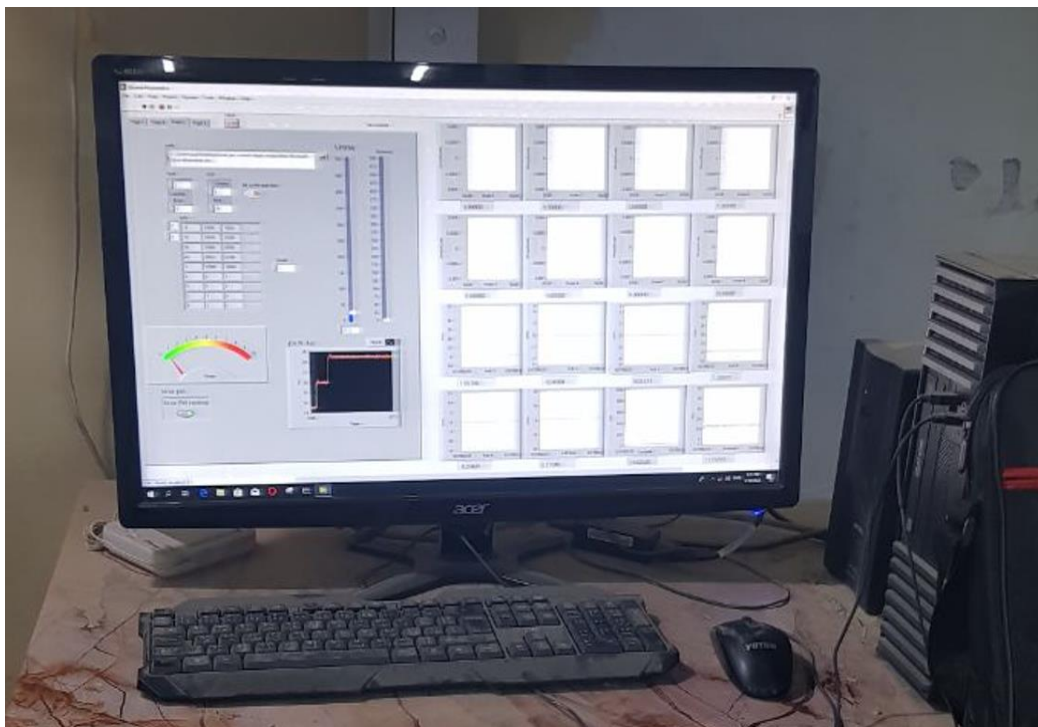


**Figure 3.16:** Strain Indicator Device and Software Interface Window.

### 3.11.3 Microscopic Observation

One of the serviceability requirements for structural concrete members is crack width. Because of concrete's poor tensile strength, cracks in reinforced concrete members are to be expected under service loads. Controlling cracking is critical for achieving a good look and ensuring the long-term durability of concrete buildings. A high-resolution microscope with a lens that magnifies and clarifies the micro-cracks up to 10 times was utilized; this high-resolution microscope runs via an adjustable light source powered by high-power batteries. **Figure 3.16** depicts the tiny crack meter device.



**Figure 3.17:** Crack Meter Microscopic Device.

### 3.12 Loading Test Setup

The test setup was installed at the structural laboratory in the Department of Civil Engineering / College of Engineering / University of Kerbala. The test was carried out with a frame in load-control mode, measuring 5.5 m in width and 3m in height. A steel frame of the I-section was fixed at the load frame by welding and bolts to support and carry the crane, which is used for lifting and positioning the tested beams. **Figure 3.17** illustrates a schematic depiction of the specimen's test setup. The positioning was then maintained by applying a modest pre-load. Up to a



load intensity of 30 kN, the load was applied in 5.0 kN increments, and for greater loads, the load was applied in 2.5 kN increments. The time of each loading increment consisted of 10 min/stage. A load cell was used to record the applied load, and LVDT-KTR-50 mm was used to record the vertical deflections beneath the load and at mid-span.

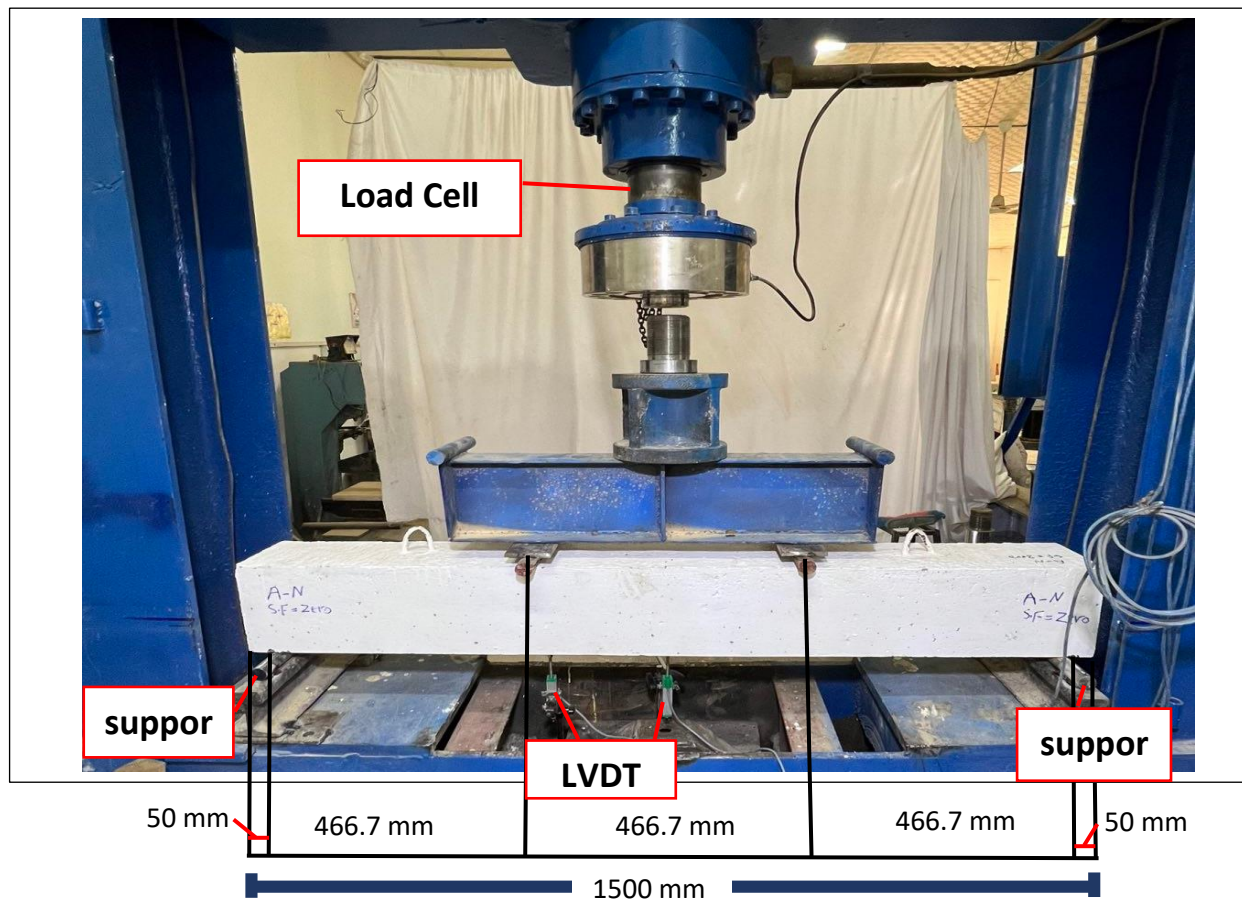
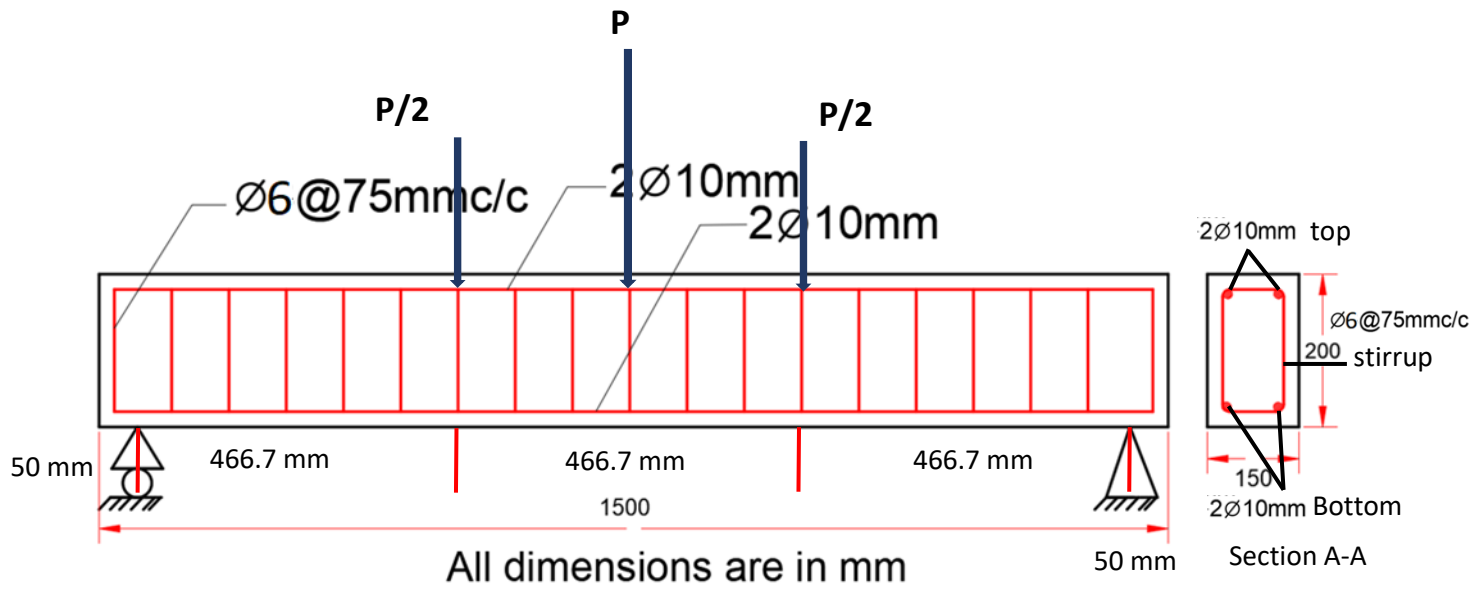


**Figure 3.18:** Test Setup.



# Chapter four

## Experimental Results and Discussion

### 4.1 Introduction

Fourteen reinforced concrete (RC) beams were designed as simply supported beams constructed using SIFCON concrete. This chapter discusses the results of fourteen beams that are defined as reference beams (without SIFCON; one with CFRP sheets and the other without CFRP) tested under monotonic loads. Various factors, such as the percentage of added steel fibers, CFRP sheets, and thickness of the SIFCON layer, will be compared to understand the impact of the various variables on the behavior of studied RC beams. For the tested beams, the experimental results have been presented. Observation of load against deflection under monotonic load tests, ductility factor, crack pattern, and failure mechanism are all important considerations for each specimen. Crack propagation was documented using images following the monotonic load test, and the cracks were labelled as the loading progressed. And in order to investigate the effect of steel fibers on the compressive strength and the flexural strength of SIFCON concrete, other specimens were examined and separated into four main groups according to the percentage of steel fibers.

### 4.2 Test Results of Control Specimens

#### 4.2.1 Compressive Strength

Test results indicated that the compressive strength of normal concrete ( $f_{cu}$ ) was 28.56 and 39.68 MPa for specimens aged 7 and 28 days, respectively. **Table 4.1** shows the compressive strength values for SIFCON with different percentages of steel fibers. It can be concluded from **Table 4.1** that the percentage of steel fiber has an impact on the compressive strength; the increase in the percentage of steel fiber led to an increase in the compressive strengths by about (18, 39, and 73%) for

the added steel fiber percentage of 2, 4 and 6% concerning the reference specimen for age seven days, respectively. Indeed, the increase in the percentage of steel fiber has a significant effect on the compressive strength ( $f_{cu}$ ) at a later age as the increase of the percentage of steel fiber increased the compressive strengths by about (30, 55, and 77%) for the added steel fiber percent of 2, 4 and 6% concerning the reference specimen for age 28 days respectively. **Figure 4.1** shows the impact of added steel fiber percentage on compressive strength at various ages. The compressive strength ratio for SIFCON specimens with the age of 7 days to the specimens with the age of 28 days, was about 70% regardless of the percentage of added steel fibers.

**Table 4.1:** compressive strength test of SIFCON.

Specimen's age (day)	Steel fibers (%)	$f_{cu}$ (MPa)	Increase in strength (%)
7	0	35.38	Ref.
	2	41.70	18
	4	49.31	39
	6	61.22	73
28	0	48.36	Ref.
	2	62.80	30
	4	74.75	55
	6	85.58	77

\*Average of three specimens

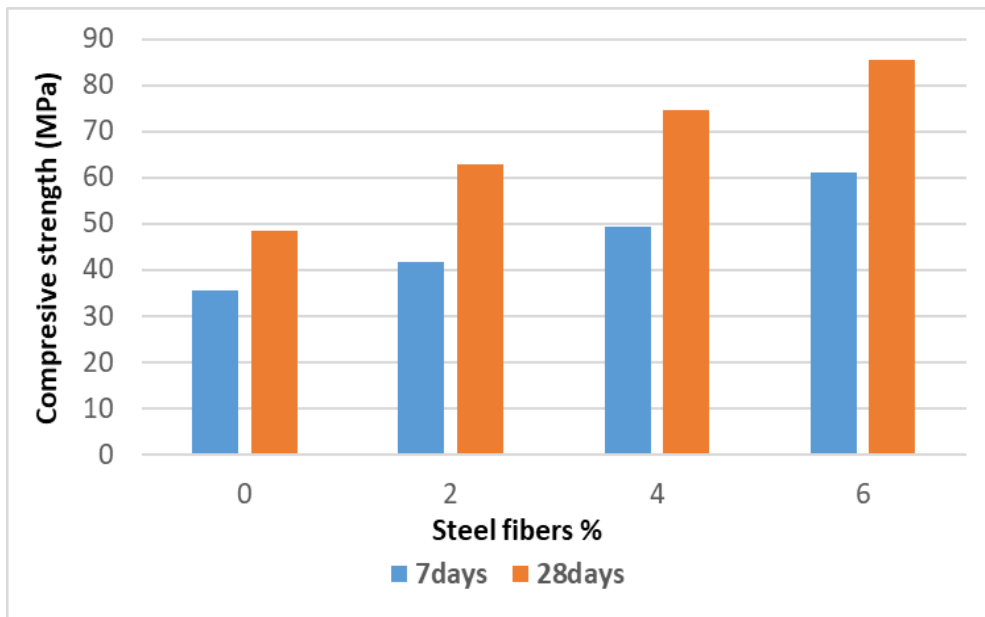


**Figure 4.1:** Effect of Steel Fiber percentage on the compressive strength at various ages.

#### 4.2.2 Splitting Tensile Strength

Test results indicate that concrete's splitting tensile strength ( $FSP$ ) was 3.36Mpa and 3.48Mpa for specimens aged 7 and 28 days, respectively, as shown in **Table 4.2**, which shows the splitting tensile strength values for SIFCON with different percentages of steel fibers. It can be concluded from **Table 4.2** that the percentage of steel fiber has an important impact on the splitting tensile strength ( $FSP$ ); for the increase of the percentage of steel fiber increased the splitting tensile strengths by about (129, 206, and 299%) for the added steel fiber percentage of 2, 4 and 6% concerning the reference specimen for age seven days respectively. Additionally, the increase of the percentage of steel fiber increased the splitting tensile strengths by about (160, 313, and 417%) for the added steel fiber percent of 2, 4 and 6% concerning the reference specimen for age 28 days, respectively. **Figure 4.2** shows the effect of steel fiber percentage on splitting tensile strength at various ages.

**Table 4.2** splitting tensile strength test results of SIFCON.

Specimen's age (day)	Steel fibers (%)	$f_{ct}$ (MPa)	Increase in strength (%)
7	0	3.36	Ref.
	2	7.70	129
	4	10.27	206
	6	13.40	299
28	0	3.48	Ref.
	2	9.06	160
	4	14.36	313
	6	18.00	417

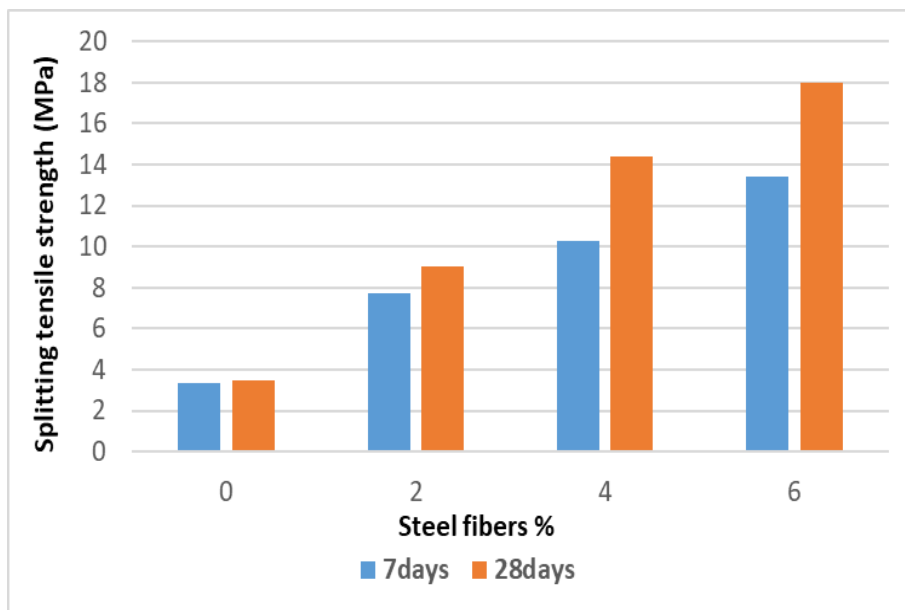


**Figure 4.2:** Effect of Steel Fiber percentage on splitting tensile strength at various Ages.

### 4.2.3 Flexural ultimate force

**Table 4.3** shows the flexural strength test result for SIFCON with different percentages of steel fibers, knowing that the flexural strength of SIFCON slurry without steel fibers was very feeble, and all specimens of this test were at the age of 7 days. **Table 4.3** indicates that the percentage of steel fiber impacts the ultimate flexural force. The increase of the percentage of steel fiber increased the ultimate flexural force by about (16 and 30%) for the added steel fiber percent of 4 and 6% concerning the reference specimen of 2% for SIFCON specimens with a thickness of 30mm, respectively. In contrast, the increase of the percent of steel fiber increased the ultimate flexural force of SIFCON by about (20 and 40%) for the added steel fiber percent of 4 and 6% concerning the reference specimen of 2% for SIFCON specimens with a thickness of 20mm respectively. Also, the ratio of the ultimate flexural force of SIFCON plates with 30mm thickness to the plates with 20 mm was 1.71, 1.66, and 1.59 for the added steel fiber percentage of 2, 4, and 6%, respectively. **Figure 4.3** shows the impact of steel fiber percentage on the ultimate flexural force at various thicknesses of SIFCON plates.

**Table 4.3:** flexural ultimate force test results of SIFCON plates.

SIFCON thickness (mm)	Steel fibers (%)	Flexural ultimate force, $P_{ult}$ (kN)	% of the increase in $P_{ult}$	The ratio of $P_{ult}$ of 30/20mm
30	2	3.5	Ref.	1.7
	4	4.06	16	1.66
	6	4.55	30	1.59
20	2	2.05	Ref.	-
	4	2.45	20	-
	6	2.87	40	-

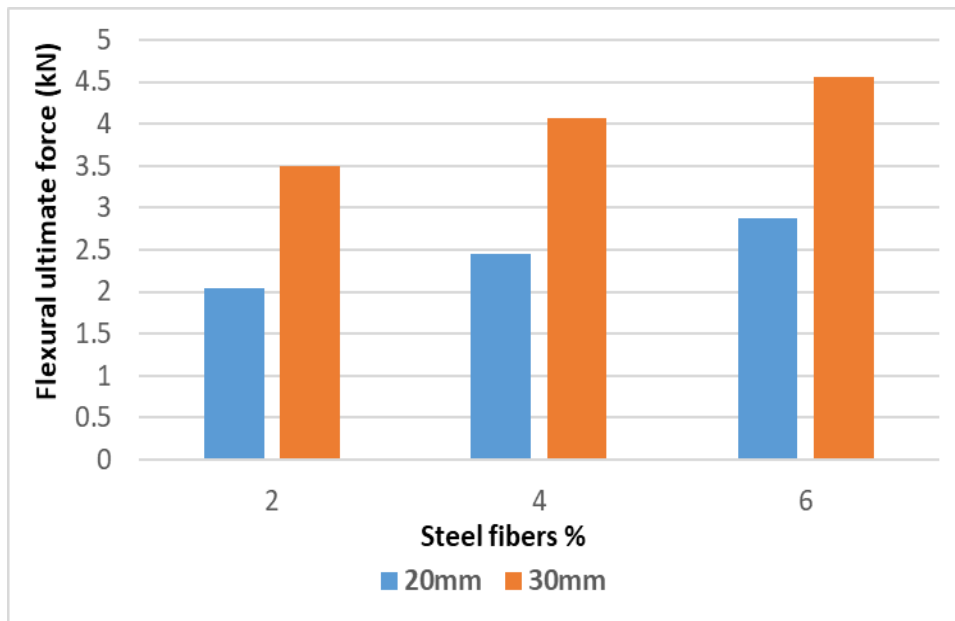


**Figure 4.3:** Effect of Steel Fiber percentage on the ultimate flexural force at various thicknesses of SIFCON Plates.

### 4.3 Crack Behavior and Failure Modes of Rc Beams

The crack formation was monitored throughout testing to assess the behavior of the strengthened specimens compared with the behavior of unstrengthened control beams, contrasting how different specimens react depending on the percentage of steel fibers, the thickness of SIFCON layer, and the length of CFRP. However, this study focused on how the sheets came apart. The cracks that led to the sheets falling will be discussed later. The following sections show the first cracking load, cracking patterns, and crack widths at ultimate loads for all specimens.

#### 4.3.1 First Crack Loads and Crack Patterns

**Table 4.4** depicts the results of the tests on the cracking loads and the ultimate loads. The first crack happened when the load (18–34 kN) was put on all of the specimens, with various first crack loads ( $P_{cr}$ ) / ultimate load ( $P_u$ ) percentage about (28 to 40 %) as shown in **Table 4.4**. This study found that extending the length of CFRP sheets decreases the  $P_{cr}/P_u$  % while increasing the amount of steel fibers likewise raises the  $P_{cr}/P_u$  percentage, with the intention of increasing the

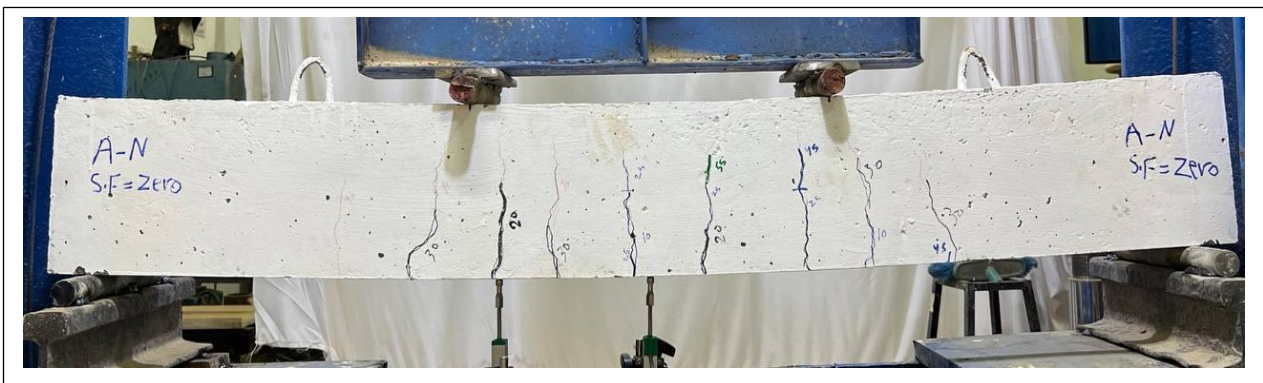


SIFCON thicknesses. When the tensile stresses in the bottom fiber of the concrete surpassed the concrete's modulus of rupture, the first flexural crack (maximal moment) appeared in the middle third of the beam. Then, cracks slowly grew along the beam's edges in the same direction as the support. At some points, more flexural cracks showed up and spread on both sides of the first crack facing the supports. When the beam broke, the cracks moved to the sides of the beam and then to the cord that held the beam together. Fractures were found in the middle third of the beam, but there were no cracks near the supports or the maximum load, which is true for all un-strengthened beams.

It was also seen that those beams didn't get any shear cracks that worked. The beams that are strengthened on the outside failure are known in a process called 'intermediate flexure crack-induced debonding failure.' The pattern of cracks in the tested specimens is shown on **Figure 4.4** to **4.17**. Adding more steel fibers has a small effect on the pattern of cracks. From these plates, it's clear that flexural cracks are roughly parallel, and it's also clear that the crack patterns for the un-strengthened beam and the externally strengthened beam behave about the same. It is obvious from **Figure 4.12** to **4.17** that the failure type of beams with CFRP changes from flexural to shear or (shear-flexural) failure.

**Table 4.4:** Cracking and ultimate loads of tested beams specimens.

Group	Beam ID	Cracking- Load (P <sub>cr</sub> )  (kN)	Increase in Cracking- Load  (%)	Ultimate -Load (P <sub>u</sub> )  (kN)	P <sub>cr</sub> /P <sub>u</sub>  (%)
A (Ref.)	A-N	18	Ref.	63.98	28
	A-NF	20	11	68.59	29
B	B20-2	22	22	70.46	31
	B20-4	28	56	78.13	36
	B20-6	33	83	83.37	40
C	C30-2	25	38	73.52	34
	C30-4	29	61	80.10	36
	C30-6	34	89	85.00	40
D	D20-2F	20	11	72.10	28
	D20-4F	28	56	80.10	35
	D20-6F	32	78	84.80	38
E	E30-2F	25.5	42	77.30	33
	E30-4F	30	67	85.00	35
	E30-6F	34	89	88.60	38

**Figure 4.4:** Cracking Pattern of Specimen A-N.



**Figure 4.5:** Cracking Pattern of Specimen A-NF.

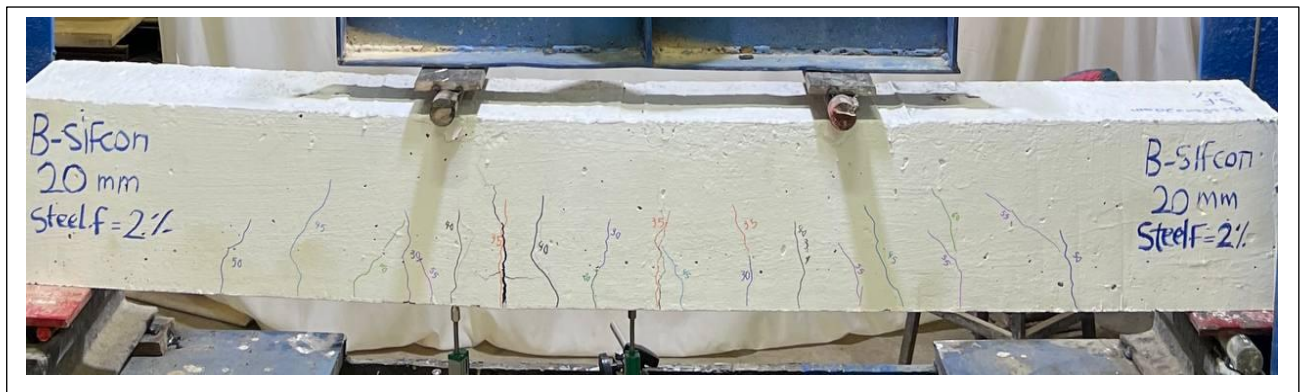


**Figure 4.6:** Cracking Pattern of Specimen B20-2.



**Figure 4.7:** Cracking Pattern of Specimen B20-4.



**Figure 4.8:** Cracking Pattern of Specimen B20-6.



**Figure 4.9:** Cracking Pattern of Specimen C30-2.



**Figure 4.10:** Cracking Pattern of Specimen C30-4.



Figure 4.11: Cracking Pattern of Specimen C30-6.



Figure 4.12: Cracking Pattern of Specimen D20-2F.



Figure 4.13: Cracking Pattern of Specimen D20-4F.



Figure 4.14: Cracking Pattern of Specimen D20-6F.



**Figure 4.15:** Cracking Pattern of Specimen E30-2F.



**Figure 4.16:** Cracking Pattern of Specimen E30-4F.



**Figure 4.17:** Cracking Pattern of Specimen E30-6F.

### 4.3.2 Failure Modes

Under flexural loads, the reference beam specimen (A-N) and all beams without CFRP worked as expected. The tensioned steel reinforcing yielding caused the failure, and the concrete in the middle of the span was crushed. The reference beam specimens A-N and A-NF were used as a starting point to compare the remaining strengthening beam specimen.

One kind of failure mode occurred in the CFRP-strengthened specimens. The intermediate flexure crack-induced debonding failure occurred in all strengthened

beams. The failure modes for the tested beam specimens strengthening with CFRP research sheets (Hawileh et al., 2014) showed different local and global failure characteristics, including concrete crushing, flexural cracks, debonding, and delamination. As shear failure also happened in SIFCON specimens made of CFRP.

### 4.3.3 Width of Crack

**Table 4.5** demonstrates the width of cracks at the maximum static load test for all tested beams without CFRP. The percentage reduction in maximum crack width was 6, and 22% for specimens B20-2 and C30-6 concerning the reference specimen A-N, respectively. **Table 4.6** demonstrates the width of cracks at the maximum of static load test for all examined beams with CFRP. The percentage reduction in maximum crack width was 3.3 and 20% for specimens D20-2F and E30-6F concerning the control beam A-NF respectively. It's obvious that increasing the added external CFRP sheets length decreases the maximum width of the crack at the ultimate load, and increasing the added steel fibers percentage decreases the maximum width of the crack at the ultimate load. Also, increasing the SIFCON thickness decreases the maximum width of the crack at the ultimate load.

**Table 4.5:** Crack width at ultimate loads of unstrengthen beams specimens.

Beam Designation	Ultimate cracks width (mm)	decreasing in Ultimate cracks width, (%)
A-N	3.2	Ref.
B20-2	3.0	6.00
B20-4	2.8	12.5
B20-6	2.6	19.0
C30-2	2.9	9.00
C30-4	2.7	16.0
C30-6	2.5	22.0
A-NF	3.0	Ref.
D20-2F	2.9	3.30
D20-4F	2.7	10.0
D20-6F	2.5	16.7
E30-2F	2.8	6.70
E30-4F	2.6	13.3
E30-6F	2.4	20.0

#### 4.4 Load-Deflection curves of RC Beams

The vertical displacement deflections at the middle of the span and the point load were documented at each increment of the load of the beam test. The service and ultimate deflections of beams were studied. Because the load behavior after the peak could not be controlled in any tested beams, the data in **Figures 4.4 to 4.17** finish at the failure load and the associated deflection value. The selected serviceability limit was the ultimate experimental load divided by 1.7, as indicated by various studies (Mansur et al., 1992) because there was no undesired breaking or deformation at this point.

In general, whenever a beam is loaded incrementally, at first, the deflection will increase at a constant rate (elastic region), then after (generation and development of cracks), the deflection will increase at a faster rate and continue to grow until yielding tension steel reinforcement, after which the slope of the curve will decrease. The test will be terminated when the deflection increases without an



increase in the applied load. **Figures 4.4 to 4.17** illustrate the load-deflection behavior for each tested beam's two points (middle of the span and the point load).

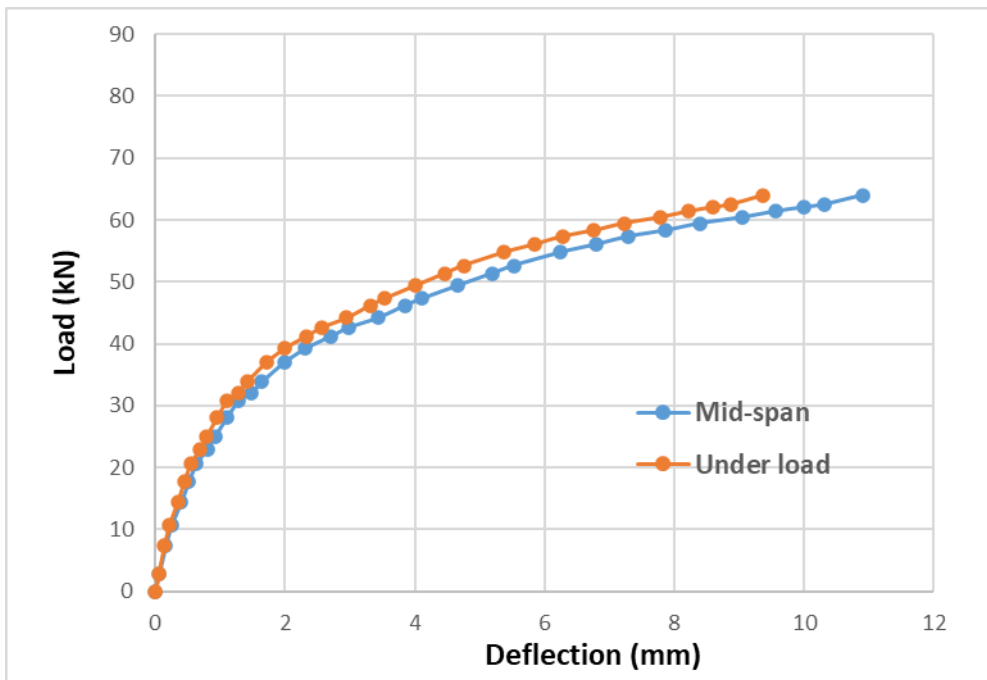


**Figure 4.18:** Load Deflection Curves for Beam A-N

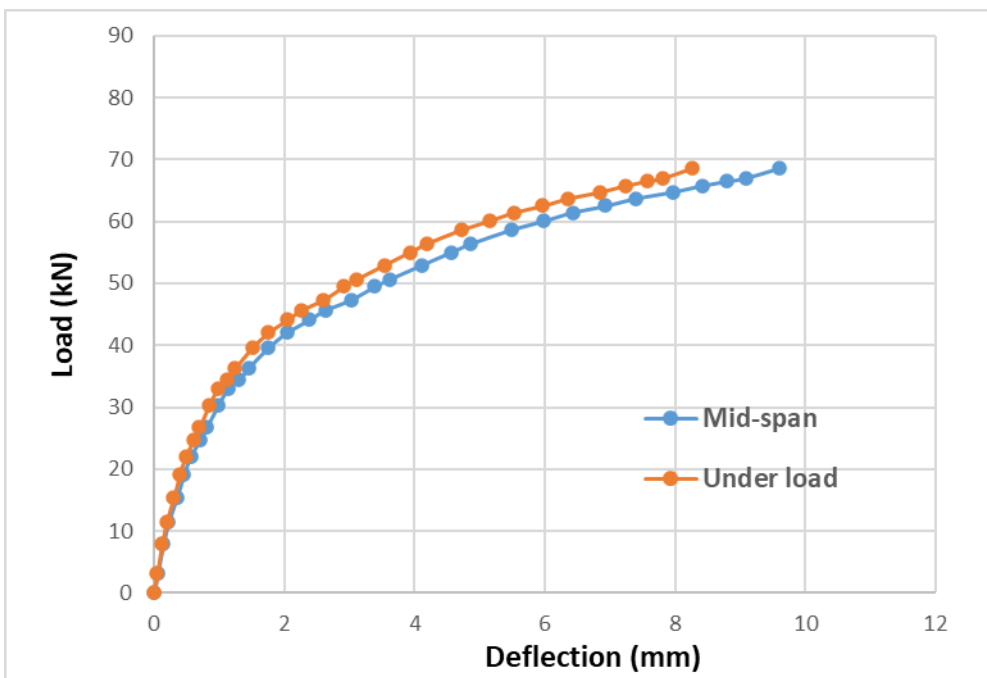


**Figure 4.19** Load Deflection Curves for Beam A-NF

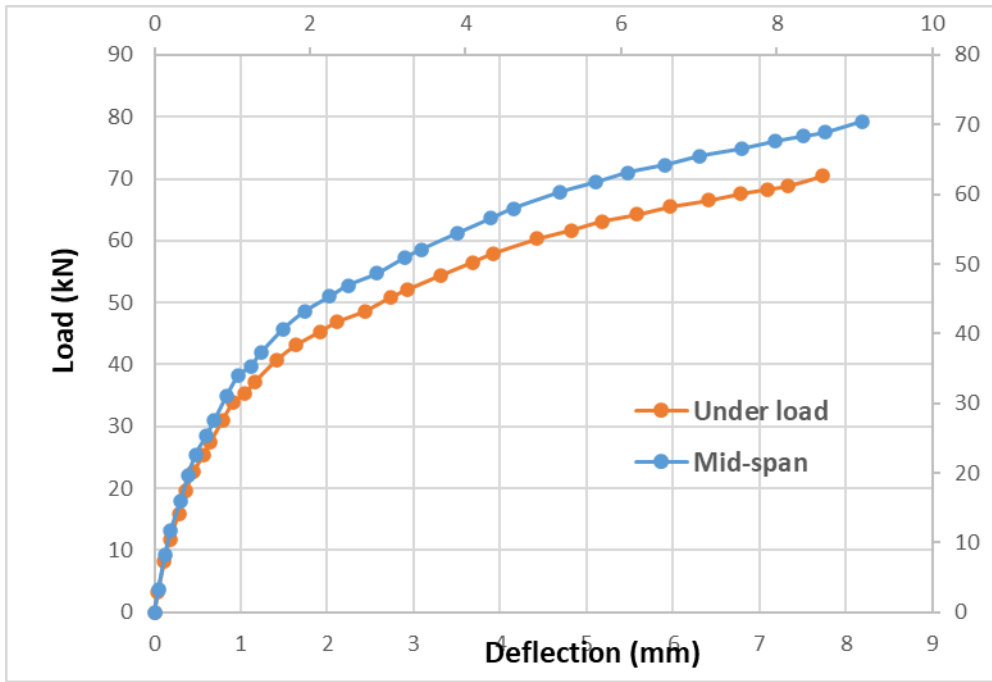


Figure 4.20: Load Deflection Curve for Beam B20-2.

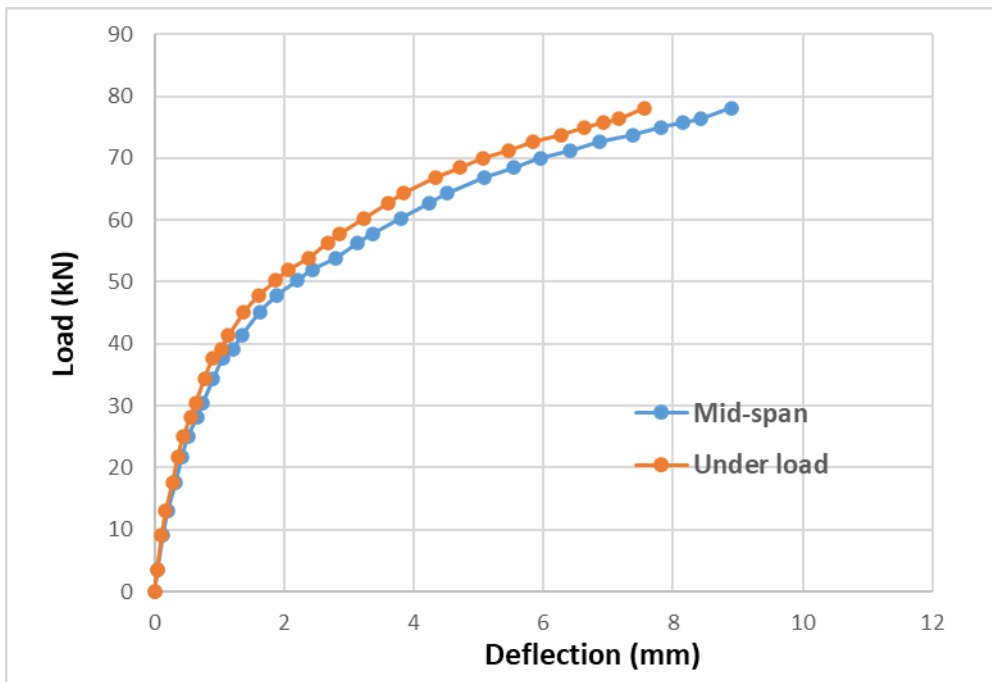


Figure 4.21: Load Deflection Curve for Beam B20-4.

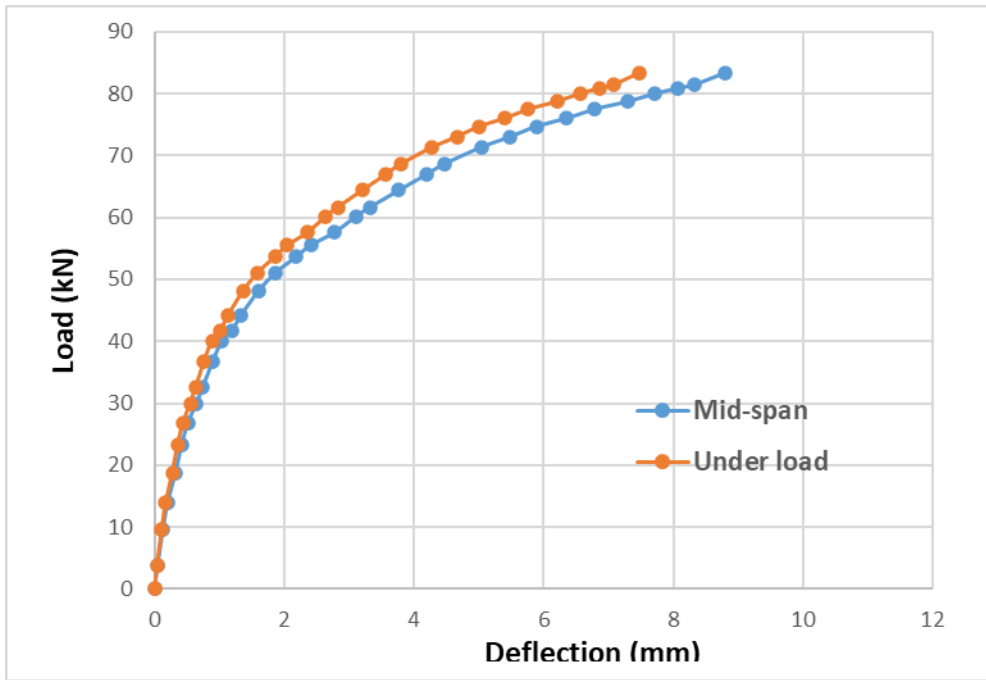


Figure 4.22: Load Deflection Curve for Beam B20-6.

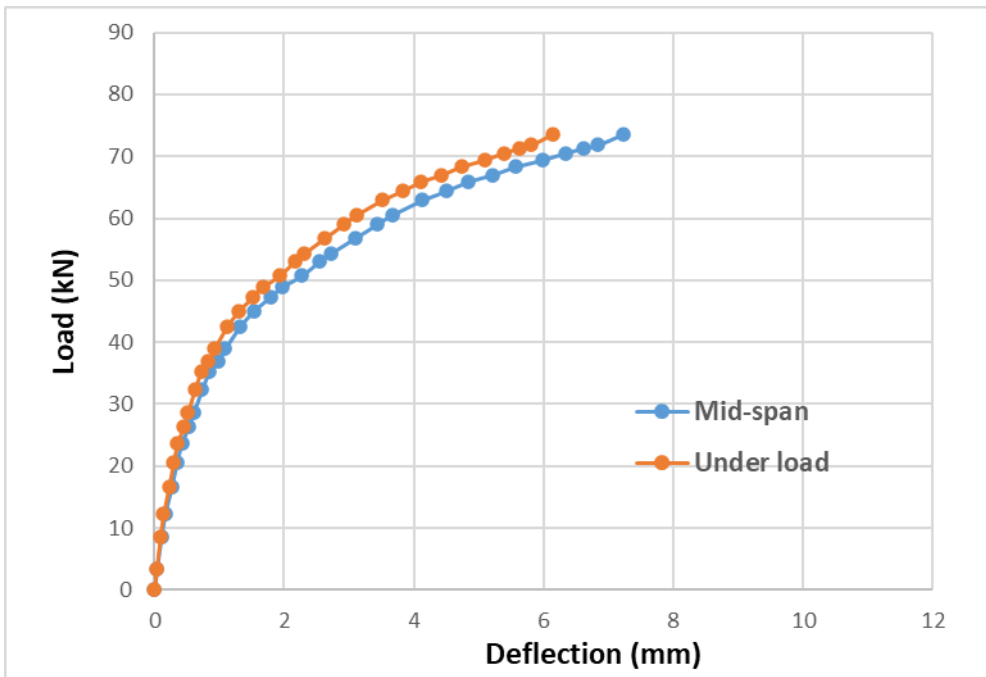


Figure 4.23: Load Deflection Curve for Beam C30-2.

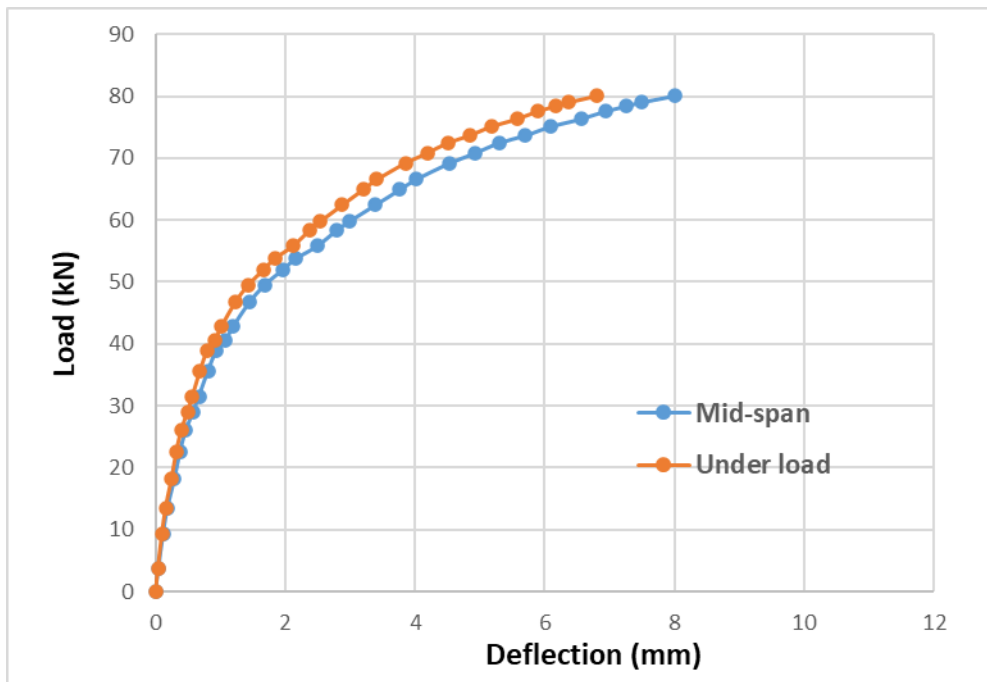


Figure 4.24: Load Deflection Curve for Beam C30-4.

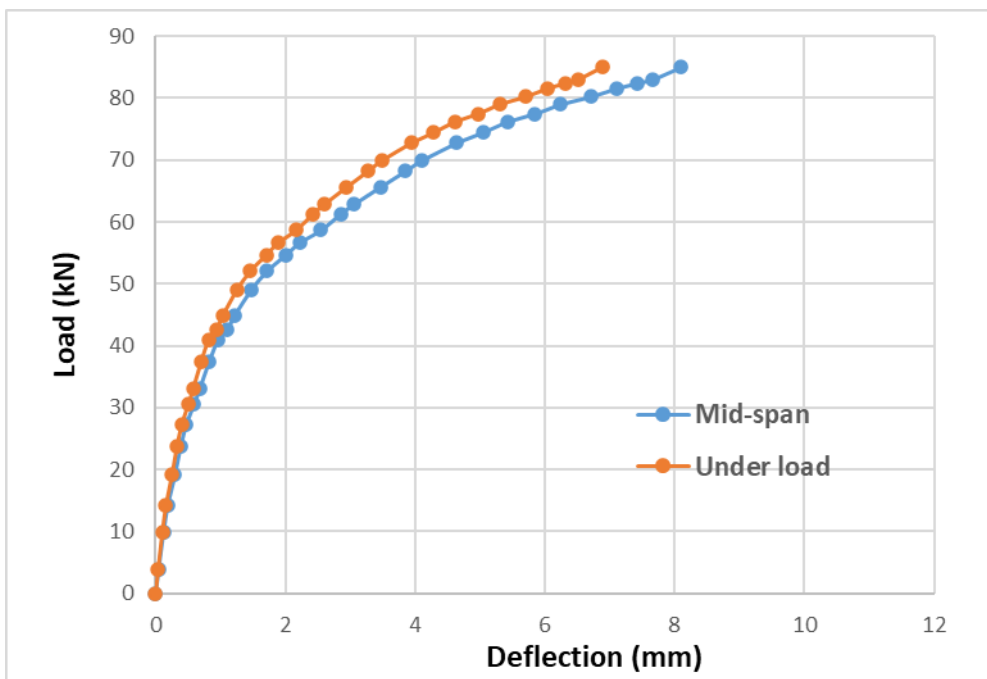


Figure 4.25: Load Deflection Curve for Beam C30-6.

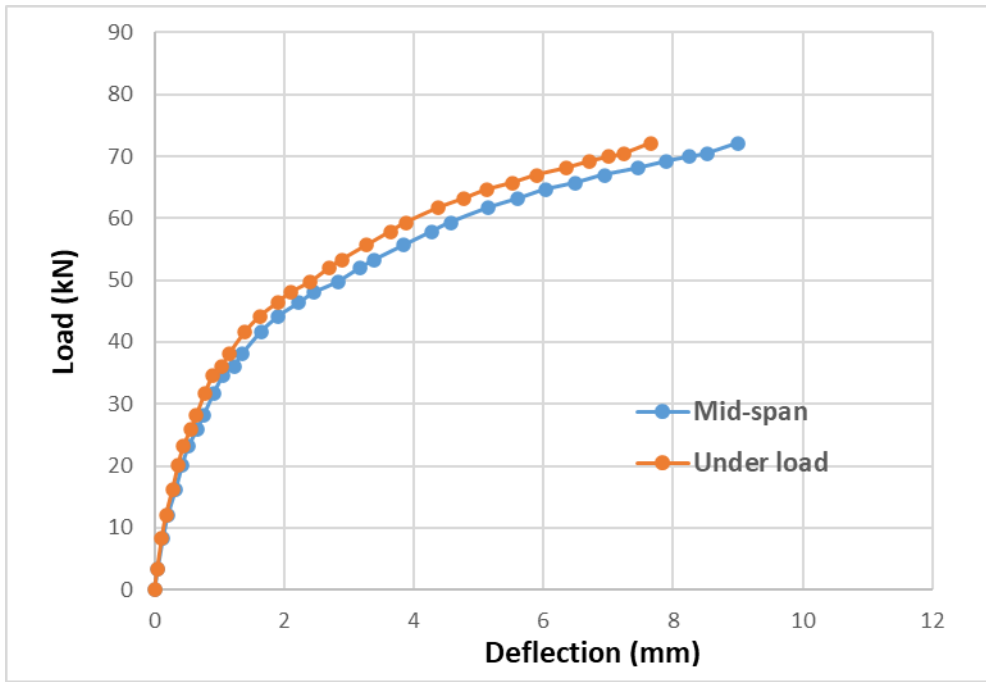


Figure 4.26: Load Deflection Curve for Beam D20-2F.

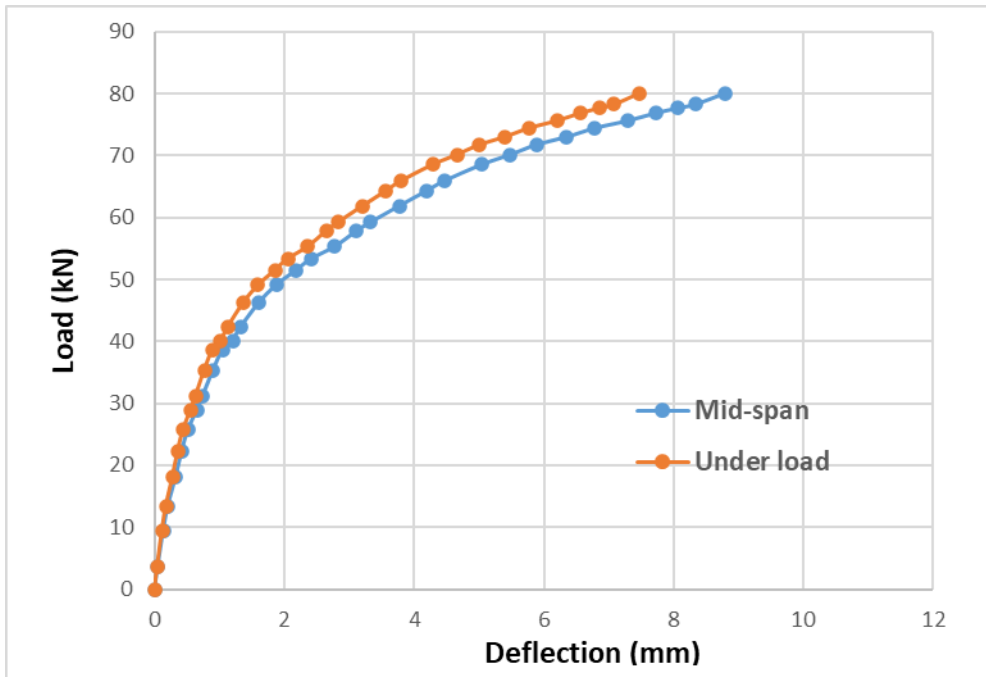


Figure 4.27: Load Deflection Curve for Beam D20-4F.

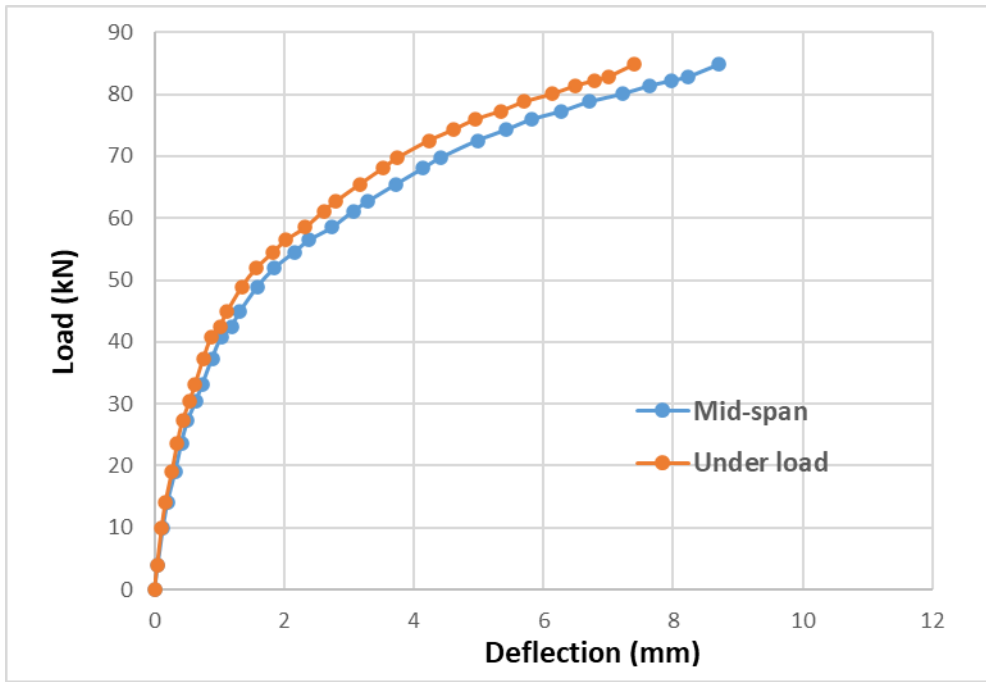


Figure 4.28: Behavior of Load Deflection Curve for Beam D20-6F.

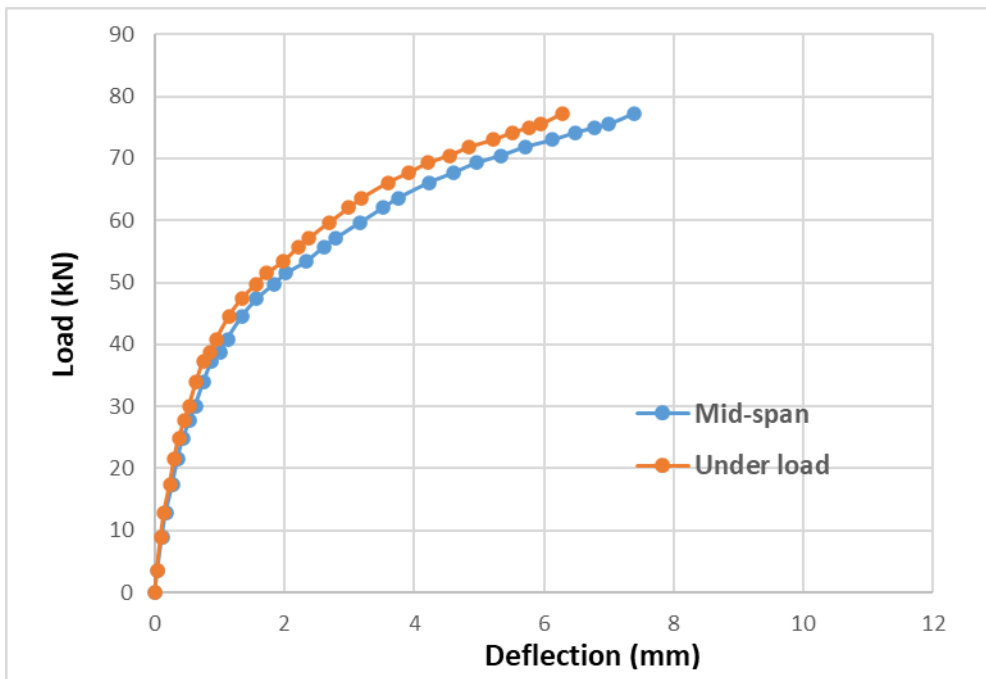


Figure 4.29: Load Deflection Curve for Beam E30-2F.

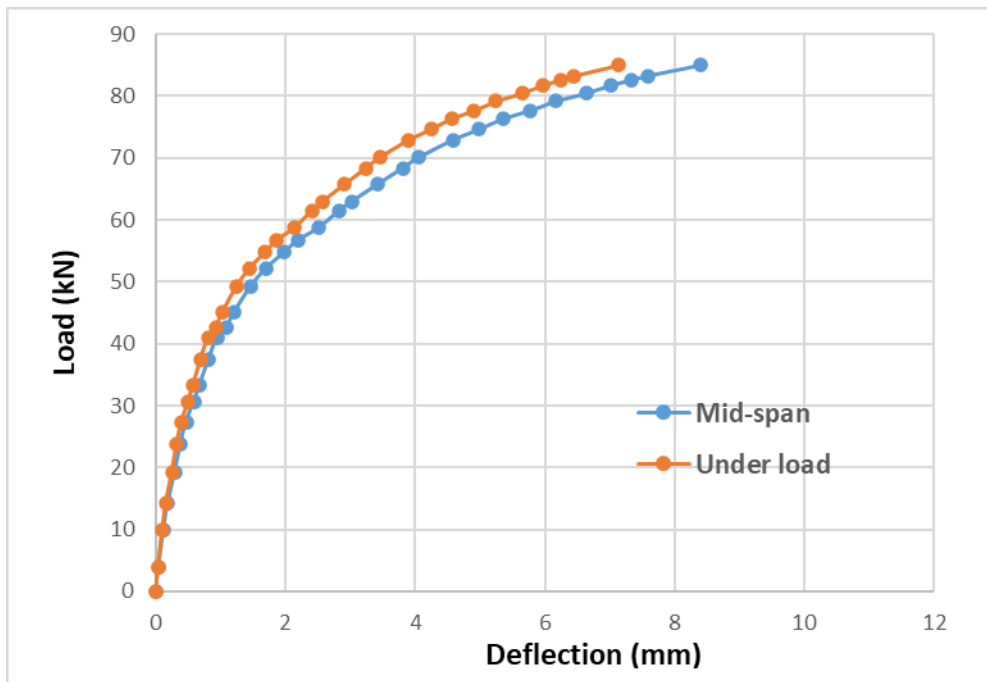


Figure 4.30: Load Deflection Curve for Beam E30-4F.

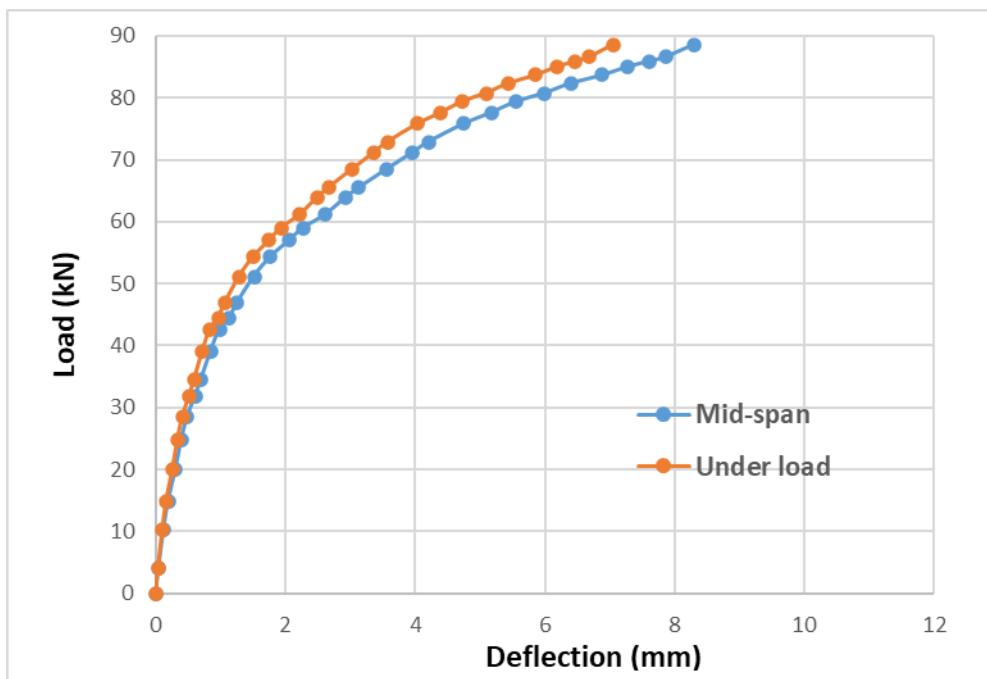
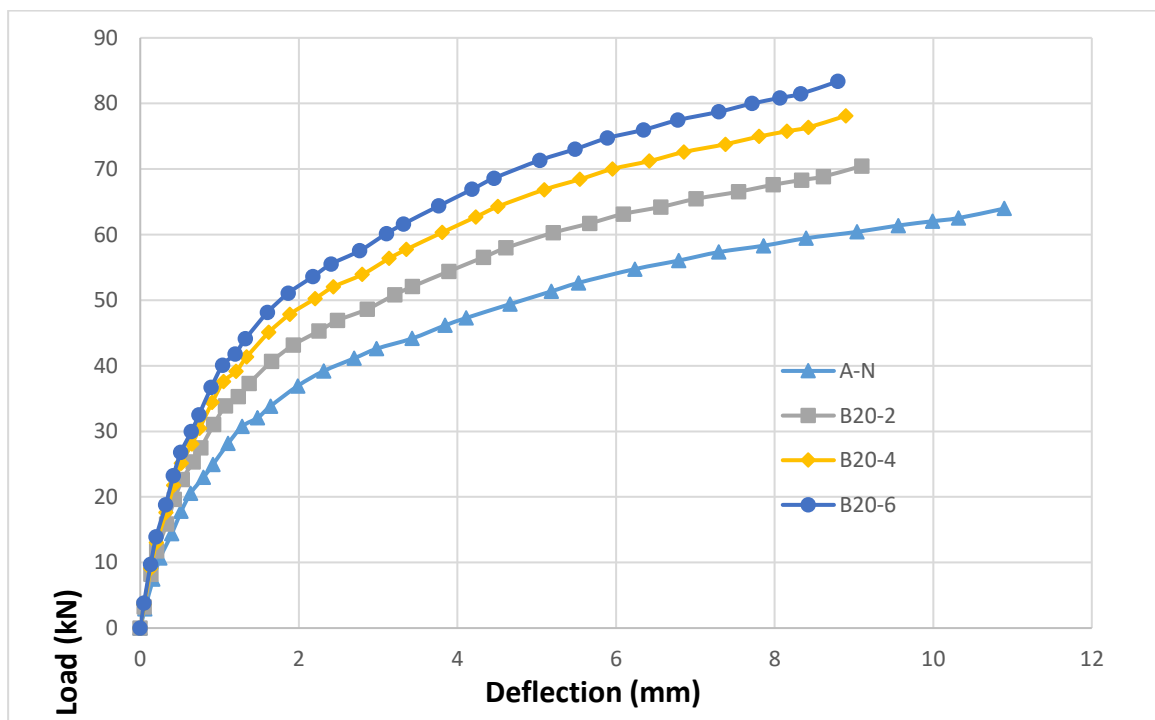


Figure 4.31: Behavior of Load Deflection Curve for th Beam E30-6F.

### 4.5 Effect of the Adopted Variables

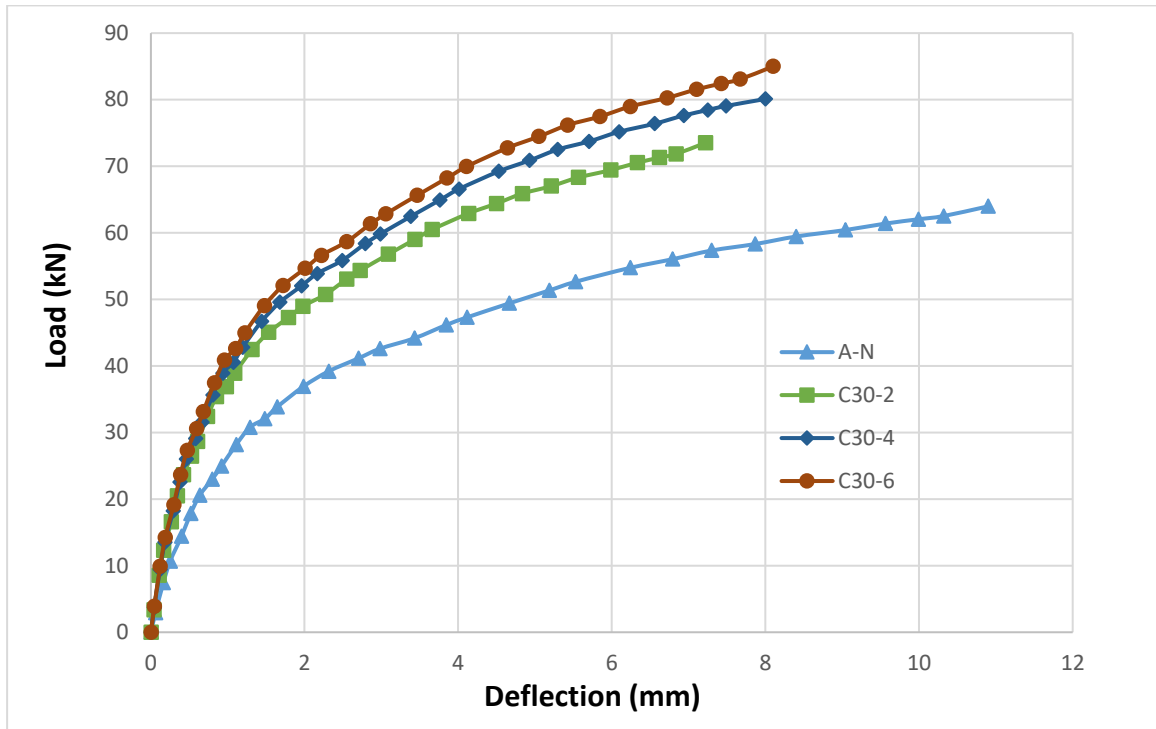
#### 4.5.1 Effect of Steel fiber

Figure 4.32 demonstrates how the percentage of steel fiber affects the performance of load deflection at the middle span for all beams. Each figure compares the outcomes of four specimens with different percentages of steel fibers (0, 2, 4, and 6%). From the load-deflection graphs, it is evident that the beams are identical in stiffness in the elastic region but that after yielding tension reinforcement, the increase of added steel fiber percentage is directly proportional with beam stiffness, or in other words, the deflection decreases with the same load level. The research indicated that the stiffness and the ultimate resistance are remarkably enhanced due to the addition of steel fibers (Oh, 1992)

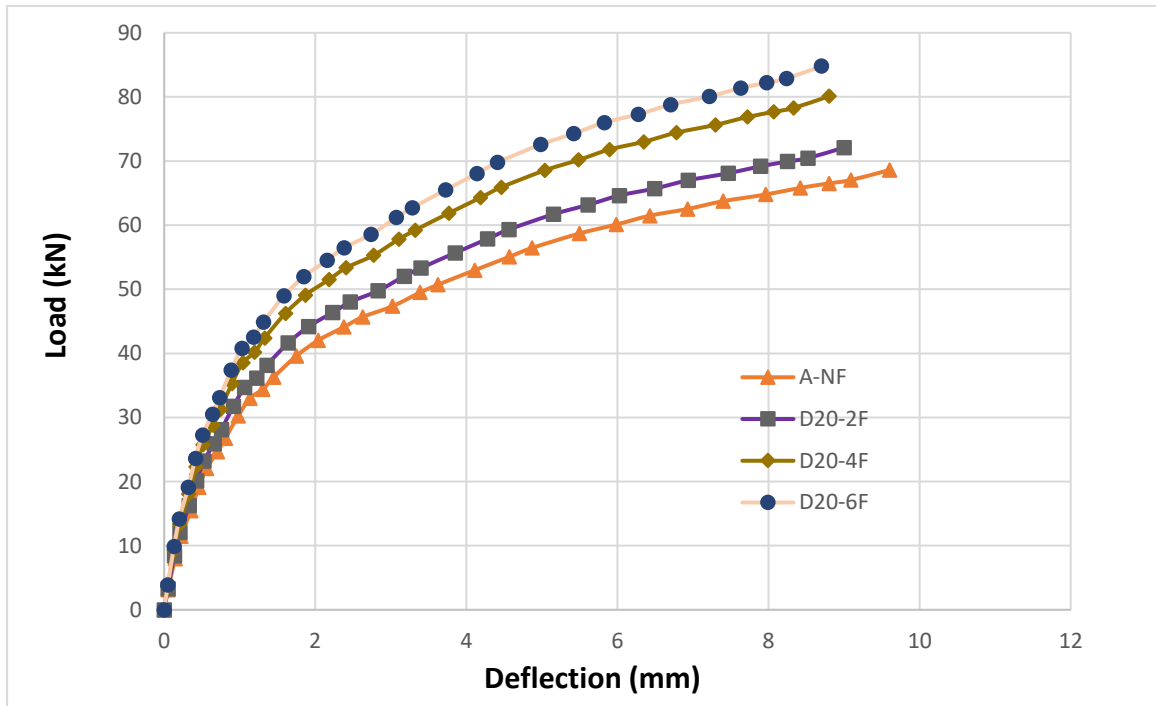


a-Group B 20 mm sifcon only

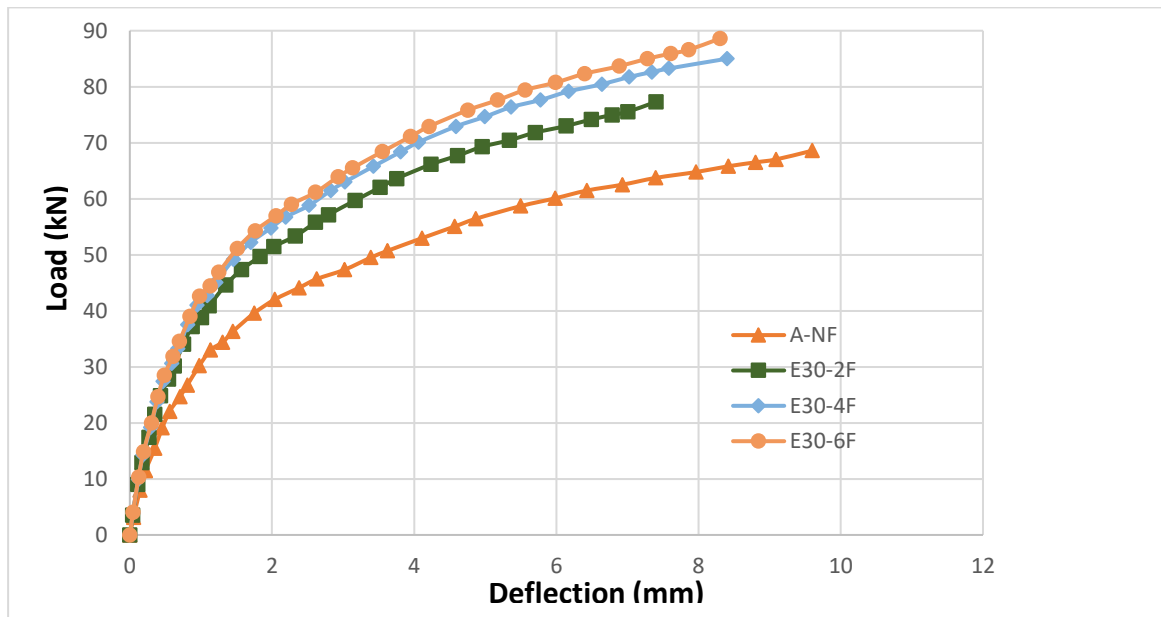




b-Group C 30 sifcon only



c-Group D 20 sifcon with CFRP



d-Group E 30 sifcon with CFRP

**Figure 4.32:** Effect of Steel Fiber on Load-Deflection Behavior.

#### 4.5.2 Effect of CFRP Sheets

**Figure 4.33** demonstrates how the load deflection behavior changes when CFRP sheets are added to the midspan point of all beams. In each figure, the results of two beams with the same percentage of steel fibers are compared with or without CFRP.

From the load-deflection curves, it is clear that the beams have the same stiffness in the elastic region, but that after the yielding of tension reinforcement, the length of added CFRP sheets is directly related to the stiffness of the beam, or in other words, the deflection decreases at the same load level for externally CFRP sheets.

The experimental outcomes of research (El Gamal et al., 2019) have demonstrated that the RC beams' flexural strengthening capacity using externally bonded CFRP sheets on bottom faces can significantly enhance the strengthened flexural capacity of the strengthened beams. The figure 4.33 also shows that the

CFRP sheets did not significantly affect the results because the stiffness of SIFCON is greater than that of normal concrete.

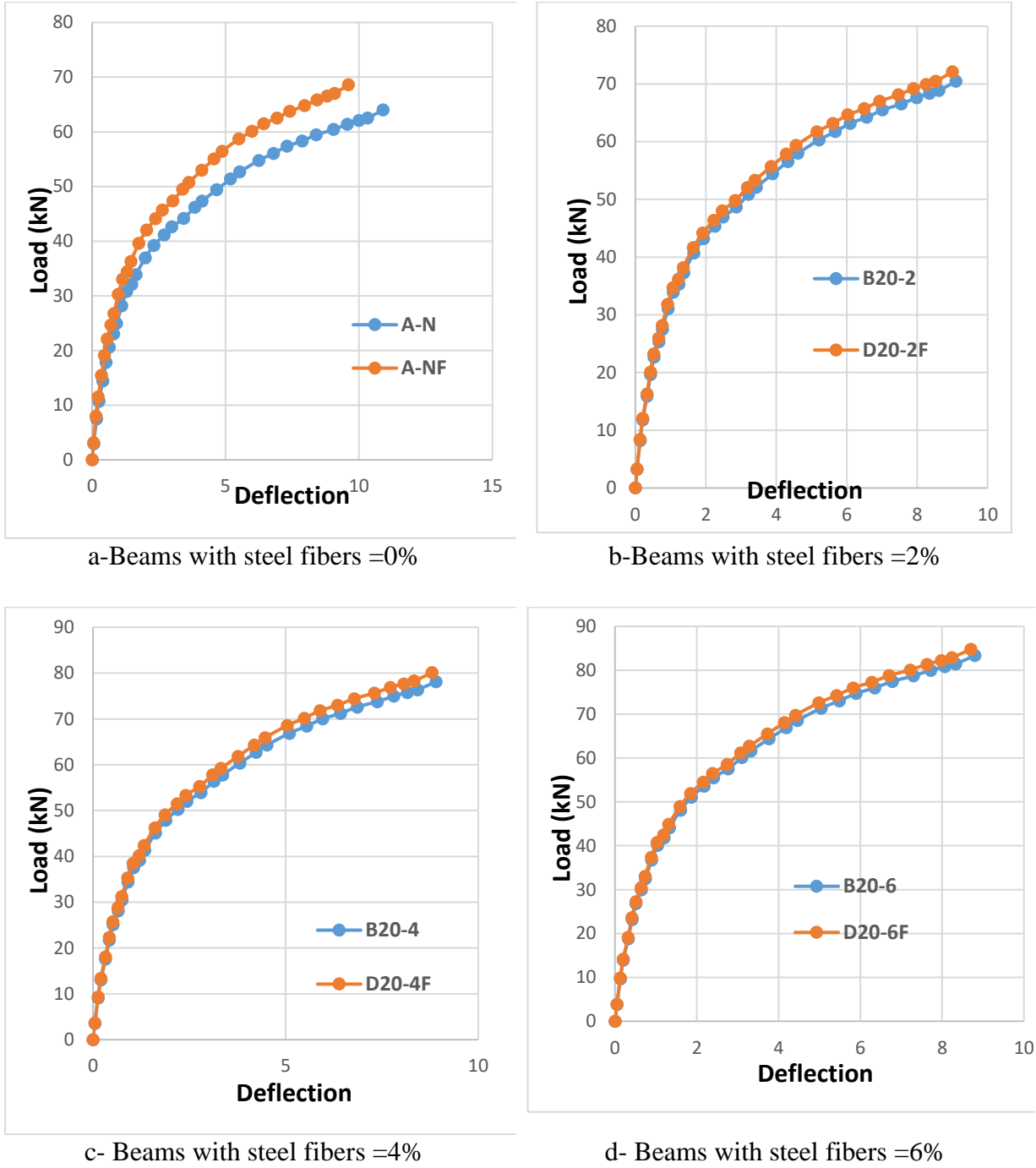
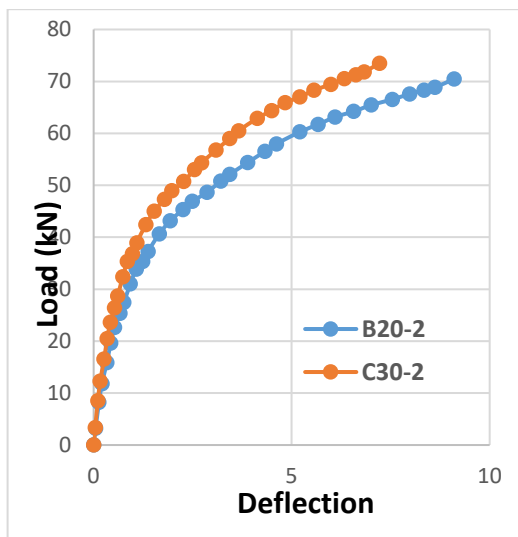


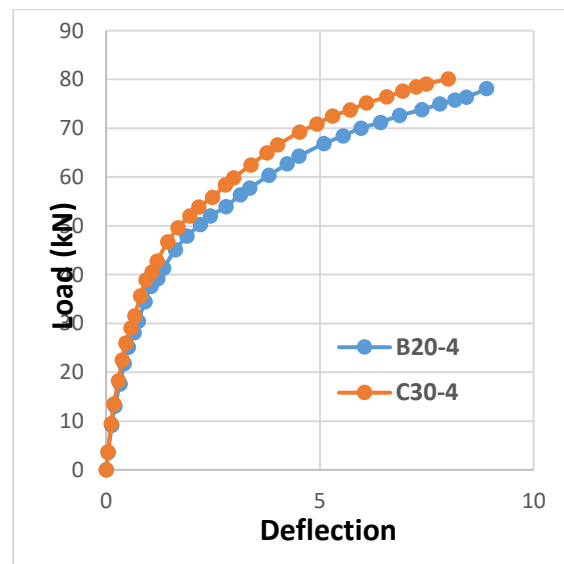
Figure 4.33: Effect of CFRP Sheets on Load-Deflection Behavior. (F=CFRP).

### 4.5.3 Effect of SIFCON Layer

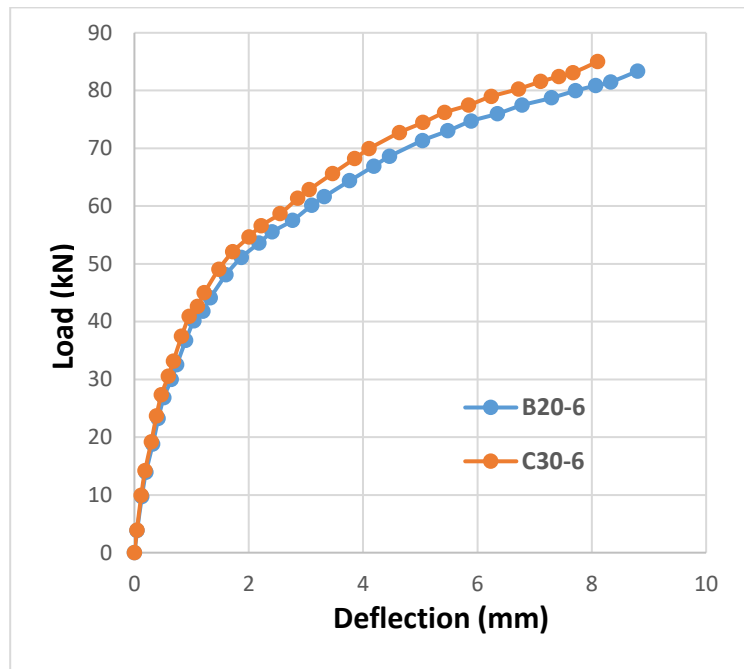
Figure 4.34 shows the effect of SIFCON layer thickness on load-deflection performance for the mid-span point for all specimens. In every figure, the results for two beams with the same steel fibers percentage are put next to each other with SIFCON layer thickness =20 and 30 mm. From the load-deflection graphs, it is clear that the beams share the same stiffness in the elastic region but that following the yielding of tension reinforcement, the rise in SIFCON layer thickness is directly related to the stiffness of the beam, or in different words, the deflection decreases at the same load level for externally CFRP sheets. When the percentage of added steel fibers decreased, the effect of the thickness of the SIFCON layer on the results was higher.



a-Beams with steel fibers =2%



b-Beams with steel fibers =4%



c-Beams with steel fibers =6%

**Figure 4.34:** Effect of SIFCON Layer on Load-Deflection Behavior.

#### 4.5.4 Deflections at Mid-span at Service and Ultimate Loads

**Table 4.7** demonstrates the deflections at the middle of the span for both the service load and the ultimate load. As we've already said, the service load is the ultimate load divided by 1.7. The added length of the CFRP sheets has a big effect on the central deflection at the service load. Also, **Table 4.6** demonstrates the deflections at mid-span for all beams at the 63.98 kN, where the percentage of drop in deflection was 28.4, and 72.9% for specimens A-NF and E30-6F respectively, concerning the reference specimen A-N.

**Table 4.6:** Deflections at mid-span at service and ultimate loads.

Specimens	Deflection at Service Load (mm)	% Decrease in Deflection at Service Load	Deflection at Ultimate Load of Ref. (63.98kN)	% Decrease in Deflection at The Ultimate Load of Ref. Specimen	Deflection at Ultimate load (mm)	% Decrease in Deflection at Ultimate Load
A-N	2.2	Ref.	10.9	Ref.	10.9	Ref.
A-NF	1.8	18.1	7.8	28.4	9.6	11.9
B20-2	1.7	22.7	6.51	40.3	9.1	16.5
B20-4	1.72	21.8	4.51	58.6	8.9	18.3
B20-6	1.74	20.9	3.72	65.9	8.8	19.3
C30-2	1.41	35.9	4.49	58.8	7.22	33.8
C30-4	1.49	32.3	3.7	66.1	8	26.6
C30-6	1.51	31.4	3.3	69.7	8.1	25.7
D20-2F	1.71	22.3	6	45	9	17.4
D20-4F	1.73	21.4	4.14	62	8.8	19.3
D20-6F	1.8	18.2	3.6	67	8.7	20.2
E30-2F	1.38	37.3	3.85	64.7	7.4	32.1
E30-4F	1.52	30.9	3.3	69.7	8.4	22.9
E30-6F	1.62	26.4	2.95	72.9	8.3	23.9

## 4.6 Ductility Index

The ductility index measures the capacity of a structural element to withstand large deformations. In other words, it is the ratio of the mid-span deflection at ultimate loads to the mid-span deflection at the initial yielding of tension of the main reinforcement bars. The ductility index for each specimen is shown in **Table 4.7**. **Figure 4.35** shows that as the number of CFRP sheets increases, the ductility factor decreases. Also, the ductility index increases as the amount of steel fibers added increases. The research results (Oh, 1992) indicate that the ductility and the ultimate resistance are remarkably enhanced due to the addition of steel fibers. **Figure 4.35** also shows that increasing the SIFCON thickness increases the ductility factor.

The ductility index is greatly affected by the percentage of added steel fibers and the thickness of the SIFCON layer in the presence of CFRP because the failure is controlled by debonding of the SIFCON layer, which makes it close to failure in the absence of CFRP. This indicates that the CFRP fixation length is insufficient to increase the ductility index.

**Table 4.7:** Ductility Index of Tested beams Specimens.

Beam ID	Yield - Deflection (mm)	Ultimate - Deflection (mm)	Ductility Index
A-N	3.5	10.9	3.11
A-NF	3.2	9.6	3
B20-2	2.9	9.1	3.14
B20-4	2.8	8.9	3.18
B20-6	2.71	8.8	3.25
C30-2	2.28	7.22	3.17
C30-4	2.45	8	3.27
C30-6	2.42	8.1	3.35
D20-2F	2.9	9	3.103
D20-4F	2.8	8.8	3.143
D20-6F	2.7	8.7	3.222
E30-2F	2.35	7.4	3.15
E30-4F	2.6	8.4	3.231
E30-6F	2.5	8.3	3.32
Ductility index = Ultimate Deflection / Yield Deflection			

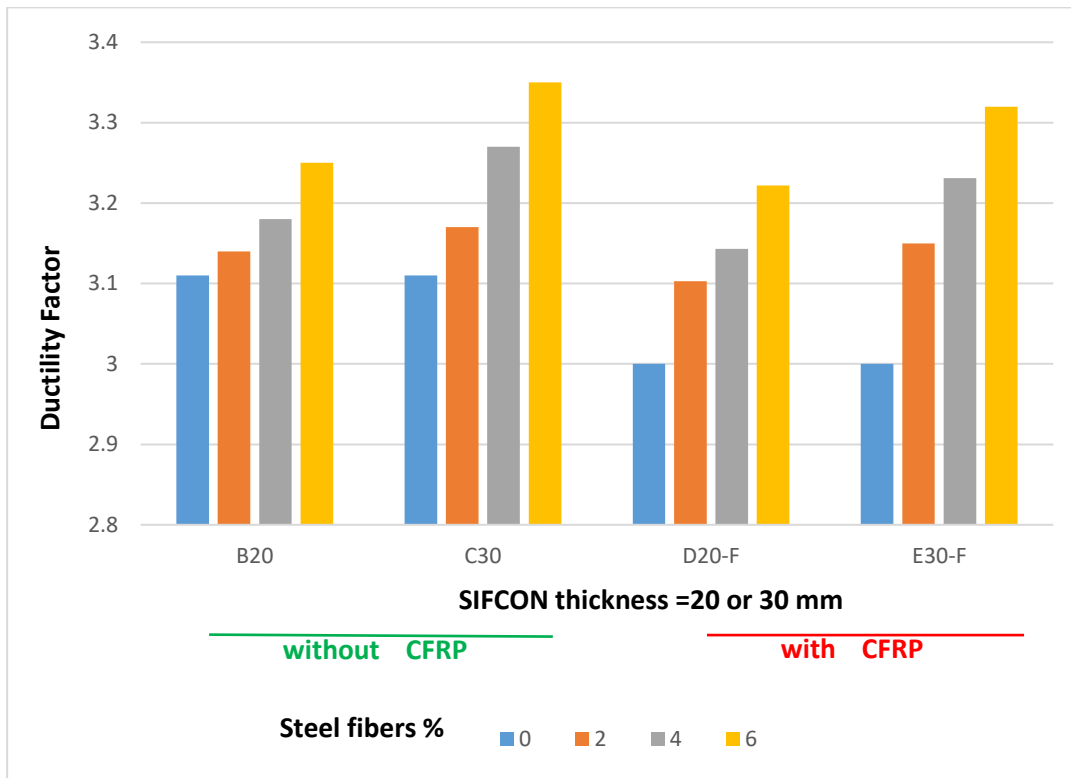


**Figure 4.35:** A comparison in ductility factor for tested beams.

## 4.7 Ultimate Load

All the un-strengthened and strengthened RC beam specimens were tested up to failure. The recorded ultimate loads and failure modes for these beam specimens are presented in **Table 4.9**. It is observed that adding CFRP sheets increases the ultimate load, whereas the ultimate load of the strengthened beam A-NF increased by 7.2% concerning the un-strengthened beam A-N for the reference group. The effect of CFRP sheets on the ultimate load was small because the CFRP fixation length was insufficient, which led to the debonding of the SIFCON layer and CFRP at the end. Finally, it is observed that increasing the thickness of the SIFCON layer increases the ultimate load for all beams, whether strengthened or un-strengthened. **Figure 4.36** demonstrates a comparison in ultimate load for examined beams, and increasing the CFRP length increases the ultimate load.



**Table 4.8:** Ultimate Loads of Tested Beams Specimens.

<b>Specimens</b>	<b>Ultimate Load (P<sub>u</sub>) (kN)</b>	<b>% Increase in Ultimate Load concerning Ref. A-N</b>	<b>Failure Mode</b>
A-N	63.98	Ref.	F1*
A-NF	68.59	7.2	F2**
B20-2	70.46	10.1	F1*
B20-4	78.13	22.1	F1*
B20-6	83.37	30.3	F1*
C30-2	73.52	14.9	F1*
C30-4	80.1	25.2	F1*
C30-6	85	32.9	F1*
D20-2F	72.1	12.7	F2**
D20-4F	80.1	25.2	F2**
D20-6F	84.8	32.5	F2**
E30-2F	77.3	20.8	F2**
E30-4F	85	32.9	F2**
E30-6F	88.6	38.5	F2**
F1*: yielding of tension steel reinforcement followed by crushing of concrete.			
F2**: intermediate flexure crack-induced debonding failure.			

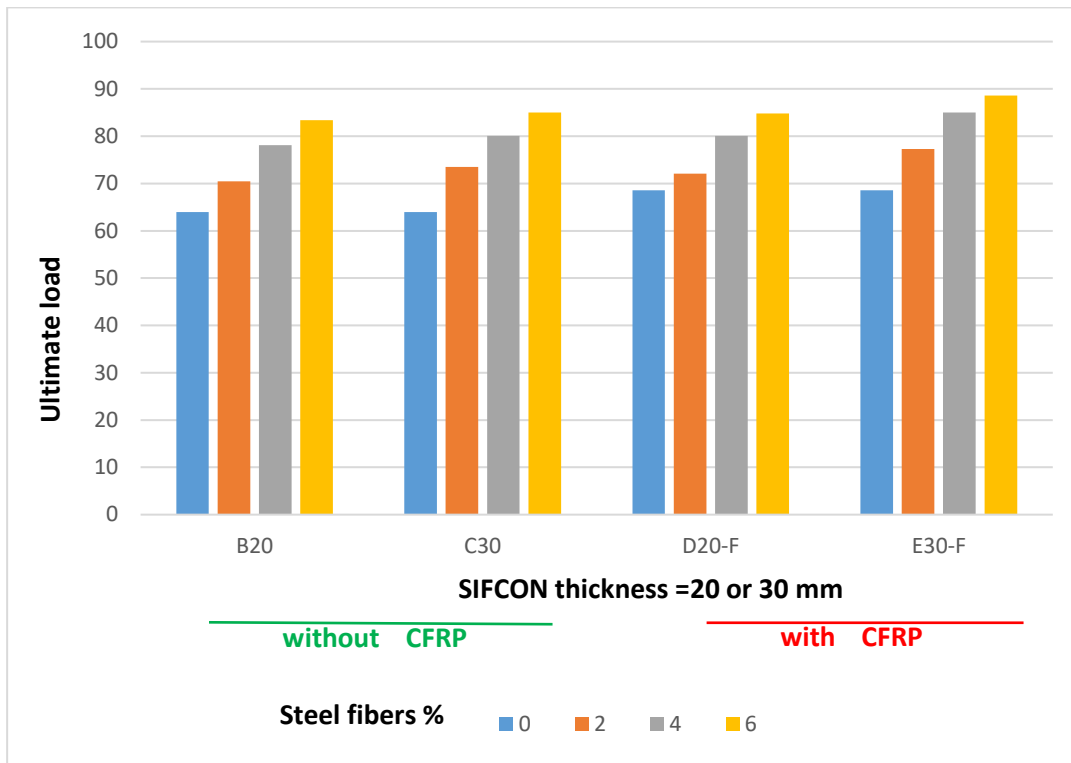


**Figure 4.36:** Ultimate load comparisons of specimen beams Specimens.

## 4.8 Flexural Toughness

One definition of flexural toughness is the capacity to resist crack formation. Another way to think about it is that flexural toughness is the measure of energy absorption capacity. The performance of regions under the load-deflection curve is being measured here. The area under the curve was calculated using AutoCAD. **Table 4.10** and **Figure 4.37** illustrates the toughness values of all tested beams. **Figure 4.37** also shows that the effect of SIFCON thickness on toughness was very small, and the effect of added steel fibers percentage on toughness was not uniform; however, the percentage of 2% gave the lowest values of toughness, while the percentage of 6% gave the largest values of toughness for all groups. (Dong et al., 2019)

**Table 4.9:** Toughness of tested beams.

Beam-ID	Toughness (kN.mm)
A-N	524.6
A-NF	495.3
B20-2	482.3
B20-4	523.0
B20-6	551.8
C30-2	399.3
C30-4	488.4
C30-6	525.0
D20-2F	488.1
D20-4F	530.2
D20-6F	554.9
E30-2F	430.3
E30-4F	546.1
E30-6F	553.1

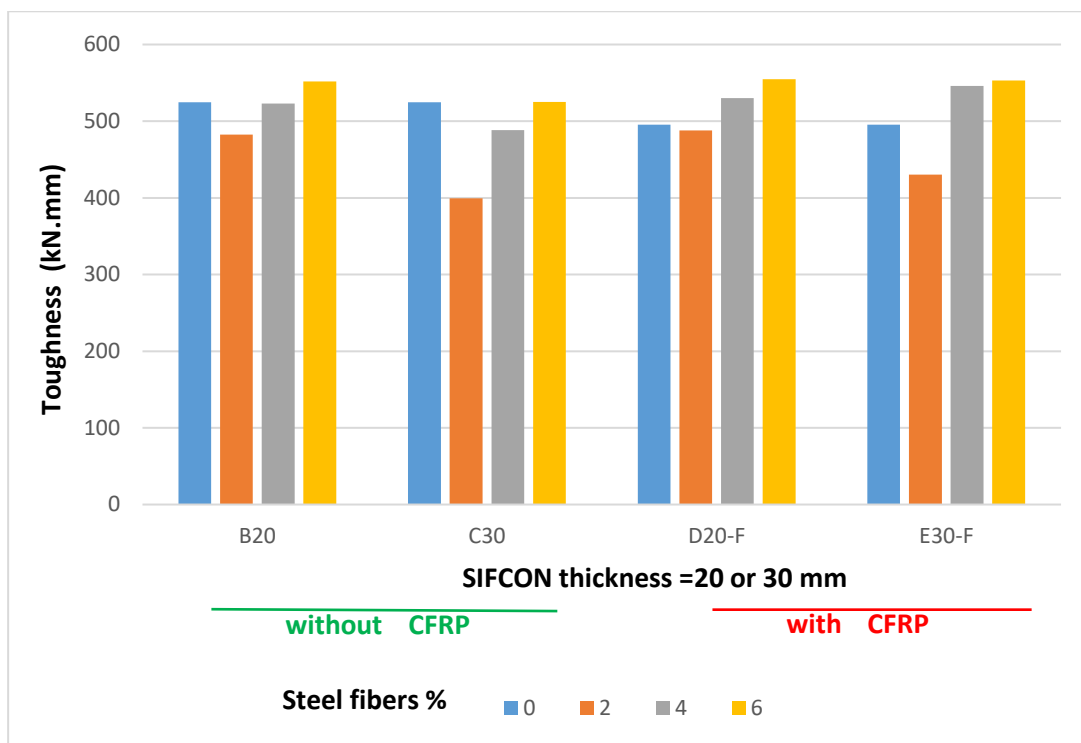


**Figure 4.37:** A comparison of the toughness of tested beams.

## 4.9 Flexural Stiffness

The flexural stiffness ( $k$ ) was determined by calculating the slope ( $\Delta F/\Delta\delta$ ) of the linear portion of the load-deflection curves between (10% and 50%) of the maximum load [Najim, 2012]. **Table 4.11** shows the stiffness of tested beams, and **Figure 4.38** compares the stiffness values of tested beams. It is observed that increasing adding CFRP sheets increases the stiffness, as shown in **Figure 4.38**. Also, increasing the percentage of added steel fibers increases the stiffness, and increasing the SIFCON layer thickness from 20 to 30 mm increases the stiffness by a small amount. The percentage increase in stiffness was 25.4% and 84.7% for specimens A-NF and E30-6F concerning the reference specimen A-N respectively. When the thickness of SIFCON was small (20mm), the effect of the percentage of added steel fibers on the stiffness was significant. While in the case of a thickness of 30 mm, the effect of the percentage of added steel fibers on the stiffness was small.

**Table 4.10:** Stiffness of tested beams.

Beam ID	Stiffness (kN/mm)	% Increase in Stiffness
A-N	18.9	Ref.
A-NF	23.7	25.4
B20-2	25.4	34.0
B20-4	28.9	53.0
B20-6	30.9	64.0
C30-2	33.1	75.0
C30-4	33.2	75.7
C30-6	34.3	82.0
D20-2F	26.0	38.0
D20-4F	29.6	57.0
D20-6F	31.7	68.0
E30-2F	33.8	79.0
E30-4F	34.2	81.0
E30-6F	34.9	84.7

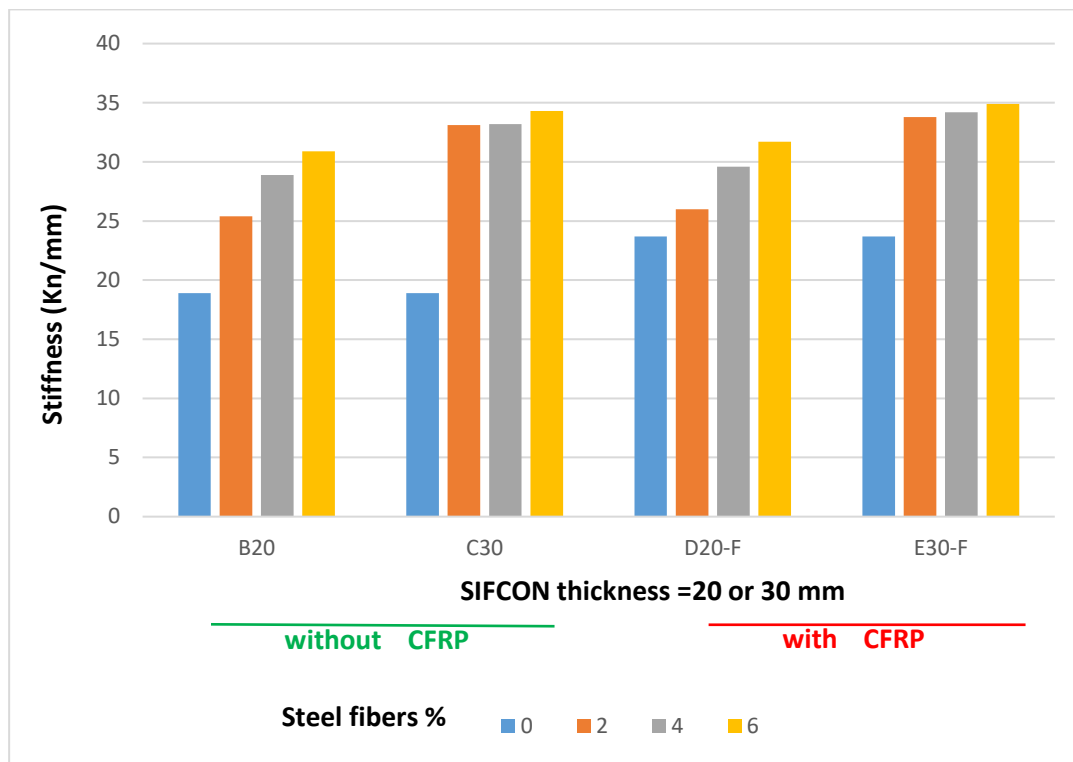


**Figure 4.38:** A Comparison in Stiffness Values of Tested Beams.

## Chapter five

# Conclusions and Recommendations

### 5.1 Introduction

The main objective of this thesis is to investigate the behavior of reinforced SIFCON concrete beams externally strengthened with CFRP attached to their bottom sides. The experimental work's main variables were the CFRP sheet's length, the percentage of added steel fiber, and the thickness of the SIFCON layer. In the present study, tested beams are divided into five groups according to the thickness of the SIFCON layer and the existing CFRP sheet; each group has three specimens with different percentages of added steel fiber (0, 2, 4, and 6). Also, laboratory tests of hardened SIFCON concrete were done.

### 5.2 Conclusions

The following conclusions are drawn from the study's experimental findings and data analysis.

- 1- It is concluded that the percentage of steel fiber has an impact on the compressive strength of SIFCON, for the increase in the percentage of steel fiber can increase the compressive strengths by about (18, 39, and 73%) for the added steel fiber percentage of 2, 4, and 6% with respect to the reference specimen at the age of 7 days, respectively. Moreover, the percentage of steel fiber has an important impact on the compressive strength of SIFCON as the increase of the percentage of steel fiber can increase the compressive strengths by about (30, 55, and 77%) for the added steel fiber percent of 2, 4, and 6% with respect to the reference specimen at the age of 28 days, respectively.
- 2- The ratio of the splitting tensile strength for SIFCON specimens aged 7 days compared to the specimens aged 28 days decreased with the increase

- in the added steel fibers. This ratio was 97, 85, 73, and 74% for the percentages of added steel fibers of 0, 2, 4, and 6%.
- 3- The percentage of steel fiber has a crucial impact on the ultimate flexural force of SIFCON, the increase of the percentage of steel fiber increased the ultimate flexural force by about (16 and 30%) for the added steel fiber percentage of 4 and 6% with respect to the reference specimen of 2% for SIFCON specimens with a thickness of 30mm respectively. At the same time, the increase of the percentage of steel fiber increased the ultimate flexural force of SIFCON by about (20 and 40%) for the added steel fiber percentage of 4 and 6% with respect to the reference specimen of 2% for SIFCON specimens with a thickness of 20mm respectively.
  - 4- The ratio of the ultimate flexural force of SIFCON for specimens with a thickness of 30mm to the specimens with a thickness of 20mm was 1.71, 1.66, and 1.59 for the added steel fiber percentage of 2, 4 and 6%, respectively.
  - 5- The first flexural crack happened for all samples, with various initial crack load ( $P_{cr}$ ) / ultimate load ( $P_u$ ) percentage of about (28 to 40 %). Which concluded that increasing the CFRP sheets' length decreases the  $P_{cr} / P_u$  percentage while increasing the added steel fibers percentage increases the  $P_{cr} / P_u$  percentage. Also, increasing the SIFCON thickness increases the  $P_{cr} / P_u$  percentage.
  - 6- Increasing the added external CFRP sheets length decreases the maximum width of the crack 3.3-20 % at the ultimate load, on the other hand, increasing the added steel fiber percentage decreases the maximum width of the crack 6-22 % at the ultimate load. Also, increasing the SIFCON thickness decreases the maximum width of the crack at the ultimate load.
  - 7- In the elastic zone, the beams share the same stiffness. Still, following the yielding of tension reinforcement, the rise in the percentage of added steel

fibers is directly proportional to beam stiffness. On the other hand, the deflection reduces for a given load.

- 8- The increased CFRP sheet length is directly proportional to beam stiffness or, in other words, the deflection decreases at the same load level. And increasing SIFCON layer thickness is directly proportional to beam stiffness.
- 9- The ductility index is greatly affected by the percentage of added steel fibers and the thickness of the SIFCON layer in the presence of CFRP because the failure is controlled by the debonding of the SIFCON layer, which makes it close to failure in the absence of CFRP. This indicates that the CFRP fixation length is insufficient to increase the ductility index.
- 10- For beams without CFRP, increasing the percentage of added steel fibers increases the ultimate load, where as the ultimate load increased by 10.1, 22.1, 30.3, 14.9, 25.2, and 32.9% for all beams respectively, with respect to the un-strengthened beam BR. While the ultimate load increases for beams with CFRP as the percentage of added steel fibers increases, the ultimate load increased by 5.1%, 16.8%, 23.6%, 12.7%, 23.9%, and 29.2% for all beams respectively.
- 11- Stiffness is increased by adding CFRP sheets, stiffness is also increased by increasing the percentage of steel fibers added, and it is slightly increased by raising the thickness of the SIFCON layer from 20 to 30 mm.



### **5.3 Recommendations for Future Research Work**

Based on the results of this work, the following fields are suggested for further research.

- 1- Studying the performance of reinforced SIFCON concrete beams with CFRP under dynamic and impact loads.
- 2- Examining the performance of reinforced SIFCON concrete beams with CFRP under fire effect.
- 3- Investigating the performance of reinforced SIFCON concrete beams partially prestressed.
- 4- Revealing the performance of thick reinforced SIFCON concrete one-way slabs with CFRP sheet internally and externally under monotonic and repeated loads.
- 5- Inspecting the performance of preloaded thick reinforced SIFCON concrete one-way slabs repaired with NSM-CFRP plates.
- 6- Extending CFRP length along the beam.

## References

- ABD-ALI, M. & ESSA, A. 2019. Mechanical properties of slurry infiltrated fibrous concrete (SIFCON) with variation steel fiber ratios and silica fume. *J. Adv. Res. Dyn. Control. Syst*, 11, 1863-1872.
- ABDULKAREEM, B. F. & IZZET, A. F. Post Fire Residual Concrete and Steel Reinforcement Properties. IOP Conference Series: Earth and Environmental Science, 2021. IOP Publishing, 012058.
- AL-ABDALAY, N. M., ZEINI, H. A. & KUBBA, H. Z. 2020. Investigation of the behavior of slurry infiltrated fibrous concrete. *Journal of Advanced Research in Fluid Mechanics and Thermal Sciences*, 65, 109-120.
- AL-MAHMOUD, F., CASTEL, A., FRANÇOIS, R. & TOURNEUR, C. 2009. Strengthening of RC members with near-surface mounted CFRP rods. *Composite structures*, 91, 138-147.
- ALI, A. S. & RIYADH, Z. 2018. Experimental and Numerical Study on the Effects of Size and type of Steel Fibers on the (SIFCON) Concrete Specimens. *International Journal of Applied Engineering Research*, 13, 1344-1353.
- BALAGURI, P. & SHAH, S. 1992. Fiber Reinforced Cement Composites, McGrawHill. Inc, Singapore.
- BALAJI, S. & THIRUGNANAM, G. 2018. Behaviour of reinforced concrete beams with SIFCON at various locations in the beam. *KSCE Journal of Civil Engineering*, 22, 161-166.
- BARRIS, C., SALA, P., GÓMEZ, J. & TORRES, L. 2020. Flexural behaviour of FRP reinforced concrete beams strengthened with NSM CFRP strips. *Composite Structures*, 241, 112059.
- BASHANDY, A. A. 2013. Flexural strengthening of reinforced concrete beams using valid strengthening techniques. *Archives of Civil Engineering*.
- BERG, A. C., BANK, L. C., OLIVA, M. G. & RUSSELL, J. S. 2006. Construction and cost analysis of an FRP reinforced concrete bridge deck. *Construction and Building Materials*, 20, 515-526.

- DAGAR, K. 2012. Slurry infiltrated fibrous concrete (SIFCON). *International Journal of Applied Engineering and Technology*, 2, 99-100.
- DONG, S., ZHOU, D., ASHOUR, A., HAN, B. & OU, J. 2019. Flexural toughness and calculation model of super-fine stainless wire reinforced reactive powder concrete. *Cement and Concrete Composites*, 104, 103367.
- DUTHINH, D. & STARNES, M. 2001. Strength and Ductility of Concrete Beams Reinforced with FRP and Steel. *National Institute of Standards and Technology, NISTIR*, 6830, 493-498.
- EL GAMAL, S., AL-NUAIMI, A., AL-SAYDY, A. & AL-SHANFARI, K. 2019. Flexural behavior of RC beams strengthened with CFRP sheets using different strengthening techniques. *The Journal of Engineering Research [TJER]*, 16, 35-43.
- ELAVARASI, M. 2016. KSR, “performance of slurry infiltrated fibrous concrete (Sifcon) with silica fume.”. *International Journal of Chemical Sciences*, 14, 2710-2722.
- G. KARAYANNIS, C., K. KOSMIDOU, P.-M. & E. CHALIORIS, C. 2018. Reinforced concrete beams with carbon-fiber-reinforced polymer bars— Experimental study. *Fibers*, 6, 99.
- HAWILEH, R. A., RASHEED, H. A., ABDALLA, J. A. & AL-TAMIMI, A. K. 2014. Behavior of reinforced concrete beams strengthened with externally bonded hybrid fiber reinforced polymer systems. *Materials & Design*, 53, 972-982.
- JERRY, A. H. & FAWZI, N. M. 2022. The effect of using different fibres on the impact-resistance of slurry infiltrated fibrous concrete (SIFCON). *Journal of the Mechanical Behavior of Materials*, 31, 135-142.
- KHAN, A., BALUCH, M. & AL-GADHIB, A. Repair and strengthening of reinforced concrete structures using CFRP plates. Proceedings of international Bhurban conference on applied sciences and technology v. 2, 2004.

- LAMANNA, A. J., BANK, L. C. & SCOTT, D. W. 2004. Flexural strengthening of reinforced concrete beams by mechanically attaching fiber-reinforced polymer strips. *Journal of composites for construction*, 8, 203-210.
- LANKARD, D. Preparation, properties and applications of concrete-based composites containing 5% to 20% steel fiber. Steel Fiber Concrete, US-Sweden Joint Seminar, 1985. 199-217.
- LANKARD, D. R. 1984. Slurry infiltrated fiber concrete (SIFCON): Properties and applications. *MRS Online Proceedings Library*, 42, 277-286.
- LAU, D. & PAM, H. J. 2010. Experimental study of hybrid FRP reinforced concrete beams. *Engineering Structures*, 32, 3857-3865.
- LEE, D., CHENG, L. & YAN-GEE HUI, J. 2013. Bond characteristics of various NSM FRP reinforcements in concrete. *Journal of Composites for Construction*, 17, 117-129.
- LIN, X. & ZHANG, Y. 2013. Bond–slip behaviour of FRP-reinforced concrete beams. *Construction and Building Materials*, 44, 110-117.
- LIU, Z., LU, Y., LI, S., ZONG, S. & YI, S. 2020. Flexural behavior of steel fiber reinforced self-stressing recycled aggregate concrete-filled steel tube. *Journal of Cleaner Production*, 274, 122724.
- MANOLIA, A., SHAKIR, A. & QAIS, J. The effect of fiber and mortar type on the freezing and thawing resistance of Slurry Infiltrated Fiber Concrete (SIFCON). IOP Conference Series: Materials Science and Engineering, 2018. IOP Publishing, 012142.
- MANSUR, M., HUANG, L., TAN, K. & LEE, S. 1992. Deflections of reinforced concrete beams with web openings. *Structural Journal*, 89, 391-397.
- MEIER, U. 1987. Bridge repair with high performance composite materials. *Material und Technik*, 4, 125-128.
- MOHAMMED, G. K., SARSAM, K. F. & GORGIS, I. N. 2020. Flexural Performance of Reinforced Concrete Built-up Beams with SIFCON. *Engineering and Technology Journal*, 38, 669-680.

- OH, B. H. 1992. Flexural analysis of reinforced concrete beams containing steel fibers. *Journal of structural engineering*, 118, 2821-2835.
- RAO, H. S., GHORPADE, V. G., RAMANA, N. & GNANESWAR, K. 2010. Response of SIFCON two-way slabs under impact loading. *International Journal of Impact Engineering*, 37, 452-458.
- SALIH, S., FRAYYEH, Q. & ALI, M. Fresh and some mechanical properties of sifcon containing silica fume. MATEC Web of Conferences, 2018. EDP Sciences, 02003.
- SHANNAG, M., BARAKAT, S. & JABER, F. 2001. Structural repair of shear-deficient reinforced concrete beams using SIFCON. *Magazine of Concrete Research*, 53, 391-403.
- SHANTHINI, D. & MOHANRAJ, E. 2015. Mechanical behavior of SIFCON beams. *International Journal of Science and Engineering Research (IJOSE)*, 3, 3.
- SHARIFIANJAZI, F., ZEYDI, P., BAZLI, M., ESMAEILKHANIAN, A., RAHMANI, R., BAZLI, L. & KHAKSAR, S. 2022. Fibre-reinforced polymer reinforced concrete members under elevated temperatures: a review on structural performance. *Polymers*, 14, 472.
- SHELORKAR, A. & JADHAO, P. 2018. Determination of Mechanical Properties of Slurry Infiltrated Steel Fiber Concrete Using Fly Ash and Metakaolin. *International Journal of Engineering and Technology*, 7, 262-267.
- STANDARD, A. 2006. C305. Standard practice for mechanical mixing of hydraulic cement pastes and mortars of plastic consistency. *Annual book of ASTM standards*.
- SUNDAR, N., RAGHUNATH, P. & DHINAKARAN, G. 2016. Flexural behavior of RC beams with hybrid FRP strengthening. *International Journal of Civil Engineering and Technology*, 7, 2016.
- VALERIO, P. 2009. *Realistic shear assessment and novel strengthening of existing concrete bridges*. University of Bath.

YANG, J., HAGHANI, R., BLANKSVÄRD, T. & LUNDGREN, K. 2021.  
Experimental study of FRP-strengthened concrete beams with corroded  
reinforcement. *Construction and Building Materials*, 301, 124076.

## APPENDIX A

### BEAM SPECIMEN DESIGN CALCULATION ACCORDING TO ACI318-19

#### A.1 Calculation of flexural capacity for a beam without strengthening

Beam clear span (L)	1400mm
Compressive strength ( $f_c'$ )	35 MPa
Yield strength ( $f_y$ )	420 MPa
Height of beam section (h)	200 mm
Width of beam section (w)	150 mm
Effective depth (d)	169mm
Cover (c)	20 mm
Diameter of long. reinforcement	10 mm
Diameter of shear reinforcement	6 mm
Steel modulus of elasticity ( $E_s$ )	200000 MPa
Concrete modulus of elasticity	27806 MPa

Use bar 2  $\emptyset 10$

$$\rho = \frac{A_s}{b \times d} = 0.012$$

$$\rho_{min} = \frac{0.25\sqrt{f_c'}}{f_y} = 0.0033 \quad \text{OR} \quad \rho_{min} = \frac{1.4}{f_y} = 0.0035$$

$$\therefore \rho_{min} = 0.0035 \quad \dots\dots\dots \text{ACI318 -14 (9.6.1.2)}$$

$$\beta_1 = 0.80 \quad \dots\dots\dots \text{ACI318 -14 (Table 22.2.2.4.3)}$$

$$\rho_b = 0.85 \times \beta_1 \times \frac{f_c'}{f_y} \times \frac{600}{600+f_y} = 0.033$$

$$\rho_t = 0.85 \times \beta_1 \times \frac{f_c'}{f_y} \times \frac{0.004}{0.004+\epsilon} = 0.021$$

$$\rho_{max} = 0.85 \times \beta_1 \times \frac{f_c'}{f_y} \times \frac{0.003}{0.003+\epsilon} = 0.024$$

$$\therefore \rho_{min} < \rho < \rho_{max}$$

$$M_n = 0.243 + 0.692P$$

$$M_n = \rho b d^2 F_Y \left(1 - 0.59\rho \frac{f_y}{f_{c'}}\right) = 17.78 \text{ KN.m} ,$$

$$17.78 = 0.243 + 0.692P$$

$$P = 25.43 \text{ kN}$$

## A.2 Calculation of shear capacity for a beam without strengthening

$V_C$  = nominal shear strength provided by concrete, KN

$V_S$  = nominal shear strength provided by shear reinforcement, KN

$V_n$  = nominal shear strength, KN

$$V_u = 1.6 p + 1.2 (24 * 0.15 * 0.2 * 1.5) / 2 = 40.97 \text{ kN}$$

$$V_{ud} = 40.74 \text{ kN}$$

$$V_C = \frac{1}{6} \sqrt{f_c'} b d = 25.49 \text{ KN}$$

$$V_C / 2 = 12.75 \text{ kN}$$

$$V_S = V_{ud} - V_C = 28.83 \text{ kN}$$

$$V_S < 2V_C \rightarrow$$

$$1- d/2 = 84.5 \text{ mm}$$

$$2- 600 \text{ mm}$$

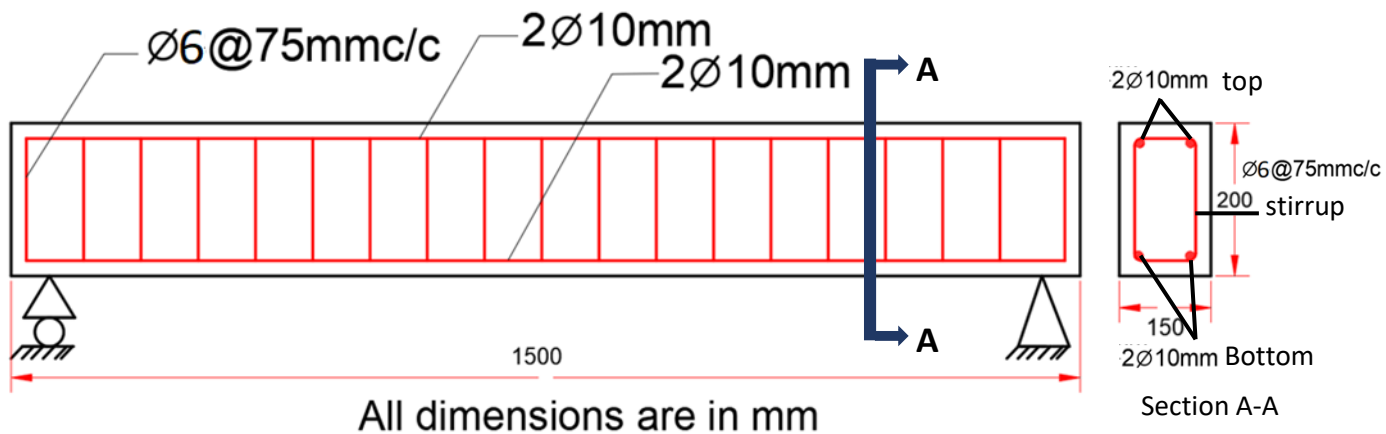
$$3- 3A_v f_y / b = 475 \text{ mm}$$

$$4- 16 A_v f_y / b \sqrt{f_c'} = 428.2 \text{ mm}$$

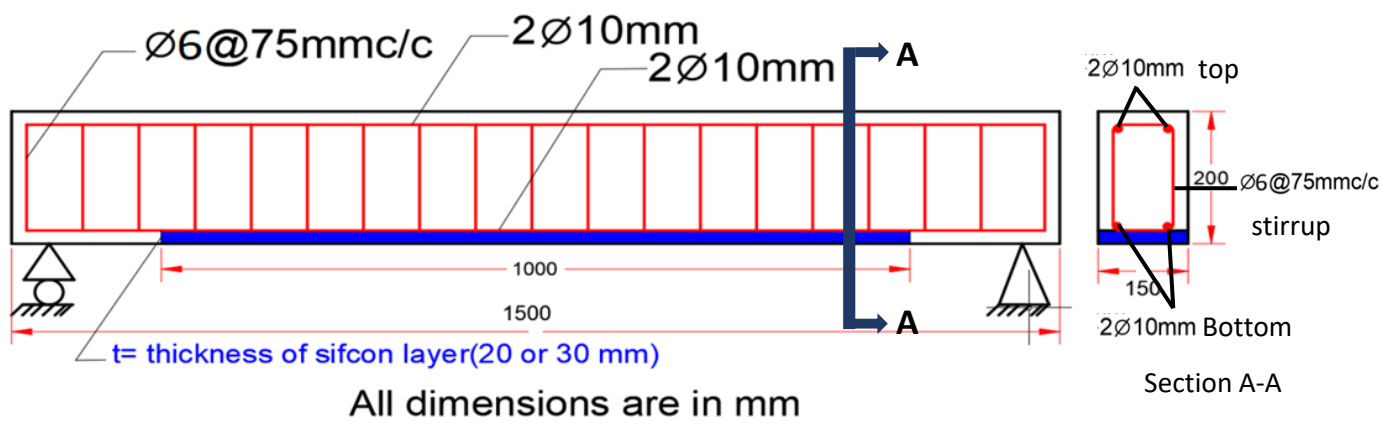
So  $S_{\max} = 83.5 \text{ mm}$  , use  $S_{\max} = 80 \text{ mm}$

$$S = \frac{A_v f_y d}{V_S} = 480.5 > 80 \quad \text{OK}$$



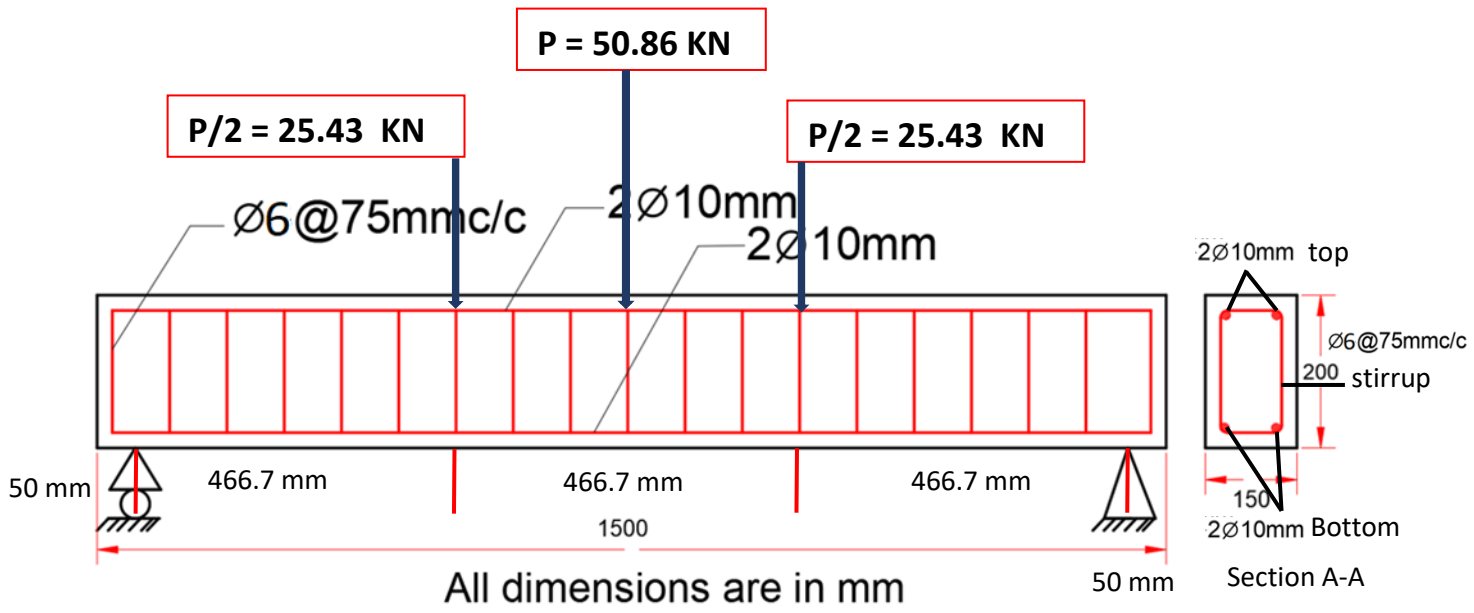


**A-without SIFCON**



**b-with SIFCON**

**Figure 3.13** Schematic Layout of Beams and Details of Steel Reinforcement



## الخلاصة

تعتبر خرسانة المونة المتسللة ضمن الألياف (SIFCON) أحد الاستخدامات الجديدة للخرسانة التي أصبحت أكثر أهمية لنجاح استخدامها كطريقة لتدعيم واصلاح الهياكل القديمة وتحديثها او نتيجة زيادة الاحمال الناتجة عن الاخطاء التصميمية.

تتميز الخرسانة الهجينة (سيفكون) بمادة مطيلة للغاية وطاقة كامنة ممتازة لامتناسص الحمل المفاجئ. بالإضافة إلى ذلك، تتمتع بمقاومة عالية للصددمات المرتدة عن الانفجارات. قد تعمل المادة الرابطة في الخرسانة الهجينة الناتجة كعضو مركب لتوزيع الأحمال وامتصاص الصدمات على العضو الإنشائي بسبب القيم العالية للمرونة والطاقة الكامنة للألياف الحديدية.

ان الهدف من هذه الدراسة الحالية هو التحري من سلوك وأداء الاعتاب الخرسانية المسلحة الحاوية على (SIFCON) والمقواة بأشرطة اللدائن المقوى بألياف الكربون (CFRP) والمثبتة في مناطق الشد.

يتضمن العمل المختبري تصنيع واختبار أربعة عشر نموذجاً من الاعتاب الخرسانة المسلحة مقسمة الى خمسة مجاميع حسب نسبة الالياف الفولاذية وسمك طبقة السيفكون والتقوية بألياف الكربون البوليميرية. أظهرت النتائج المختبرية الى أن زيادة نسبة الألياف الفولاذية لها تأثير على مقاومة الانضغاط للأعتاب الخرسانية الحاوية على SIFCON اذ ان زيادة النسبة المئوية للألياف الفولاذية زادت من مقاومة الانضغاط بحوالي (30 و 55 و 77%) للألياف الفولاذية المضافة بنسبة 2 %، 4 %، و 6% مقارنة بالعينة المرجعية لعمر 28 يوماً على التوالي.

علاوة على ذلك، فقد ثبت أن زيادة النسبة المئوية للألياف الفولاذية لها تأثير كبير على مقاومة الشد للأعتاب الخرسانية (fct) الحاوية على Sifcon. حيث ان زيادة النسب المئوية المضافة للألياف الفولاذية البالغة 2 و 4 و 6% بالنسبة للأعتاب المرجعية للعمر 28 يوماً ، زادت قوة الشد بحوالي (160 إلى 417%) على التوالي.

أظهرت النتائج المختبرية أيضاً أن النسبة المئوية للألياف الفولاذية لها تأثير على قوة الانحناء القصوى للأعتاب الحاوية على SIFCON ؛ حيث ان زيادة النسبة المئوية للألياف الفولاذية ، زادت قوة الانحناء النهائية بحوالي (16 و 30%) لنسبة الألياف الفولاذية المضافة بنسبة 4 و 6% عند مقارنتها بالأعتاب المرجعية بنسبة 2% للأعتاب الحاوية على SIFCON بسمك 30 ملم على التوالي. في الوقت نفسه ، أدت زيادة النسبة المئوية للألياف الفولاذية إلى زيادة قوة الانحناء القصوى فيما يتعلق بالأعتاب المرجعية بنسبة 2% والحواوية على SIFCON بسمك 20 ملم على التوالي.

اثبتت النتائج المختبرية أيضا ان زيادة النسبة المئوية لالياف الفولاذ لها تاثير في زيادة معامل الليونة او المطالية للأعتاب الحاوية على SIFCON مقارنة بالأعتاب المرجعية .  
أيضا اثبتت النتائج المختبرية ان زيادة النسبة المئوية لألياف الفولاذ وسمك طبقة السيفكون والياف الكربون كلها تؤدي الى زيادة الحمل التشققي الاولي مع تقليل مقدار الهطول.



جمهورية العراق

وزارة التعليم العالي والبحث العلمي

جامعة كربلاء / كلية الهندسة

قسم الهندسة المدنية

**كفاءة الاعتاب الخرسانية المسلحة الحاوية على SIFCON و**

**المدعمة باستخدام CFRP**

رسالة مقدمة الى قسم الهندسة المدنية في كلية الهندسة /جامعة كربلاء

كجزء من متطلبات نيل شهادة الماجستير في علوم الهندسة المدنية

من قبل

**عصام يوسف جبار**

(بكالوريوس في الهندسة المدنية – 1996)

اشراف

**أ.د. ليث شاكر رشيد**

**أ.م.د. وجدي شبر صاحب**